Distribution Category:
Energy Storage (General) (UC-201)

ANL--89/35

ANL-89/35

DE90 010262

ARGONNE NATIONAL LABORATORY
9700 South Cass Avenue
Argonne, Illinois 60439

PRACTICAL SUPERCONDUCTOR DEVELOPMENT FOR ELECTRICAL POWER APPLICATIONS

ANNUAL REPORT FOR FY 1989

Roger B. Poeppel, Coordinator
Kenneth C. Goretta, Compiler

Contributors:

U. Balachandran
I. Bloom†
S. E. Dorris
J. T. Dusek
J. E. Emerson
K. C. Goretta
K. E. Gray*
M. Hatch†
J. R. Hull
S. A. Johnson†
R. T. Kampwirth*
M. Kullberg
D. S. Kupperman
M. T. Lanagan
S. Majumdar
V. A. Maroni†
R. L. McDaniel
J. H. Meiser†
J. J. Picciolo
J. P. Singh
C. A. Youngdahl

Materials and Components Technology Division

September 1989

Work supported by U. S. Department of Energy,
Office of Energy Storage and Distribution,
under Contract W-31-109-Eng-38

*Materials Science Division.
†Chemical Technology Division.

MASTER

LEGIBILITY NOTICE

A major purpose of the Technical Information Center is to provide the broadest dissemination possible of information contained in DOE's Research and Development Reports to business, industry, the academic community, and federal, state and local governments.

Although a small portion of this report is not reproducible, it is being made available to expedite the availability of information on the research discussed herein.

Contents

Figures

Table

PRACTICAL SUPERCONDUCTOR DEVELOPMENT FOR ELECTRICAL POWER APPLICATIONS

ANNUAL REPORT FOR FY 1989

Abstract

Development of useful high-critical-temperature (high-T_c) superconductors requires the synthesis of various superconducting oxide compounds; the fabrication of wires, tapes, and thin films from these compounds; the capability to form composite structures that incorporate integral insulators or stabilizers; and the design of efficient components and systems. This report describes the technical progress in and status of research efforts aimed at producing superconducting components based on the oxide systems YBCO, BSCCO, and TCBCO. Topics discussed are synthesis and heat treatment of high-T_c superconductors; formation of monolithic and composite wires and tapes; design and fabrication of superconductor/metal connections; characterization of microstructures and of superconducting, electrical, and mechanical properties; and fabrication and electrical properties of thin films. Interactions with industry and academia are also documented, and a list of selected program publications is provided.

1 Introduction

The superconductor program at Argonne National Laboratory (ANL) includes the development of both bulk and thin-film processing directed toward improving the properties of high-critical-temperature (high-T_c) superconductors and the development of fabrication methods for production of commercial conductors. Establishment of team relationships with industrial and academic partners is integral to this program. The objective of the ANL program is to develop, as quickly as possible, methods to fabricate and use structurally reliable high-T_c superconductors for the generation, transmission, and storage of electrical energy. Ceramic processing, fabrication, and joining techniques are being developed to provide useful conductors from one or several of the high-T_c superconductors. Initial work is focused on superconductors based on yttrium-barium-copper oxide (YBCO), bismuth-strontium-calcium-copper oxide (BSCCO), and thallium-calcium-barium-copper oxide (TCBCO).

There are several requirements for monolithic and composite conductors in the form of wires, tapes, films, and other shapes. The conductors must be capable of carrying large currents in the presence of large magnetic fields and must be strong, flexible, and chemically and cryogenically stable. The principal impediments to the use of bulk high-T_c superconductors are low critical current density (J_c) and poor mechanical properties. Processing methods for the improvement of both have been, and will continue to be, developed. The goals of ceramic fabrication include maximizing flux pinning through microstructural control, promoting high conductivity by obtaining phase-pure materials and imparting favorable grain alignment, and increasing flexibility and reliability by minimizing microstructural flaws and optimizing the toughness of each material.

This report reviews the technical progress in and status of (1) synthesis and heat treatment of high-T_c superconductors; (2) forming of monolithic and composite wires and tapes; (3) design and fabrication of superconductor/metal connections; (4) characterization of superconducting and electrical properties, microstructures, and mechanical properties; and (5) fabrication and property evaluations of thin films. Interactions with industry and academia are also documented.

2 Technical Progress in 1989

2.1 Synthesis and Heat Treatment

2.1.1 Y-Ba-Cu-O System

High-temperature ceramic superconductors are normally prepared by the solid-state reaction of oxides, carbonates, or nitrates. For $YBa_2Cu_3O_x$ (YBCO), the mixed precursors are calcined at 890-980°C for 20-100 h. Intermittent grinding is necessary to obtain relatively phase-pure and homogeneous YBCO powders (Coretta et al., 1988; Poeppel et al., 1987; Cava et al., 1989). The high temperatures used in the conventional method can

induce formation of liquids and nonsuperconducting phases such as Y_2BaCuO_5 and $BaCuO_2$ (Goretta et al., 1988). The presence of these nonsuperconducting phases, especially at grain boundaries, reduces J_c (Shi et al., 1988). In addition to producing undesirable phases, the conventional processes are time-consuming and produce coarse particles.

During calcination of the YBCO precursor, simultaneous decomposition of $BaCO_3$ and reaction among the three constituent oxides form the desired perovskite phase. The CO_2 released by decomposition of $BaCO_3$ can, however, react with YBCO to form $BaCO_3$, Y_2O_3, CuO, and $Y_2Cu_2O_5$, depending on temperature (Smith, 1987; Fjellvag et al., 1988). Kingon et al. (1989) have also suggested that a Ba-Cu-C oxide forms when YBCO is exposed to CO_2.

We have developed a synthesis route to obtain phase-pure orthorhombic YBCO powders at 800°C in flowing O_2 at reduced pressure. The procedure is as follows: Y_2O_3, $BaCO_3$, and CuO were mixed as a 1-kg batch and calcined for 4 h in flowing O_2 at a pressure of 2-20 mm Hg and a temperature of 800°C. During cooling, the vacuum was discontinued and ambient-pressure O_2 was passed. A 3-h hold at 450°C was incorporated into the cooling schedule to promote oxygenation of the resulting powder. A Bomem Michelson 100 Fourier transform infrared (FTIR) spectrophotometer with 4-cm^{-1} resolution was used to monitor the evolution of CO_2 during calcination. As shown in Fig. 1, the weight loss attributable to CO_2 evolution during heating the precursor powders begins at about 750°C at the ambient pressure of 1 x 10^5 Pa (curve b); it begins at about 620°C, however, at 2.7 x 10^2 Pa (curve a). More weight was lost from the low-pressure mixture because additional O_2 was also liberated. Heating the powders at less than 20°C h^{-1} in the range of 700-800°C enabled CO_2 levels to be maintained at less than 2% of the O_2 (see Fig. 2). Faster heating rates resulted in higher CO_2 concentrations and yielded powders containing Y_2BaCuO_5 and other impurity phases. Phase-pure powders, as determined by differential thermal analysis and X-ray diffraction, were obtained when the total pressure was maintained at 2.7 x 10^2 Pa. Analysis of the orthorhombic X-ray diffraction peak split and comparison against published data (Wong-Ng et al., 1987) revealed that no tetragonal phase was present in the powder. The particle size of the powder resulting from the low-pressure synthesis was 1 to 4 μm. This relatively small particle size is due to the low processing temperature. Calcination could be carried out at 800°C, rather than 890°C or greater, because diffusional kinetics in YBCO are faster in reduced O_2 pressures (Chen et al., 1989; von Stumberg et al., 1989). A partial vacuum was used, instead of a mixture of O_2 and a noble gas, because CO_2 was removed with increased efficiency.

The resultant YBCO powder was cold-pressed into pellets and sintered in O_2 to make dense superconductors. For sintering from 915 to 980°C, pellet densities ranged from 90 to 96% of theoretical, and similar superconducting properties were achieved. The J_c values, measured in zero field at 77 K with a criterion of 1 μV/cm, were about 1.0 x 10^3 A/cm^2. The J_c as a function of external magnetic field, H, for samples sintered at 915 and 980°C is shown in Fig. 3. In addition to pellets, wire samples were extruded from the vacuum-calcined YBCO powder, and the sintered wires exhibited J_c of more than 1000 A/cm^2 at 77 K in zero applied field.

Recently, another compound in the YBCO system, with stoichiometry $YBa_2Cu_4O_8$ ("124") was observed, first as a lattice defect in partially decomposed 123 powders (Zandbergen et al., 1988), and then as an ordered defect structure in 123 thin films

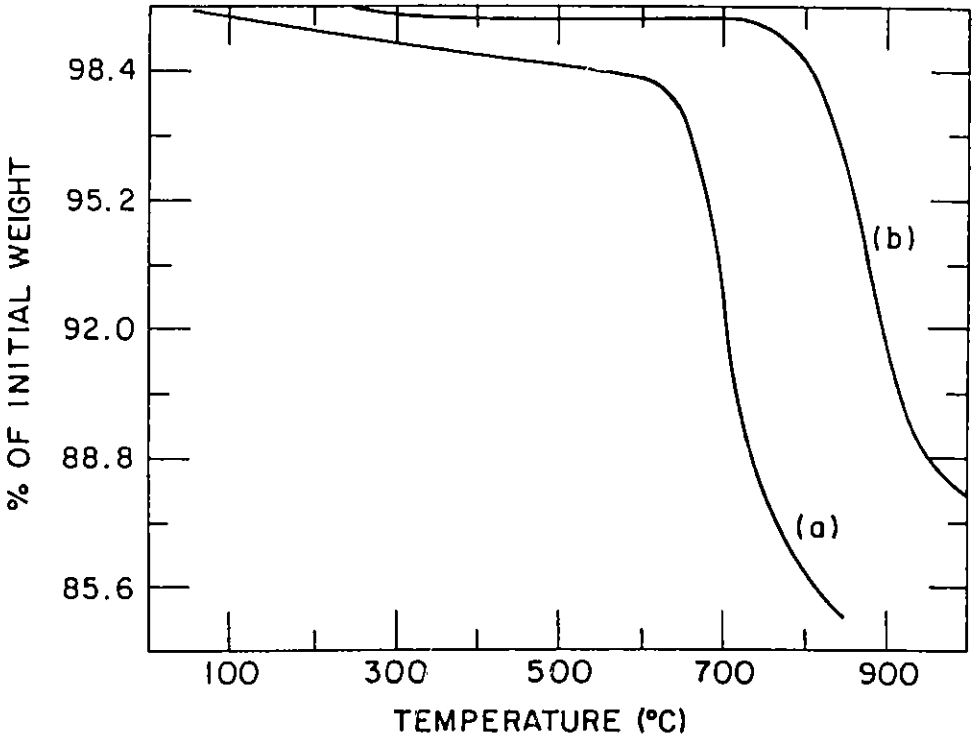

Fig. 1. Change in Mass Observed by Thermogravimetric Analysis during Heating of YBCO Precursor Powders: (a) Pressure of 2.7 x 10^2 Pa; (b) Ambient Pressure.

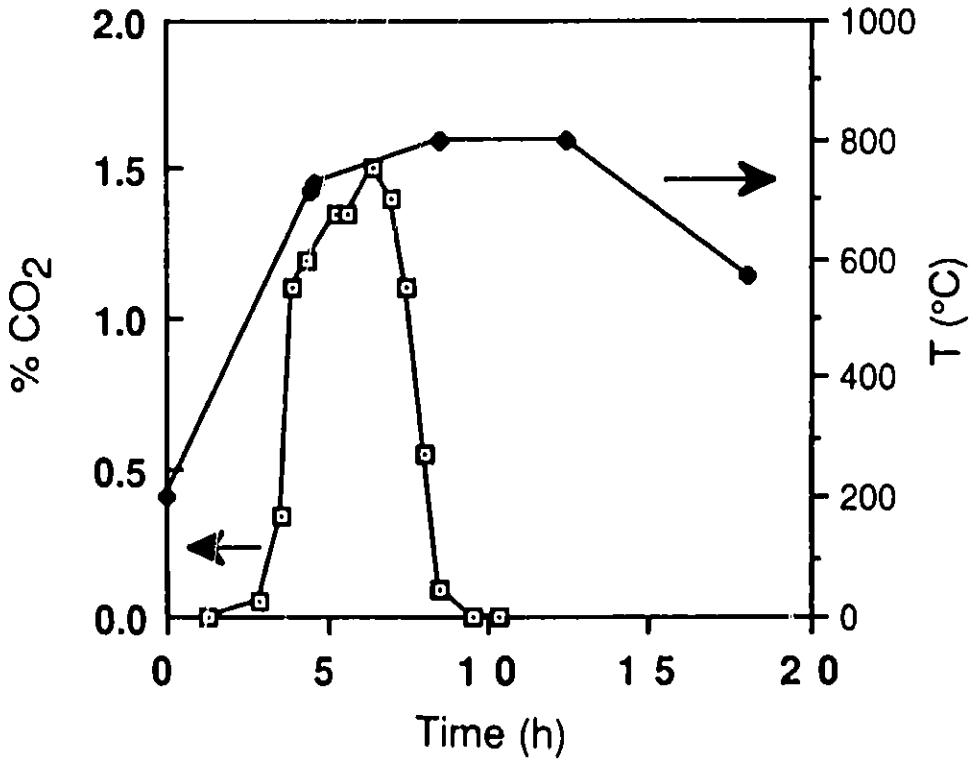

Fig. 2. CO_2 Evolution vs. Time during Vacuum Calcination of YBCO Precursor; Temperature Profile vs. Time Is Also Given.

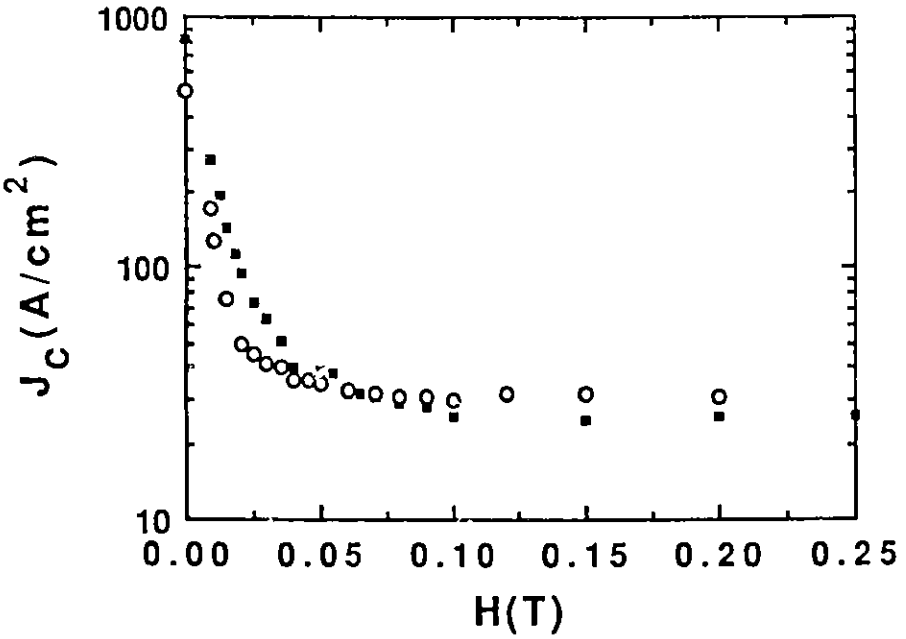

Fig. 3. J_c vs. Field for YBCO Pellets Sintered at 915 and 980°C in Oxygen.

(Kogure et al., 1988; Marshall et al., 1988; Zandbergen and Thomas, 1988). The 124 phase was then prepared as a distinct phase in thin films (Mandich et al., 1988; Kwo et al., 1988; Char et al., 1988). Films of 124 superconduct with a transition temperature of 80-81 K. The crystal structure of 124 was determined by Marsh et al. (1988); it differs from 123 in that the single Cu-O chain has been replaced by a double Cu-O ribbon. The proposed structure for 124 has a c-axis spacing of ≈27 Å.

High oxygen pressures were considered necessary to synthesize bulk 124, and because of specialized equipment needs, this compound has not been investigated extensively (Karpinski et al., 1988; Morris et al., 1989). Cava et al. (1989) reported a two-step process for the synthesis of the 124 phase (containing some impurity phases) in flowing oxygen at atmospheric pressure. In their method, an equal volume of alkali carbonates is added as catalyst to a prereacted stoichiometric 124 mix. The materials made by this method are, in general, not single phase, but are at least as phase-pure as materials prepared at high oxygen pressures. We have developed a novel synthesis route to obtain phase-pure orthorhombic 124 powders, without the use of alkali carbonates, at 800°C in flowing oxygen at reduced pressure followed by high-temperature annealing in ambient-pressure oxygen. The procedures are similar to those for synthesizing 123.

The observed X-ray diffraction pattern, for 2θ = 20-70°, of the 124 powder annealed at 800°C for 24 h is shown in Fig. 4. In addition to the diffraction peaks shown here, two others at 2θ = 6.55 and 13.10° were also observed. All of the diffraction peaks are indexed on the basis of atomic positional coordinates worked out by Marsh et al. (1988) for the 124 structure. As seen from Fig. 1, the 124 powder prepared by this method is single phase. Neutron diffraction experiments confirmed the phase purity of the powder. Magnetic susceptibility revealed a T_c of 80 K.

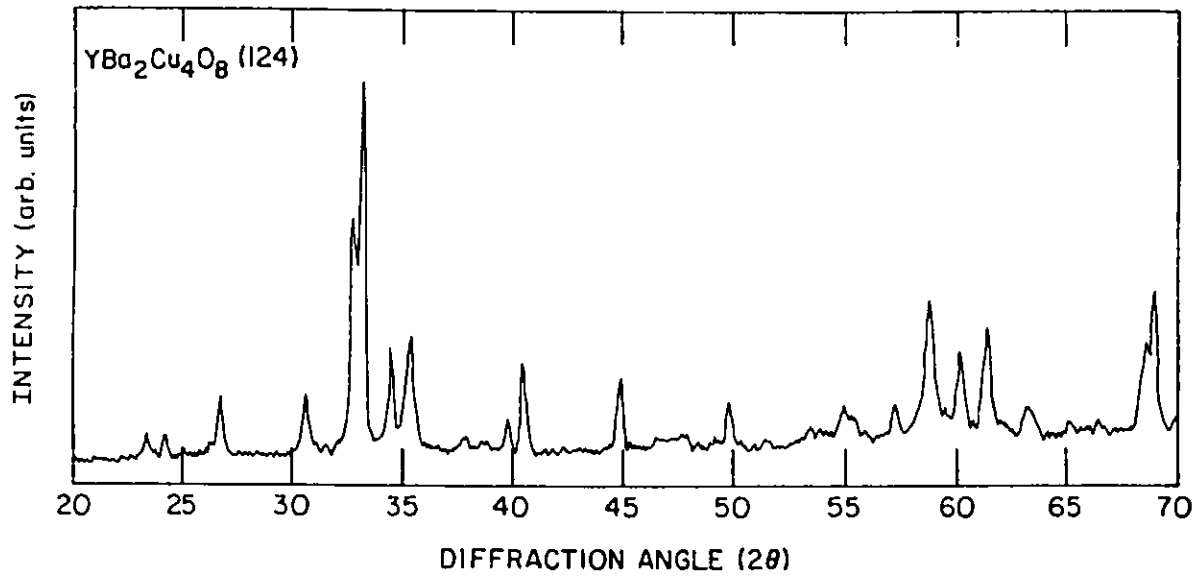

Fig. 4. X-Ray Powder Diffraction Pattern of $YBa_2Cu_4O_8$ Annealed at 800°C for 24 h.

Thermogravimetric analysis (TGA) shows that 124 begins to decompose at about 880°C in 1-atm oxygen. However, the weight of 124 samples decreased by only 0.06% at 600°C, 0.12% at 700°C, and 0.16% at 800°C. The 123 compound, on the other hand, loses about 0.5, 1.0, and 1.4 % by weight at 600, 700, and 800°C respectively (Balachandran et al., 1989; Gallagher, 1987). The oxygen content of the 124 superconductor is stable up to the decomposition temperature. Differential thermal analysis (DTA) traces exhibit three endothermic peaks with onset temperatures of 880, 960, and 990°C. The first endothermic peak with onset at 880°C is due to the decomposition of 124 to 123 and CuO. There is, as observed in the TGA, a corresponding weight loss at this temperature. The peak with the onset at ≈960°C is attributed to a peritectic reaction between 123 and CuO that forms Y_2BaCuO_5 ("211") and a liquid (Aselage and Keefer, 1988). The peritectic reaction may not have reached completion at the heating rate of 3°C/min used in our experiment, and the unreacted CuO upon further heating undergoes another peritectic reaction with 211 to form $Y_2Cu_2O_5$ and a liquid phase. The onset of this reaction is at about 990°C. Selective manipulation of decomposition may yield microstructures containing flux pinning sites. Investigation of this possibility is underway. In addition, since 124 appears to be more stable than 123, further investigations into the properties of 124 are planned.

Sintering of YBCO has been studied extensively in the past year. Two investigations have been completed. The first involves heating before and after sintering; the second involves sintering in various atmospheres. For these studies, the YBCO was derived from solid-state reaction or obtained from Rhône-Poulenc, Inc.

The effects of heating schedules have been published (Chen et al., 1988; Bloom et al., 1989), and the results can be summarized briefly. YBCO appears more stable relative to impurity phases at lower temperatures. (As stated previously, this is also found in synthesis.) The greater the time spent in O_2 from 400 to 900°C, the better the superconductor. For specimens of low phase-purity, the benefits are appreciable. For example, as shown in the DTA trace in Fig. 5, holding phase-impure YBCO at 860°C for

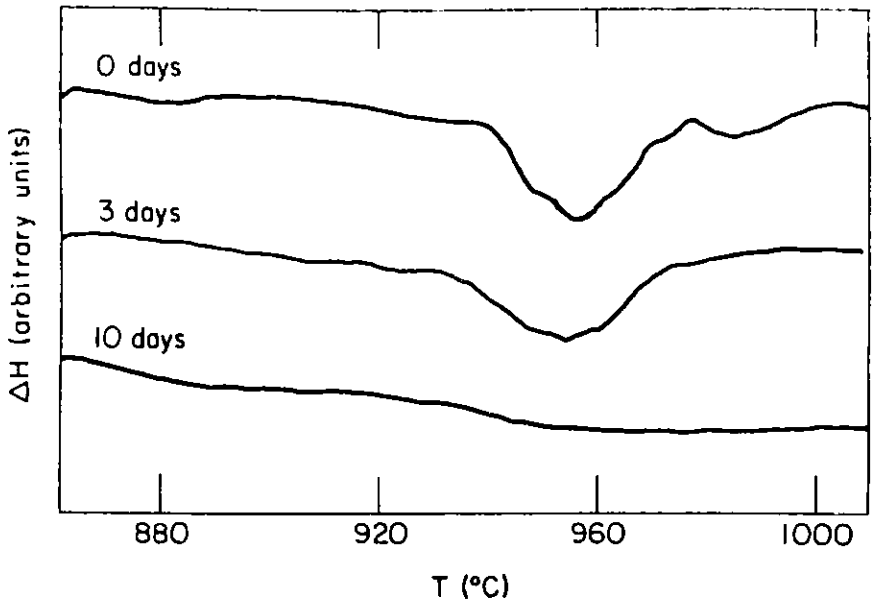

Fig. 5. DTA Trace of YBCO Powder after Anneals at 860°C for Three Time Periods.

10 days resulted in almost complete elimination of low-temperature melting associated with impurity phases. An increase in J_c of about 100% was associated with the enhanced phase purity.

It has been found that sintering of YBCO is strongly affected by its oxygen content. Diffusion rates in nonstoichiometric oxides (Kofstad, 1972) are generally functions of oxygen partial pressure, $P(O_2)$. Sintering kinetics and high-temperature plastic deformation are generally governed by diffusion of minority defects (Routbort, 1982). Mass transport of the slowest-diffusing species determines the rate of the process. Furthermore, detailed knowledge of the majority point defects does not often allow one to predict the relationship between $P(O_2)$ and minority-species-controlled properties; experiments are necessary.

Sintering experiments were conducted from 850 to 910°C in mixtures of 0.2%, 3%, and 17.9% O_2 in Ar and in 100% O_2. Sintering kinetics militated against use of significantly lower temperatures. Lower $P(O_2)$ mixtures were avoided because of YBCO decomposition at low $P(O_2)$. Sintering studies were conducted in two ways. First, the effects of oxygen partial pressure on shrinkage during sintering were investigated isothermally by a dilatometric technique. Second, densification was studied by sintering in furnaces.

Shrinkage profiles in the dilatometer were obtained for several temperatures and oxygen partial pressures. Representative data are shown in Fig. 6. As expected, initial shrinkage rates increased with increasing temperature (Fig. 6a). Initial shrinkage rates also increased with decreasing $P(O_2)$, even for temperatures at which no liquid phase was present (Fig. 6b). Densification data taken from sintering experiments parallel the shrinkage data. Use of higher temperatures or lower $P(O_2)$ increased densification.

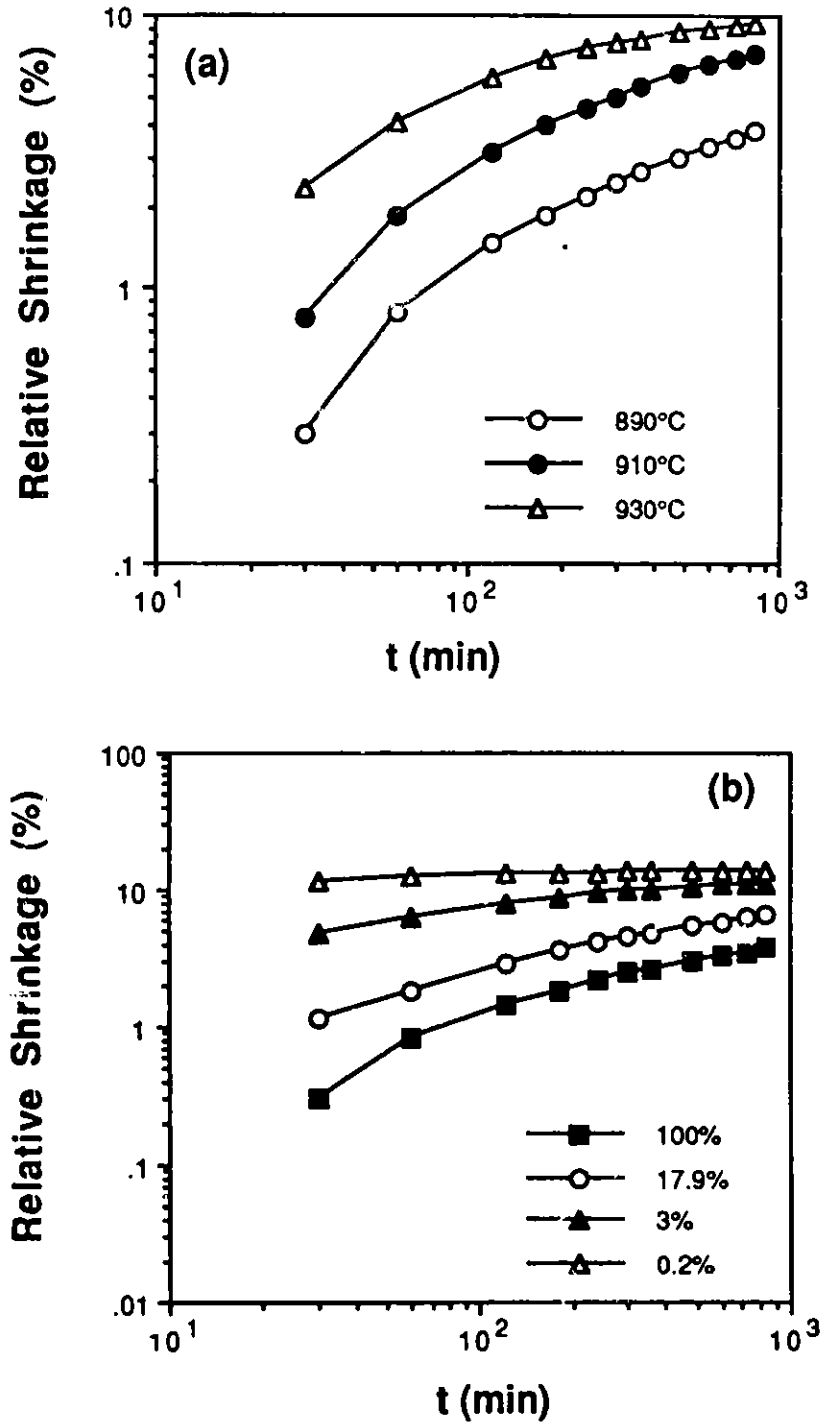

Fig. 6. Dilatometer Shrinkage Curves for YBCO (a) in O_2 at Various Temperatures and (b) at 890°C in Various Oxygen Contents.

A summary of J_c data obtained is shown in Fig. 7. It is clear that J_c increases with densities up to about 87% and decreases at higher densities. Furthermore, the J_c values for the specimens sintered in 3% O_2 are higher than those for specimens sintered at higher $P(O_2)$.

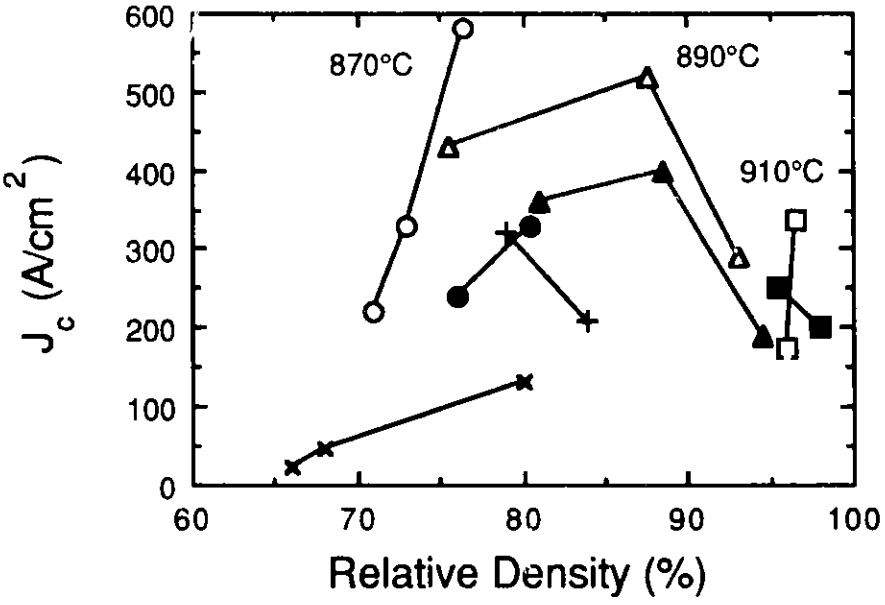

Fig. 7. J_c as Function of Specimen Density (open symbols denote specimens sintered in 3% O_2; temperatures shown are for this oxygen content only).

From the standpoint of attempting to make a better bulk superconductor, four results were most significant: (1) as $P(O_2)$ decreased, the melting points of both YBCO and the impurity phase decreased; (2) for a given temperature, solid-state sintering kinetics were fastest for lower $P(O_2)$; (3) J_c was correlated with density, with specimens of 80-85% density giving the highest J_c; and (4) for specimens with the same density, those sintered in 3% O_2 had higher J_c values.

Recently, similar experiments have been conducted on phase-pure powder. Effects of liquid phase are thus avoided. The finding that lower temperatures and lower $P(O)_2$ yield better properties was borne out.

2.1.2 Bi-Sr-Ca-Cu-O System

Superconductivity with onset at 120 K and zero electrical resistivity at 106 K has been obtained in the system (Bi,Pb)-Sr-Ca-Cu-O. The T_c and room-temperature resistivity of the samples depend on the rate of cooling from the sintering temperature (Figs 8 and 9). Sintered pellets showed J_c of ≈200 A/cm^2, and extruded wires demonstrated values of ≈300 A/cm^2. A series of experiments, in which phase composition was monitored by DTA, determined that 30% Pb substitution for Bi yielded the highest fraction of the 110 K phase. A second set of experiments revealed that the use of low calcination temperatures of about 820°C was beneficial in producing the 110 K phase $Bi_{0.7}Pb_{0.3}SrCaCu_{1.8}O_x$. The Pb-doped Bi-Sr-Ca-Cu-O system is complex, and additional studies aimed at producing higher-quality powders in shorter times are in progress.

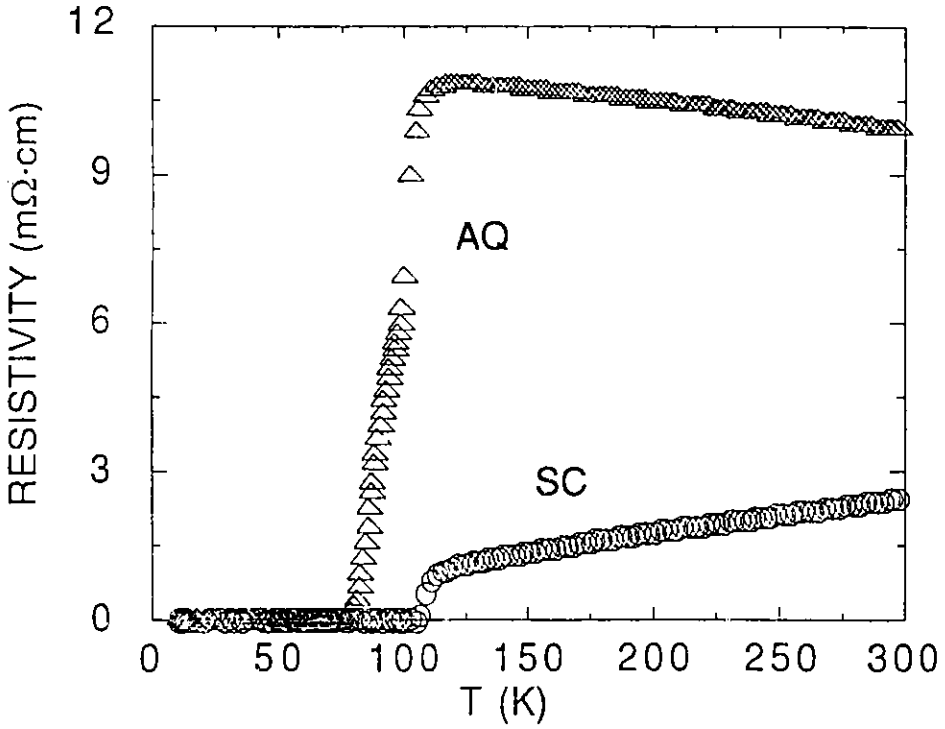

Fig. 8. Temperature Dependence of Electrical Resistivity of Pb/BSCCO: Sample AQ Was Air-Quenched; Sample SC Was Slow-Cooled.

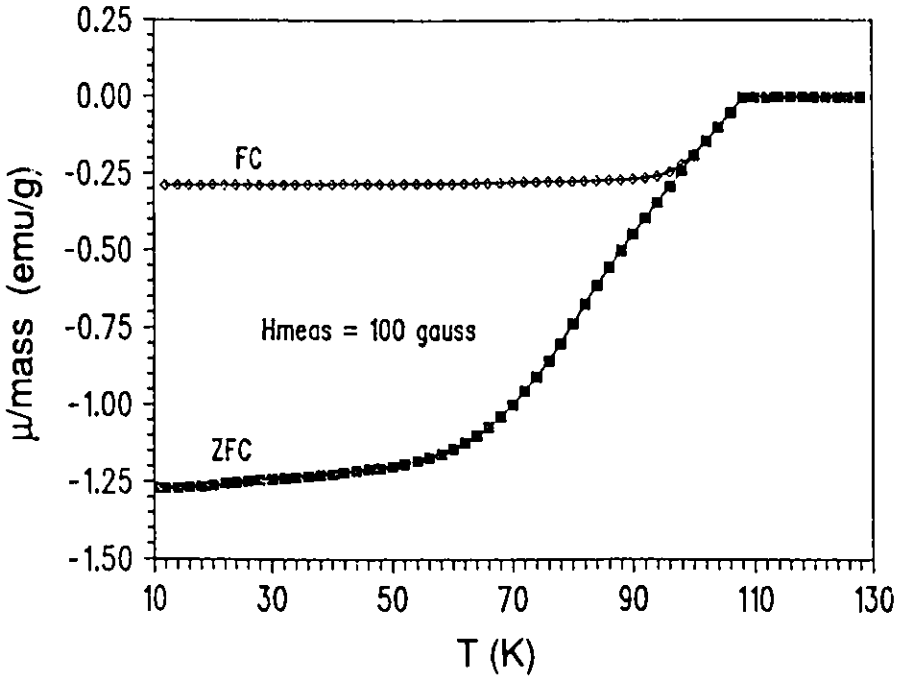

Fig. 9. Magnetic Susceptibility vs. Temperature for Pb/BSCCO Pellet.

$Bi_2Sr_2CaCu_2O_x$ (2212) of high phase purity has recently been synthesized. The actual composition of the superconducting phase is Sr-deficient, i.e., approximately $Bi_2Sr_{1.7}CaCu_2O_x$. Bulk specimens have been formed and processed by sintering in the solid state, in the presence of a liquid phase, or by sinter-forging. Figure 10 shows the J_c of 2212 specimens as a function of sintering temperature. DTA performed in air at a heating rate of 5°C/min revealed an onset of melting for the powder at 875°C. Attempts at sintering in the solid state, i.e., at temperatures below 875°C, resulted in porous specimens with very low J_c values. Liquid-phase sintering is rapid and generally leads to high densities, extensive grain growth, and higher J_c values. Sinter-forging to impart favorable grain alignment in 2212 specimens was attempted at 870°C and 900°C, temperatures below and above that at which liquid forms. Within experimental error, no improvement in J_c was found in any sinter-forged specimen.

2.1.3 Tl-Ca-Ba-Cu-O System

Thallium-based superconductors have been reported to have zero-resistance temperatures (T_0) as high as 125 K, although the T_c of bulk forms is generally below 120 K (Ginley et al., 1988). Synthesis of powder for bulk specimens has been accomplished by using compositions rich in Ca and Cu. To make a large fraction of the high-T_c phase $Tl_2Ca_2Ba_2Cu_3O_x$ (2223), the starting composition 1313 has been shown to be effective (Lee et al., 1988). Because liquid-phase sintering occurs during synthesis, bulk parts can be fabricated during the reaction that generates the high-T_c phase.

Many researchers begin with Tl-excess mixtures to compensate for Tl evolution at high temperatures. Efforts at ANL have focused on encapsulation to avoid Tl volatilization. This approach is necessary for fabrication because it is impractical to change formulations for every geometry used. The ANL procedure begins by forming oxide precursors of the Ca, Ba, and Cu species: Ca_2CuO_3, Ba_2CuO_3, and $Ba_2Cu_3O_5$. Phase-pure materials can be made by calcining at 900 to 950°C. Encapsulation can then be successful, because no CO_2 is evolved during heating. Heating of 1313 mixtures has been studied as follows: Maximum temperature was varied from 860 to 925°C; time at temperature ranged from 0.2 to 12 h; the atmosphere included 1% O_2 in N_2, air, and O_2; and post-sintering annealing at 750°C in O_2 was conducted for up to 16 h (Goretta et al., 1989).

Results indicate that (1) T_0 rises with processing temperature, reaching a maximum at 118 K for temperatures of 910 to 920°C (for 910°C, more than 8 h is needed to obtain the high T_0, for 920°C, only 2 h at temperature is required); (2) T_0 rises with increasing oxygen partial pressure, but use of hyperbaric O_2 is ineffective; (3) the phase purity of all specimens is imperfect, and only about 90% of any specimen is the high-T_c phase; and (4) J_c values for all specimens range to 700 A/cm^2, with ≈100 A/cm^2 typical for specimens with T_0 greater than 100 K.

Results 3 and 4 are in agreement with much of the literature (Ginley et al., 1988). Results 1 and 2 have not been reported previously in any systematic way. Specimens not encapsulated are generally processed at 850 to 870°C. Encapsulation dictates use of higher processing temperatures. The initial trend in T_0 with oxygen partial pressure had suggested that hyperbaric conditions may be useful for synthesizing 2223. This speculation has been tested to a pressure of 6×10^5 Pa. No improvement in phase purity or T_c resulted. Current work is based on findings for the YBCO and BSCCO systems. For those materials,

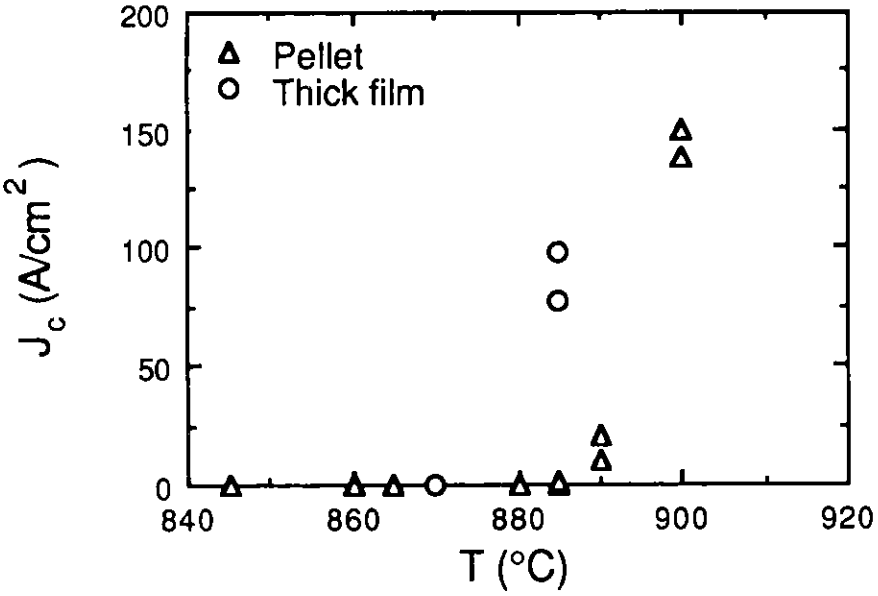

Fig. 10. J_c of 2212 Specimens as Function of Sintering Temperature.

use of low pressures improved phase purity. Because of the high volatility of Tl, low-pressure processing must still provide for a Tl overpressure. Creation of a static vacuum should enable Tl pressure to be maintained. Experiments are now in progress on three TCBCO compositions to determine whether phase-pure 120-K TCBCO can indeed be formed. Subsequent work will focus on fabrication of thick films and on J_c enhancement.

References for Section 2.1

T. Aselage and K. Keefer, J. Mater. Res. *3*, 1279 (1988).

U. Balachandran, et al., Mater. Lett. *8*, 454 (1989).

I. Bloom, et al., J. Mater. Res. *4*, 1093 (1989).

G. Bussod, et al., J. Am. Ceram. Soc. *72*, 137 (1989).

R. J. Cava, et al., Nature *338*, 328 (1989).

K. Char, et al., Phys. Rev. B *38*, 834 (1988).

N. Chen, M.S. thesis, Illinois Institute of Technology (1988).

N. Chen, D. Shi, and K. C. Goretta, J. Appl. Phys. *66*, 2485 (1989).

H. Fjellvag, et al., Acta Chem. Scand. *A42*, 178 (1988).

P. K. Gallagher, Adv. Ceram. Mater. *2*, 632 (1987).

D. S. Ginley, et al., Physica C, 152, 217 (1988).

K. C. Goretta, et al., Mater. Lett. *7*, 161 (1988).

K. C. Goretta, et al., Supercond. Sci. Tech. *2*, 192 (1989).

J. Karpinski, et al., Nature *336*, 660 (1988).

A. I. Kingon, et al., in *Abstract Book, 91st Annual Meeting of the American Ceramic Society*, Indianapolis, April 23-27, 1989, p. 151.

P. Kofstad, *Nonstoichiometry, Diffusion and Electrical Conductivity in Binary Metal Oxides* (Wiley-Interscience, New York, 1972).

T. Kogure, et al., Physica C *156*, 45 (1988).

J. Kwo, et al., Appl. Phys. Lett. *52*, 1625 (1988).

W. H. Lee, et al., Physica C *152*, 345 (1988).

M. L. Mandich, et al., Phys. Rev. B *38*, 5031 (1988).

P. Marsh, et al., Nature *334*, 141 (1988).

A. F. Marshall, et al., Phys. Rev. B *37*, 9353 (1988).

D. E. Morris, et al., Physica C *158*, 287 (1989).

R. B. Poeppel, et al., in *Chemistry of High-Temperature Superconductors*, edited by D. L. Nelson, M. S. Whittingham, and T. F. George (American Chemical Society, Washington, DC, 1987) p. 261.

P. E. Reyes-Morel, W. Wu, and I-W. Chen, in *Ceramic Superconductors II*, ed. M. F. Yan (Am. Ceram. Soc., Westerville, OH, 1988) p. 590.

S. J. Rothman, J. L. Routbort, and J. E. Baker, Phys. Rev B *40*, 8852 (1989).

J. L. Routbort, Acta Metall. *30*, 663 (1982).

D. Shi, et al., Mater. Lett. *6*, 217 (1988).

D. W. J. Smith, J. Chem. Educ. *64*, 480 (1987).

A. W. von Stumberg, et al., J. Appl. Phys. *66*, 2079 (1989).

W. Wong-Ng, et al., Adv. Ceram. Mater. *2*, 565 (1987).

H. W. Zandbergen, et al., Nature *331*, 596 (1988).

H. W. Zandbergen and G. Thomas, Phys. Stat. Solidi. A *105*, 207 (1988).

2.2 Bulk Conductor Production

2.2.1 Monolithic Conductors

Coils of high-T_c superconductors, which are essential for the development of highly efficient motors and generators, have been fabricated by plastic extrusion. Wires have been extruded in long continuous lengths, wrapped into coils, and subsequently sintered. Coils, 2 cm in diameter and comprising up to 30 turns, have been made with critical current density (J_c) of about 250 A/cm^2 at 77 K. Recently, multilayer coils have been extruded.

Large-scale implementation of high-T_c superconductors will depend greatly on the ability to process these ceramic materials into useful shapes and on achieving high J_c in large magnetic fields. Monolithic and composite superconductors in the form of wires and tapes are candidates for a wide array of potential applications, including conducting rings for magnetic energy storage, windings for power generation, and long continuous wire for power transmission lines.

The extrusion process originates with a well-characterized YBCO powder, which is combined with a set of organics and mixed in a sigma-blade blender for optimal homogeneity. A solvent provides the basic vehicle into which the oxide powder and other organics are placed. Typical organic solvents include methyl ethyl ketone, methanol, and xylene. Dispersants are used to deflocculate the inorganic particles in the solvent and to assist in obtaining higher green densities. Binders impart strength to the green body, and plasticizers promote flexibility.

Extrusion itself consists of placing a high pressure (approximately 20 MPa) on the plastic mass and forcing it through a small aperture. Wires with radii of 0.1 to 1.5 mm have been manufactured in lengths of well over 200 cm. The wire has great flexibility in the unfired state, and 3-5-cm diameter coils of 1 to 70 turns have been fabricated. Some degree of particle alignment can occur as a result of the high shear stresses induced during the process. Texturing may enhance the critical current density because of the anisotropic transport properties observed in YBCO.

The extruded wire must be heated to consolidate the powder. The heat treatment schedule for fabricated shapes is divided into three parts: removal of organics, sintering, and annealing. Initially, a slow increase in temperature is required to remove organics from the green body. If the organics are removed rapidly, the final product will have large voids and a bloated appearance. Sintering temperature is about 870 to 990°C for YBCO. Annealing is carried out at about 450°C for several hours to transform the tetragonal phase to the superconducting orthorhombic phase.

Density and J_c are dependent upon sintering temperature (see Fig. 11). A small degree of uncontrolled variation in the macroscopic properties can be seen from the separate firings at 930°C. A correlation between J_c and theoretical density is also seen in the figure. The increase in J_c with density is attributed to the effective cross-sectional area of the wire.

In Fig. 11, the data are shown for 0.7-mm diameter wires, with the exception of one data point for a 0.2-mm wire. The relationship between wire diameter and critical current density was studied statistically because of the inherent uncertainty in the J_c data. Random

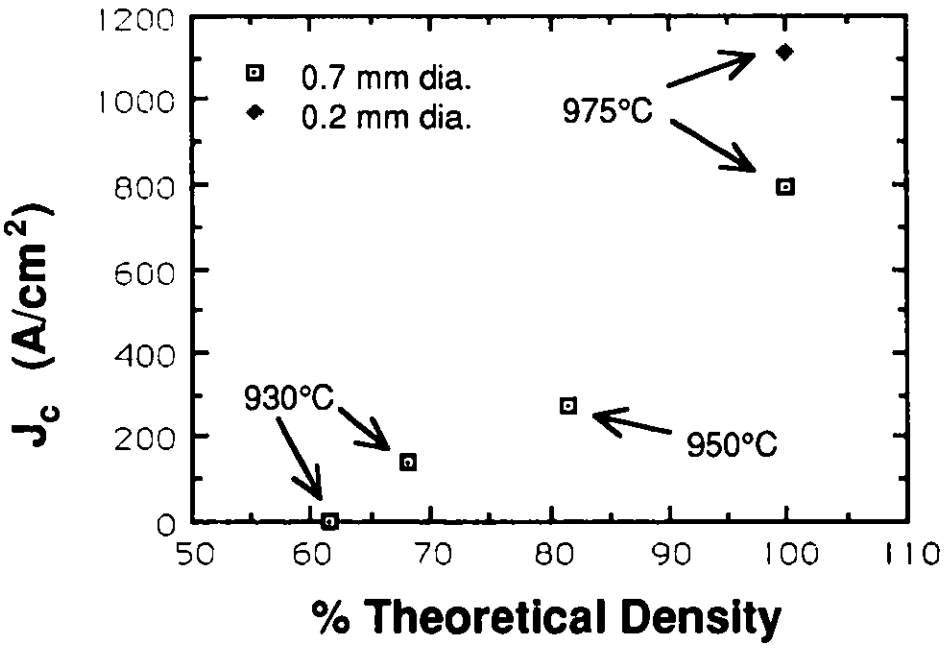

Fig. 11. J_c as Function of Wire Diameter.

defects such as porosity and microcracking may cause a wide variation in the J_c values. In this study, 10 wire samples each of 0.7- and 0.2-mm diameter were processed identically. The sintering temperature was 950°C. The 0.7-mm wire had a mean J_c of 273, with a standard deviation of 24.5 A/cm^2. The 0.2-mm wire had a mean J_c of 545, with a standard deviation of 104 A/cm^2. It is concluded with a 99% confidence level that the 0.2-mm wire had a significantly higher J_c than the 0.7-mm wire.

The effect of specimen geometry on J_c has been observed by others (Stephens, 1989). It was attributed to weak coupling between superconducting grains. Microcracking, spurious phases, and distortion in the crystal lattice at the grain boundaries all contribute to reduced J_c. The magnetic field generated by the measuring current will cause the links to become resistive and thus limit the current carrying capacity of the entire specimen. Smaller wires generate a lower magnetic field for an equivalent current density and thus will have a higher J_c.

The magnetic flux density calculated from Ampere's circuital law and the critical current in the wire is on the order of 10 gauss and is consistent with the effect on J_c of an externally applied magnetic field. Large reductions in J_c (on the order of 50%) have been observed in YBCO wire specimens measured in fields of 10 gauss. Preliminary data show that the size dependence is not observed in a small applied magnetic field.

Coils are fabricated by wrapping the wire around a mandrel in the unfired state. These coils are subsequently sintered, annealed, and tested. Since the beginning of our program, approximately 400 coils have been processed through the firing stage, and electrical properties of 200 coils have been measured. Each coil was assigned an extrusion number and a coil number within the batch. This allowed the coil to be tracked through the process (Table 1). The sintering conditions, fired density, and specimen geometry were

Table 1. Spreadsheet Used to Record Specimen Data

	A	B	C	D	E	F	G	H	I	J
88	EXT. NUMBER	DATE	COIL NUMBER	FIRING TIME	Jc VALUE	NO. OF TURNS	BOOK/PAGE #	DENSITY %	DENSITY	DIAMETER
90	EXT-41	1/27/89	-	S/930/24	361	WIRE SAMPLE	LB75-P134			
91	EXT-41	1/27/89	-	S/930/24	71	WIRE SAMPLE	LB75-P134			
92	EXT-41		-	S/930/24		WIRE SAMPLE	LB75-P134		5.944	
93	EXT-41	3/24/89	-	S/950/24	364	WIRE SAMPLE	LB110-P4	94	5.526	
94	EXT-41	2/22/89	-	S/930/24	371	WIRE SAMPLE	LB75-P145	88	-	
95	EXT-42	1/31/89	1	S/930/24	135	16 TURNS	LB75-P134	-		
96	EXT-42	2/23/89	2	S/930/24	146	17 TURNS	LB75-P145		5.052	
97	EXT-42	2/22/89	4	S/930/24	179	19 TURNS	LB75-P145	80.1	-	
98	EXT-42	3/24/89	6	S/930/24	122	19 TURNS	LB110-P4	-	4.882	
99	EXT-42	1/27/89	8	S/930/24	140	18 TURNS	LB75-P134	78	-	
100	EXT-42	3/10/89	8	S/930/24	161	19 TURNS	LB75-P161	-	4.738	
101	EXT-42	1/31/89	9	S/930/24	188	30 TURNS	LB75-P134	75	6.055	
102	EXT-42		10	S/950/24	144	20 TURNS	LD110-P4	96	5.436	
103	EXT-42	1/31/89	10	S/930/24	252	0.5 TURN	LB75-P134	86		
104	EXT-42	3/28/89	11	S/930/24	124	23 TURNS	LB110-P9		5.842	
105	EXT-42	3/17/89	12	S/930/24	260	10 TURNS	LB75-P161	93	4.533	
106	EXT-42	1/27/89	13	S/930/24	512	0.5 TURN	LB75-P134	72	-	
107	EXT-42	1/27/89	13	S/930/24	183	12 TURNS	LB75-P134	-	-	
108	EXT-42	1/31/89	-	S/930/24	304	WIRE SAMPLE	LB75-P134	-		
109	EXT-42	1/31/89	-	S/930/24	336	WIRE SAMPLE	LB75-P134			
110	EXT-42	2/22/89	-	S/930/24	117	WIRE SAMPLE	LB75-P145		5.262	
111	EXT-42	1/27/89	-	S/930/24	298	WIRE SAMPLE	LB75-P134	84	-	
112	EXT-42	1/27/89	-	S/930/24	318	WIRE SAMPLE	LB75-P134	-	-	
113	EXT-42	1/27/89	-	S/930/24	402	WIRE SAMPLE	LB75-P134	-	-	
114	EXT-42	1/27/89	-	S/930/24	338	WIRE SAMPLE	LB75-P134	-	-	-
115	EXT-43	2/23/89	1	S930/24	-	# TURNS ?	LB75-P145	-	-	
116	EXT-43	2/23/89	2	S/930/24	13	13 TURNS	LB75-P145	-	3.766	-
117	EXT-43	3/2/89	4	-	BSC	18 TURNS	-	90	-	-
118	EXT-43	-	5	S930/24	2	# TURNS ?	-	57	4.722	
119	EXT-43	3/7/89	6	S/950/24		19 TURNS	LB108-P4	75	3.7642	
120	EXT-43	2/23/89	8	S/930/24	NO SC FOUND	28 TURNS	LB75-P145	60	3.859	
121	EXT-43	2/24/89	9	S/930/24	0.7	WIRE SAMPLE	LB75-P145	62	-	-
122	EXT-43	3/2/89	10	-	2.41	# TURNS ?	-	-	4.21	-
123	EXT-43	-	11	S930/24	58.77	# TURNS ?	LB108-P4	67	4.94	
124	EXT-43	3/27/89	12	S/950/24	66	19 TURNS	LB110-P4	78	4.434	
125	EXT-43	3/28/89	13	S/930/24	NO SC FOUND		LB110-P9	70		
126	EXT-43	3/25/89	14		0	-	LB110-P4		-	
127	EXT-43	3/16/89	16	S/930/24	NO SC FOUND	15 TURNS	LB75-P161	-	2.832	
128	EXT-43	3/27/89	18	S/950/24	NO SC FOUND	29 TURNS	LB110-P4	45		
129	EXT-43	3/7/89	19	S/950/24	70	34 TURNS	LB108-P4			
130	EXT-43	3/16/89	20	S/930/24	NO SC FOUND	10 TURNS	LB75-P161		3.236	-
131	EXT-43	3/2/89	-	-	4.406	WIRE SAMPLE	-	51	4.405	-
132	EXT-43	-	-	S950/24	39	WIRE SAMPLE	LB108-P4	70	4.299	

recorded. As can be seen from Table 1, wide variations can occur between different extrusion batches and within a single extrusion batch.

The criterion for measuring J_c is a 1-μV drop over the entire coil length. A J_c of 250 A/cm^2 has been measured in a 30-turn coil (total wire length = 240 cm). The highest J_c value for a sample about 1 cm long was 1300 A/cm^2. Data were taken at 77 K in zero magnetic field. The J_c values for coils are generally lower than those for wire samples 1 cm long, thus demonstrating the statistical nature of the J_c measurement. The probability of encountering a current-limiting defect in a 240-cm-long coil is far greater than in a sample 1 cm in length.

Single-layer coils have been fabricated and characterized extensively during the past year. An apparatus has been recently employed to wind multilayer coils, and three-layer coils with more than 100 turns have been fabricated in the green state. Differential shrinkage of coil layers during heat treatment is a current problem that needs to be resolved. Another difficulty is that the windings cannot be separated easily after sintering;

this can be resolved by coating the wire with an insulating layer prior to wrapping on the mandrel. A slurry of Y_2BaCuO_5 has been used to coat the wire and has been successfully cofired with YBCO wire.

In conclusion, increased density has been found to enhance the J_c of extruded YBCO wire. Weak links limit J_c, as indicated by the observed effects of sample geometry on the J_c. The effect of processing on microstructure is a subject of continuing research, with the aim of improving electrical and mechanical properties.

2.2.2 Composite Conductors

One possible application of superconductors is in superconducting coils used for generating magnetic fields. Two coil fabrication methods are extrusion and tape casting. With either of these methods, it may be necessary to cofire the superconductor with an insulating material to prevent electrical short circuits between the individual turns of the coil during sintering. In this section, efforts to develop an insulator that is compatible with YBCO are summarized, and methods for coating YBCO with the insulator are described. There are two principal requirements for the insulator. The first is that it should be chemically compatible with the superconductor at high temperature (900-1000°C), since it will be cofired with the superconductor. YBCO tapes have been seen to react with the insulators Al_2O_3, ZrO_2, and MgO; however, the Y_2O_3-BaO-CuO phase diagram (Roth et al., 1988) shows that $BaCuO_2$ and Y_2BaCuO_5 (211) are both compatible with YBCO. Because of their chemical compatibility, efforts to develop an insulator have focused on 211 and $BaCuO_2$. The second requirement is that shrinkage of the insulator during firing should be similar enough to that of the superconductor to prevent cracking during firing. Pure YBCO by itself is very brittle, so it can withstand only a slight shrinkage mismatch; however, additions of Ag to YBCO increase its fracture toughness and enable it to withstand substantial shrinkage mismatch with the insulator (Singh et al., 1989).

Current efforts to fabricate coils employ 211 as the insulator, with tests showing that YBCO and 211 are chemically compatible during firing; however, the shrinkage and thermal expansion of 211 are not ideal. The shrinkage of 211 during firing is ~5-7% and can be increased to ~12% with the addition of 25 vol.% YBCO, but the shrinkage of YBCO is ~25% (Poeppel et al., 1989). Additions of YBCO greater than ~25 vol.% were not seen to increase the firing shrinkage of the 211/YBCO layer any further, and such large additions might form a continuous path of YBCO through the insulator. The coefficient of thermal expansion (α) for 211 ranges from 11×10^{-6} °C^{-1} to 16×10^{-6} °C^{-1} over the temperature range 30-900°C, with an average value of 14.3×10^{-6} °C^{-1}. By comparison, α of YBCO has an average value of 16.9×10^{-6} °C^{-1}, but reaches ~30×10^{-6} °C^{-1} as a result of the tetragonal-to-orthorhombic phase transition. In addition, the stiffness of 211 is higher than that of YBCO (Dorris et al., 1989). Although the mismatches in stiffness and thermal expansion are not large, the relative values are not favorable and tend to place YBCO under tension and 211 under compression during firing. As a result of the very brittle nature of pure YBCO and the mismatches in shrinkage and thermal expansion, composite tapes of pure YBCO (no Ag) and 211 shattered upon firing; however, addition of Ag to YBCO increases its strength significantly (Singh et al., 1989), and composite tapes of YBCO/Ag and 211 can now be fired routinely without cracking.

While Ag additions alleviated the problem of severe cracking of composite tapes, reduction of the 211 layer thickness was examined as a means to minimize the stresses that develop as a result of mismatches in shrinkage and thermal expansion. Very thin layers of 211 (10-25 μm) were sprayed onto tapes of YBCO/Ag. These composite tapes were stacked and fired to give a sandwich-type structure in which the 211 layer lies between two layers of YBCO/Ag. Electrical measurements were made parallel and perpendicular to the plane of the tapes to assess the J_c of the YBCO/Ag layers (parallel measurement) and the insulating properties of the 211 layer (perpendicular measurement). For the spray-coated stack, superconduction was apparent ($J_c \approx 40$ A/cm^2) in both parallel and perpendicular directions, indicating that the spray-coated layer of 211 was too thin to provide insulation between the YBCO/Ag layers. Attempts to make sandwich-type structures with thicker layers of 211 have been unsuccessful to date. Because of its high porosity, the 211 layer is very weak and splits in half during firing. Measurements on the resulting half-pieces, however, show that the YBCO layer has a J_c in the range of 500-1000 A/cm^2 (zero magnetic field), while the 211 layer has a resistivity of ≈1000 Ω-cm. This confirms that YBCO and 211 can be cofired without losing their respective properties.

$BaCuO_2$ has also been studied as a possible insulator. Since the melting point of $BaCuO_2$ (≈1010°C) is considerably lower than that of 211 (~1270°C), it undergoes more complete densification at the firing temperature of YBCO and exhibits higher shrinkage. Dilatometer measurements show that the overall firing shrinkage of $BaCuO_2$ is ≈20%. While the shrinkage match between $BaCuO_2$ and YBCO is much better than that between YBCO and 211, $BaCuO_2$ undergoes an expansion at a temperature of ≈400°C that tends to cause bloating and cracking of $BaCuO_2$/YBCO composite tapes. X-ray diffraction of a fired $BaCuO_2$ tape suggests that the $BaCuO_2$ reacts with the CO_2 evolved during binder burnout to form $BaCO_3$.

In another attempt to improve the shrinkage match between YBCO and the insulating materials, efforts focused on reducing the shrinkage of YBCO. A coarse YBCO powder (mean particle size ≈15 μm) was prepared by calcining phase-pure YBCO for periods up to 24 h. The coarse powder was added to fine YBCO powder (mean particle size of ≈4 μm) in ratios ranging from 55 wt.% coarse/45 wt.% fine to 85 wt.% coarse/15 wt.% fine. YBCO tapes were then made using the coarse/fine mixtures of YBCO with the intention of improving the particle packing in the green state and thereby reducing the firing shrinkage. The shrinkage was reduced to ~16%, but the samples were exceedingly weak even with addition of Ag, prohibiting their use.

Methods for coating YBCO with 211 are now being developed. In tape casting, YBCO can be easily coated with 211 by casting a layer of the insulator over YBCO in the green state. A strip of the composite tape can then be rolled by itself into a pancake-type coil or can be laid onto a strip of annealed Ag foil and then rolled into a coil. Alternatively, the Ag layer can be applied by cocasting Ag flakes or powder with the 211 and YBCO layers to give a three-layer composite tape. The Ag layer provides the pancake coil with mechanical support and, due to the ductility of Ag, relieves some of the stresses caused by the shrinkage mismatch between YBCO and 211 (Leu et al., 1989).

Two methods for coating extruded YBCO wires with 211 are presently being investigated. In one method, the extruded wire is passed through a slip of 211 before being wound into a coil. This method requires that the 211 dries rapidly enough that it does not

flow off the wire during winding. Slips of 211 have been made using a common binder system (acryloid resin in xylene/butanol) and three different solvents (xylene/butanol, methyl ethyl ketone (MEK), and acetone). These slips were used to coat sections of green YBCO wire: coatings made with acetone and MEK dried significantly faster than those made with xylene/butanol. With a binder system in which MEK is the base solvent, it was found that the 211 coating was dry enough to handle less than one minute after application, and in several minutes the wire was completely dry. In fact, the MEK-based coating dried so quickly that it might be difficult to wind a coil without cracking the wire; however, it should be possible to obtain an optimal drying speed by adding a less volatile solvent. In the future, 211 slip formulation will be optimized to allow coating of YBCO wires for the purpose of fabricating multilayer coils.

Coextrusion is another method that is being explored for applying a coating of 211 to YBCO wires. Plans are being made with Dennis Kountz at DuPont to set up DuPont coextrusion equipment for producing a 211-coated YBCO wire. The coextrusion will be done either by sending 211 powder from ANL to DuPont and letting them perform the coextrusion, or by having an ANL employee perform the co-extrusion at DuPont. Coextrusion will be compared to the dip-coating method described above to determine which method is most suitable for producing multilayer coils.

2.2.3 Wires in Metallic Tubes

Processing high-temperature superconductors in Ag tubes has produced J_c values of about 10^4 A/cm^2, according to several reports from Japan. J_c values of about 3000-4000 A/cm^2 appear to be reproducible; higher J_c values have not been adequately confirmed. (All measurements were taken at 77 K in the absence of a magnetic field.) Advantages of powder-in-tube processing include (1) obtaining high green densities, which obviates use of high sintering temperatures; (2) protection of the superconductor from atmospheric exposure; and (3) possible stabilization of the superconductor by the metallic sheath.

At ANL, research has included examination of swaging (Shi and Goretta, 1989) and rolling (Balachandran et al., 1989). For both YBCO and Bi-based superconductors, the results to date are simple to summarize. Swaging may be done with large areal reductions per pass. Rolling must be done with deformation limited to 10% reduction per pass. If larger reductions are attempted, tensile stresses induce transverse cracks, and low J_c values are the result. Proper heat treatment has yielded excellent, low-resistance YBCO/Ag interfaces. The BSCCO/Ag interfaces currently have higher resistance, and work in progress is seeking to modify heat treatment times and atmospheres to improve the interfaces.

The microstructures developed to date have been only modestly textured. The highest 77-K, zero-field J_c has reached 3500 A/cm^2 (Shi et al., 1989). It appears that the advantages of powder-in-tube processing are the ease with which long continuous lengths can be formed and the possibility of stabilization through the metallic sheath. Because this wire fabrication method is highly directional, it may prove possible to impart favorable texture (Hikata et al., 1989; Osamura et al., 1989). Current work is focusing on obtaining greater extents of particle alignment. The two approaches are (1) use of powders with higher aspect ratios and (2) processing with an intermediate heat treatment to increase net plasticity of the sheath and to make possible use of favorable grain growth.

2.2.4 Thick Films

Thick films of YBCO and BSCCO were fabricated by applying a high-viscosity slurry made by mixing superconducting powder with an organic solvent. A dispersant was used to deflocculate particles and enhance rheological properties. The slurry was then painted on an Ag substrate and dried at 60°C for 4 h. The specimens were subsequently fired at high temperature and characterized by scanning electron microscopy and X-ray diffraction.

BSCCO has the advantage of a low melting temperature (885°C), which allows formation of dense films. High-density YBCO films are difficult to achieve because sintering temperatures cannot exceed the melting point of Ag. Experimentally, it was determined that the maximum sintering temperature for YBCO on Ag substrates was 930°C.

The BSCCO compound was prepared via solid state reaction using bismuth nitrate, strontium and calcium carbonate, and copper oxide. It was observed that the best films were heated above the melting temperature and then held slightly below the melting temperature for several hours. The final coating thicknesses were about 80 μm.

In addition to the high-T_c phases, impurity phases were always present in BSCCO specimens. For compositions heated above the melting point, a highly oriented structure was observed from X-ray diffraction patterns. The c-axis of the crystal lattice was found to be perpendicular to the plane of the thick film. Scanning electron microscopy revealed a platelike morphology of grains oriented parallel to the substrate plane.

Critical current density was measured as a function of sintering temperature for BSCCO. The best J_c value of 80 A/cm^2 was measured for a specimen sintered at 910°C. A parallel resistance model was used to determine the resistivity of BSCCO films above the J_c value. Ag plates up to 15 cm in diameter were coated with BSCCO thick films, and the microwave surface resistance was measured between 2 and 30 GHz. Details of the measurement technique have been published in a recent paper by Bohn et al. (1989).

Progress is being made on the densification of YBCO films on Ag substrates. Processing in low oxygen partial pressures promotes the densification process. Scanning electron microscopy has revealed that sintering temperatures as low as 885°C produce dense films. X-ray diffraction indicates that the film becomes more oriented as the sintering temperature is increased to 930°C. Future work on YBCO films will include quantifying their orientation and their electrical properties.

2.2.5 Electrical Contacts

The application of high-T_c ceramic superconductors in useful devices requires that some form of contact be made to the ceramic for electrical continuity, for support, and/or for stabilization. The key performance criteria for these types of composite structures dictate that the interfaces be adherent and have an interfacial electrical resistivity of less than about 10^{-6} Ω cm^2. For YBCO superconductors, reaction upon contact with common metals can cause the reduction of CuO in the orthorhombic YBCO to produce the semiconducting tetragonal phase. As a result of this transformation, the bonded interface becomes semiconducting and, consequently, has a high resistance at low temperature. In addition to solving this phase stability problem, bonding technology must be developed that

lends itself to implementation in large-scale production of a variety of practical embodiments. The objective of this task is to develop and test procedures for the preparation of suitable metallic interconnects to high-T_c ceramic materials.

The primary focus of this work over the past year has been on the testing of methods for bonding flat surfaces of high-density (in the range from 75 to 85% of theoretical density) pressed pellets of YBCO to copper or aluminum. Two techniques have been employed to accomplish this bonding. In one technique, thermocompressive diffusion is employed to join Cu to YBCO using several different bonding foils. (Aluminum was not bonded in this manner but probably can be.) The second technique involves ultrasonic bonding. Both Cu and Al have been bonded to YBCO by the ultrasonic method using two different types of bonding foils. In the thermocompressive bonding method, attachment of Cu to YBCO using indium has produced tensile strengths in excess of 900 lb/in.^{2} with interfacial resistivities (contact resistivity per contact) as low as 5×10^{-7} Ω cm^2. In very preliminary work, ultrasonic bonding of Cu to YBCO has produced bonds with a tensile strength of approximately 140 lb/in.^{2} and interfacial resistivities on the order of 10^{-4} Ω cm^2.

The key features of the thermocompressive process include special surface treatment procedures and the application by sputtering of a thin (several hundred angstroms to one micron) layer of Ag to the surfaces of the YBCO specimen. This layer not only promotes adhesion to the In bonding foil at temperatures $\leq$120°C, but also provides a buffer layer that protects the YBCO material from losing oxygen to the In foil.

In forming the contact between the Ag-sputtered YBCO and the Cu, the problem becomes one of finding suitable materials that will bond to both the Ag layer and Cu at a low enough temperature so that diffusion of the bonding agent through the entire thickness of the Ag barrier cannot occur. From the phase diagrams of the Cu-In and Ag-In systems, it is clear that in nearly pure Ag and Cu, solid solutions can be formed with In, whereas low-melting alloys of In are formed with low concentrations of Ag and Cu. In addition to pure In, several alloy systems with In were investigated as bonding agents. Among the first were two different concentrations of gallium (2% and 7%) in indium. These were chosen because of gallium's wetting ability and low melting temperature. With the 2% alloy used between Cu end pieces, the tensile strength was judged too poor even though the contact resistivity was 5.45×10^{-7} Ω cm^2 at liquid nitrogen temperature (LN). Both alloys were brittle and difficult to compress into usable foils. In spite of this, a sample with only the 2% Ga alloy between Cu blanks was prepared. Heating this sample under pressure in the usual compressive fixture at 130°C caused the contact resistivity to rise from 2.79×10^{-5} Ω cm^2 at room temperature (RT) and 6.6×10^{-6} Ω cm^2 at LN after 14.5 h of heat treatment to 3.84×10^{-5} Ω cm^2 at RT and 1.59×10^{-5} Ω cm^2 at LN after a total of 50 h of treatment. These values were approximately constant over the next 50 h. The tensile strength of this sample after 100 h was 144 lb/in.^{2}. Because of the problems cited above, the In-Ga system was not investigated further.

Alloy 13 (60% In, 40% Pb) and Alloy 14 (25% In, 75% Bi) were also prepared. Although both alloys produced bonds of sufficient strength that resistivity measurements were possible, samples containing both of these alloys shattered when slowly immersed in liquid nitrogen. This system also was judged to be unsuitable for further work. Alloy 12 (75% In, 25% Tin), however, is a soft, ductile, bright alloy that can be rolled. With only the

alloy between two Cu blanks, contact resistivity fell with increasing time. In one series of tests, resistivity dropped from 9.82 x 10^{-6} Ω cm^2 at RT and 1.05 x 10^{-5} Ω cm^2 at LN after 14.5 h of heat treatment to 1.87 x 10^{-6} Ω cm^2 at RT and 5.70 x 10^{-7} Ω cm^2 at LN after 100 h of treatment. When Ag-coated YBCO was sandwiched between Cu blanks and bonded using Alloy 12, contact resistivity tended to increase to higher values than those listed above, possibly due to increased interaction of In or Sn with the YBCO surface. Nonetheless, resistivities were sufficiently low and tensile strength measurements encouraging enough that Alloy 12 was included with pure In in a more extensive series of bonding parameter studies described later in this report.

Three alloy systems without In were tested for bond-forming properties (all percentage values are on a weight basis): Wood's metal (49.12% Bi, 24.5% Pb, 12.0% Sn, 12.24% Cd), Alloy 10 (50% Bi, 25% Sn, 25% Pb), and Alloy 11 (88% Pb, 12% Sn). Although superficial attachment appeared to take place in some experiments, true diffusion bonding was not observed. Pure Ga applied as a thin film to the YBCO and Cu gave some adhesion between two pieces of Cu, but no bonding interaction of Ga occurred with an Ag-coated YBCO surface. Work on these systems was abandoned at this stage because of lack of promise for all of the non-indium-containing foils and films.

The most recent laboratory studies of the thermocompressive bonding process have focused on optimization of the bonding parameters to (1) minimize bonding time, bonding temperature, and the as-bonded interfacial electrical resistivity; (2) maximize bond adhesive strength; and (3) maintain adhesion strength during temperature cycling from room temperature to 77 K.

Excellent bonding has been achieved with In and In_3Sn foils using processing temperatures in the 75 to 120°C range for 16 h. For comparison purposes, baseline strength and resistivity values were determined using samples with either pure In or the In_3Sn alloy between Cu blanks. Such samples exhibit tensile strengths of more than 1000 lb/$in.^2$ for the pure In and more than 500 lb/$in.^2$ for the alloy. In general, samples having lower interfacial resistivities give higher tensile strengths, indicating that increased diffusion bonding at the Cu/foil interface decreases the resistivity at that interface. Typical contact resistivities for In in the Cu/In/Cu arrangement are about 1 x 10^{-5} Ω cm^2 at RT and <1 x 10^{-5} Ω cm^2 at LN. The interfacial resistivities for In_3Sn baseline samples were not significantly different from these values. Again, for the most recent samples with silvered YBCO and In bonding foil, interfacial resistivity is about 1 x 10^{-4} Ω cm^2 at RT and <1 x 10^{-5}-Ω cm^2 at LN. With In_3Sn as bonding foil for silvered YBCO, interfacial resistivities are only slightly higher. Typical tensile strengths are 700 to 1000 lb/$in.^2$ for In bonds and 400 to 500 lb/$in.^2$ for In_3Sn bonds.

Several more observations can be made. Samples pressure-bonded under identical conditions except for temperature show lower tensile strengths at 75°C than at 100 or 120°C. Tensile strength seems little affected whether the pellet is high- or low-density YBCO. Vapor-deposited Ag that has not been annealed seems to give slightly better resistivities than are achieved for Ag-sputtered samples, but the tensile strengths of the vapor-deposited samples are considerably lower. And finally, increasing the thickness of the Ag-sputtered coating seems to reduce the interfacial resistivity. Thin, pure-Ag foils used as a bonding agent on an Ag-sputtered YBCO pellet failed to produce a satisfactory

bond between Cu and the silvered YBCO. Thickly sputtered Ag (>>1 micron) has a tendency to peel away from the surface of the YBCO.

The maximum processing pressure (i.e., at the start of bonding) is approximately 1800 lb/in.^{2}. With the use of a heatable press, it was found that in a normal heating sequence the pressure initially drops from the starting pressure but then increases by several hundred pounds per square inch over the initial starting pressure before again dropping as the In presumably begins to extrude.

Samples of YBCO containing 10 to 20 vol.% of uniformly distributed particulate Ag exhibit better performance in terms of interfacial resistivity, but are about the same as pure YBCO in terms of tensile strength. Information has been developed on the relationships between bonding time, bonding temperature, and interfacial resistivity. Of significance in all of this work is the fact that no failures have been experienced in cyclic RT $\leftrightarrow$ LN (77 K) tests with In- or In-Sn-bonded assemblies, which is attributed at least in part to the softness of In metal and the In-Sn alloy. As pointed out earlier, such failures were experienced in related studies of bonding foils composed of mixtures of Bi, Sn, and Pb.

Measurements of the superconducting properties of In-bonded Cu/YBCO assemblies have shown that the thermocompressive bonding process does not degrade either the critical temperature or critical-current-carrying capability of the YBCO samples. The thermocompressive bonding process is at the stage where tensile strengths of the bonded sample are approaching the ultimate tensile strength of the bonding foil itself. Achievement of this goal puts thermocompressive bonding in a position where both near-term application (e.g., for making contacts and stabilizing/supporting flat high-T_c embodiments) and adaptation to manufacturing operations are possible.

The second method that has been explored for the bonding of metals to high-T_c ceramics is ultrasonic welding. Using the facilities of STAPLA Ultrasonics Corp., ANL researchers have investigated the utility of that firm's ultrasonic welding machines for bonding YBCO and Bi-Ca-Sr-Cu oxide superconductors to thin Cu and Al sheets. In these tests, sandwich-type stacks, such as Cu-In foil/Ag-coated YBCO/In foil/Cu, were placed between the horn and anvil of the ultrasonic welder and energy was pulsed through the stack for fractions of a second. Preliminary tests show that bonds of fair quality ($\leq$150 lb/in.^{2} tensile strength and interfacial resistivities $<10^{-4}$ Ω cm^2) were achieved for interfaces where the Ag deposit was only 0.6 μm thick. An order of magnitude decrease could be obtained by increasing the thickness of the Ag coating. Although Cu could not be bonded directly to Ag-coated YBCO in our initial attempts, success has been achieved by STAPLA in joining Cu wire to other ceramics using a proprietary process. Aluminum was not tried in this latter mode.

In addition to the above work, attempts have been made to bond 12-gauge Cu wire to YBCO rings using the thermocompressive technique. Two different procedures were employed. In the first, the flattened Cu wire is clamped by a removable C-clamp to a piece of In positioned over an Ag-sputtered area. In the second, the Cu wire forms one-half of a clamp, which is placed over the In foil-covered, Ag-sputtered area. For this latter method, a backing plate of Cu is placed on the underside of the ring and is bolted to the copper connector. Both methods have produced adherent contacts. The levels of current carried

by these assemblies turned out to be limited by the critical current properties of the YBCO rings, not the thermocompressively bonded contacts.

Bonding by a thermocompressive method has been accomplished between 28-gauge Ag or Au wire and thin YBCO films that were ion-beam-deposited on MgO. The thin film is masked and sputtered with Ag, after which In is placed on the sputtered areas and the wires attached by small C-clamps. Such four-point attachments have exhibited very stable behavior of the recorded voltages in preliminary studies.

References for Section 2.2

U. Balachandran, et al., Proc. 3rd Annual Conf. on Superconductivity and Applications, Buffalo, NY (Sept. 1989, in press).

C. L. Bohn, et al., Appl. Phys. Lett. 55, 304 (1989).

S. E. Dorris, et al., Jpn. J. Appl. Phys. *28*, L1415 (1989).

T. Hikata, K. Sato, and H. Hitotsuyanagi, Jpn. J. Appl. Phys. *28*, L82 (1989).

H. J. Leu, J. P. Singh, S. E. Dorris, and R. B. Poeppel, Supercond. Sci. Tech. 2, 311 (1989).

K. Osamura, T. Takayama, and S. Ochiai, Supercond. Sci. Tech. 2, 111 (1989).

R. B. Poeppel et al., J. Met. *41*[1], 11 (1989).

D. Shi and K. C. Goretta, Mater. Lett. 7, 428 (1989).

D. Shi, et al., Mater. Lett. 9, 1 (1989).

J. P. Singh, et al., J. Appl. Phys. 66, 3154 (1989).

R. S. Roth, K. L. Davis, and J. R. Dennis, Adv. Ceram. Mater. 2, 303 (1988).

R.B. Stephens, Cryogenics 29, 399 (1989).

2.3 Properties of Bulk Superconductors

2.3.1 Characterization Methods

Ceramic superconductor products in the form of wires, spiral and helical coils, rings, tubes, bars, coupons, thick films, and composites are characterized to guide improvement of chemical formulations and forming and processing procedures. Product properties of primary interest are the values of the transport critical current density (J_c) and the effects of applied magnetic fields on J_c; these properties are evaluated. Closely related to J_c tests are recently initiated studies of persistent currents in superconducting ceramic rings. Results of examinations for structural defects in products, of measurements of the critical temperature (T_c) and diamagnetic response, and of tests of bulk properties of the materials prior to firing also support the materials development.

2.3.2 Critical Current Density Tests and Results

J_c tests have been performed on an average of 125 new samples each month during the reporting period. These tests were done at 77 K, with standard four-point resistance technique, direct current, a 1 μV/cm J_c criterion, and no externally applied magnetic field. Selected samples were subjected to additional tests, as described below. Most frequently, the J_c values were on the order of 100 A/cm^2, with a trend toward values of several hundred A/cm^2 in the YBCO and Bi-based compounds. The highest values produced in bulk samples at ANL have been in small-diameter extruded wires of YBCO: 1350 A/cm^2 in 0.21-mm-dia. wire and recently 1140 A/cm^2 in 0.48-mm-dia. wire. The high value to date for 0.72-mm-dia. wire in a coil was 250 A/cm^2. A sector of a YBCO ring of 0.1–cm^2 cross-sectional area displayed a J_c value of 360 A/cm^2. Tapes of YBCO containing silver powder or flakes and having thicknesses near 0.5 mm have displayed values of 500 to 1000 A/cm^2.

Arrangements have been made to measure J_c of a small number of selected samples at 4.2 and 35 K. In-house cryogenic facilities will be employed when their availability permits.

The appropriateness of the assumption of a uniform distribution of current over the cross-sectional area of the material in samples such as wires and tubes in deriving J_c values of YBCO superconductors was studied by comparing the performance of rods against that of tubes of the same outer diameter. Sample rods and tubes of the same material batches were produced especially for the experiment and were processed together, with the aim of providing identical materials in the sample pairs. The results of J_c tests of the samples at 77 K are shown in Figs. 12a and 12b. The most straightforward interpretation was that the uniform-current assumption closely applies for these materials.

To demonstrate that the J_c of a YBCO wire at 77 K is unaffected by the proximity of unpowered YBCO, a 1-mm-dia. wire of the superconductor was tested apart from a 5.1-mm-OD, 3.5-mm-ID tube sample of the same material and then within the unpowered tube. The wire's J_c (109 A/cm^2) was the same, within 1%, under the two conditions.

J_c tests of flat ring sections having 0.1 cm^2 cross-sectional area have required currents as high as 36 A. The problem of contact heating was mitigated by the use of low-resistance contacts developed by Maroni et al. The contacts were made by sputtering silver on the areas where contacts were desired on the ceramic rings and then bonding a copper

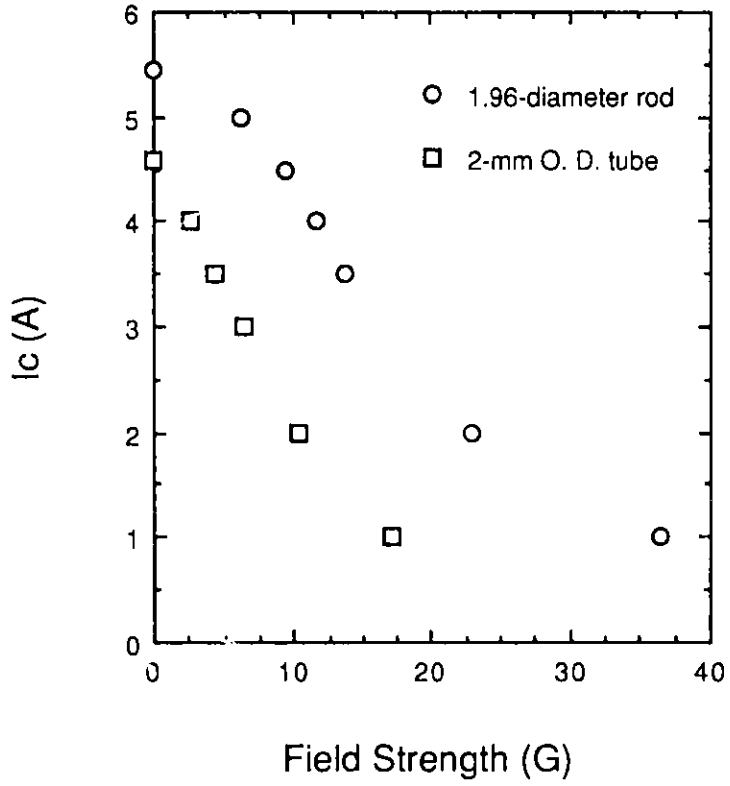

Fig. 12a. J_c versus Applied Field for YBCO Rods and Tubes of Same Outer Diameters.

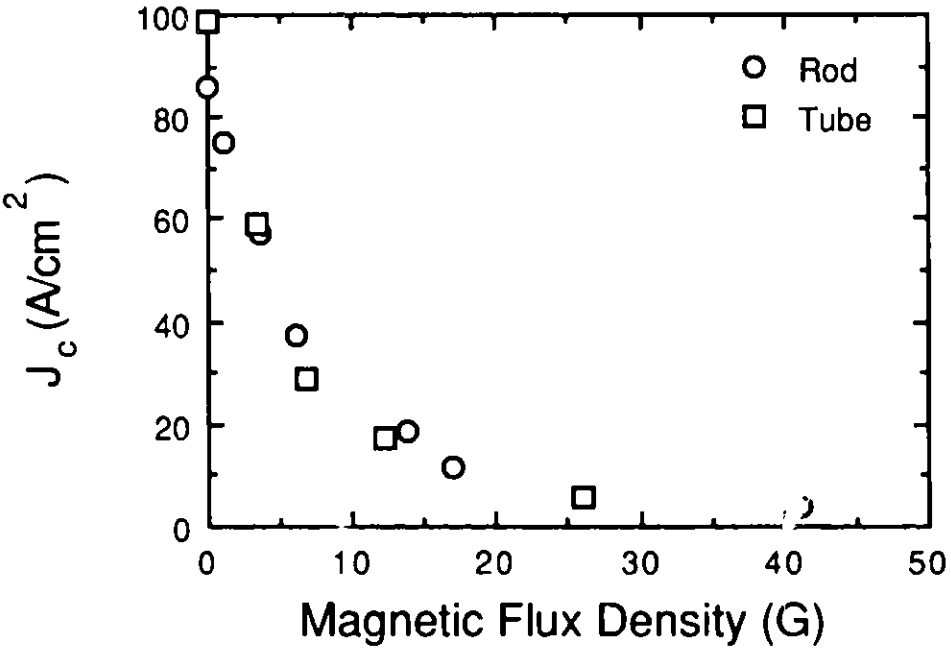

Fig. 12b. J_c versus Flux Density for YBCO Rods and Tubes of Same Outer Diameters.

conductor to each area by In foil held under pressure overnight at 120°C. The contact resistance coefficient at 77 K was as low as 0.0025 Ωcm^2 on YBCO and much lower on YBCO + silver.

J_c tests were used to monitor thermal shock damage to YBCO samples and to demonstrate the resistance to impairment by stress of YBCO containing silver. In preliminary work, the effect on a YBCO sample wire of multiple quenching cycles from room temperature to 77 K was briefly tested; J_c was substantially degraded, as shown in Fig. 13. In a similar test of YBCO containing silver at a reported concentration of 30 wt.%, the J_c (180 A/cm^2) was not impaired. When the latter material at 77 K was stressed to near its fracture strength in bending under three-point loading, the J_c was not significantly affected. More recently, the experiments were repeated with well-characterized samples produced especially for these tests. The results were the same, except that the effect of thermal shock on the unmodified YBCO was much lower. It was concluded that batch-to-batch differences are important in the response of the unmodified, polycrystalline YBCO products to thermal shock.

The effect of externally imposed magnetic fields on the J_c values of the bulk superconductors was found for selected specimens (see Fig. 14). It may be seen that as the external field is increased from zero, the reduction of J_c is approximately linear until a reduction of about 50% has resulted. The near-linearity has been used as a characteristic to aid the determination of zero-field J_c values of difficult samples: high currents that can produce excessive heating at contact areas were avoided by extrapolating to zero field the results measured with lower currents in low fields. It is encouraging to note that the rate of the fractional reduction of J_c with increasing field strength differs among samples of the same material type: the possibility is suggested that material less susceptible to the field effect can be developed. Similarly, the results from samples that differ in material type are promising: Fig. 15 shows that the fractional reductions of J_c in externally applied fields differ greatly among the various compositions tested.

Evaluation of critical currents in relatively high applied fields has been requested by designers of magnet systems. An electromagnet that produces magnetic field intensities up to 1.2 T in a gap suitable for testing 1.5-mm-diam wires has been added to our facilities, and the acquisition of an in-house 1-T electromagnet having a 25-mm gap is being arranged.

A ferromagnetic C-form core having an adjustable gap size has been provided by Reliance Electric Co. in cooperative work on ceramic superconductor coils for possible use in electric motors. Extruded coils of 25-mm ID and having about 30 turns of the ceramic wire have been produced for testing on the core. Coils constructed of YBCO + silver ring sections connected by low-resistance, normal contacts will also be tested on the core. The goal is to achieve practical field strengths in the gap by the use of a coil with <1% of the resistivity of copper at 77 K.

An experiment was conducted to demonstrate that the J_c value of a ceramic superconductor can be enhanced somewhat by cancellation of the self-field. A copper wire was inserted through the bore of a sample of YBCO tubing, and the tubing was subjected to the J_c test procedure with zero current in the wire. The J_c value was then redetermined with direct current flowing in the wire and adjusted sequentially to various values in each of the

Fig. 13. J_c Change Caused by Immersion in Liquid Nitrogen.

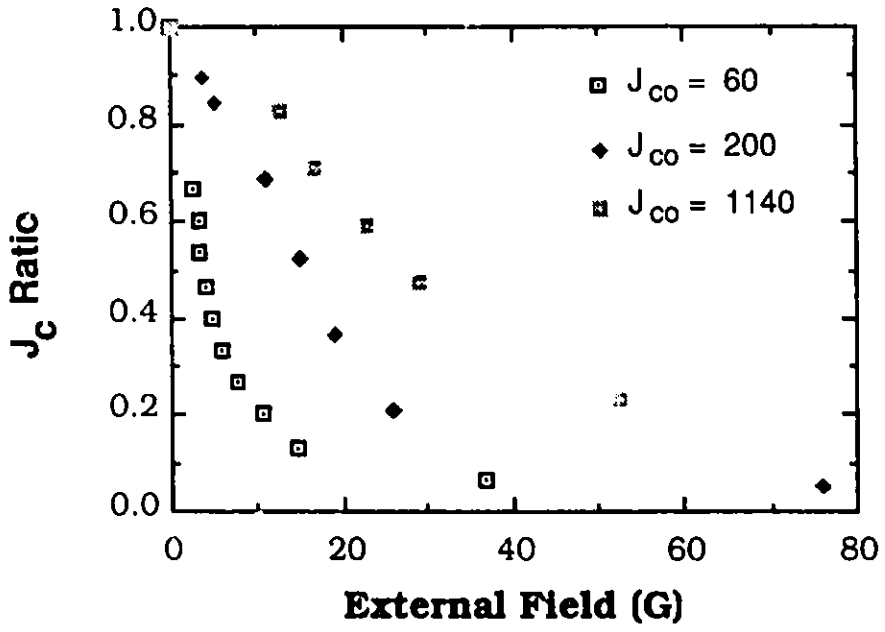

Fig. 14. Effect of External Field on J_c of Three YBCO Wires.

two possible flow directions. The results are shown in Fig. 16. The J_c of the tube was enhanced when its magnetic self-field was cancelled by the field of the wire and was diminished from the maximum when there was a net field of either polarity. In addition to demonstrating the enhancement effect, the experiment illustrated the feasibility of reducing the J_c-limiting effects of self-fields in power transfer lines made of the ceramic superconductor, not by the experimental configuration, but by geometrically commingling the outgoing and incoming leads; their self-fields will tend to cancel rather than reinforce one another.

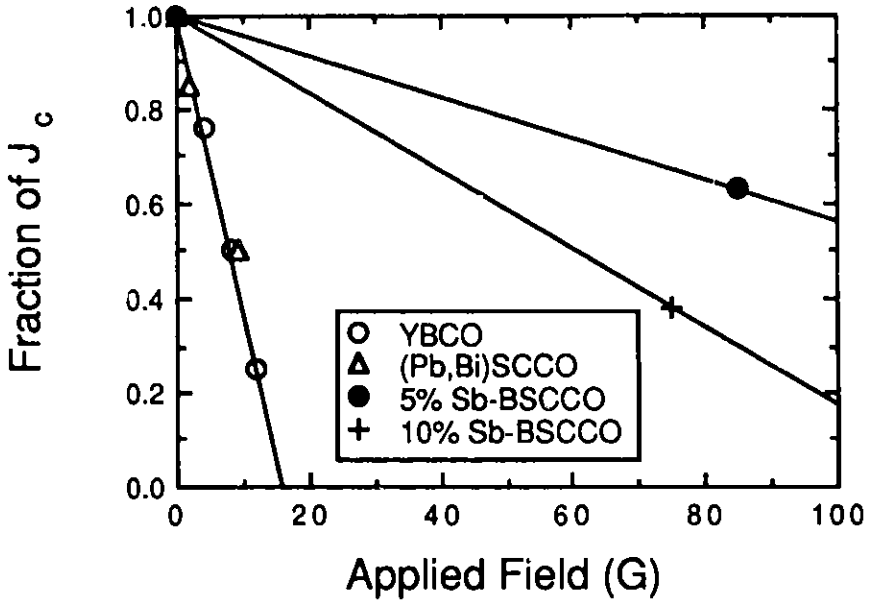

Fig. 15. Field Dependence of J_c.

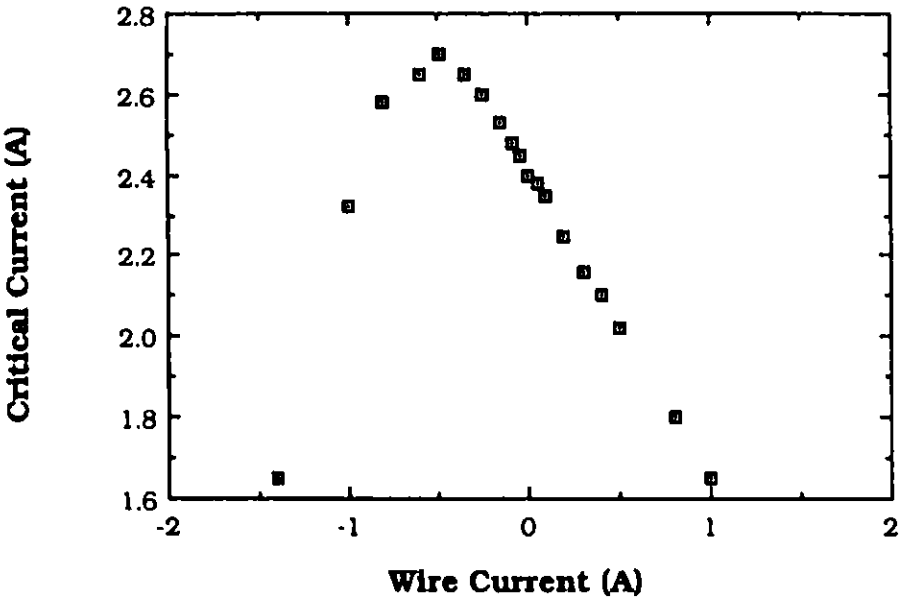

Fig. 16. Enhancement of J_c through Magnetic Field Interaction with Self-field of YBCO.

2.3.3 Persistent Current Tests

The electrical resistance of YBCO and YBCO + silver materials produced at ANL was studied with a measurement sensitivity much greater than has been possible with the conventional technique. Persistent currents were induced in rings fabricated from the superconductors, and the decay of the magnetic field produced by the current was monitored as a function of time. At 77 K in rings of 35-mm OD, 25-mm ID, and 2-mm thickness, fields consistent with circulating currents of up to 34 A were observed to persist

with very small percentage rates of decay over periods of tens of minutes and to decay more gradually with extended time. The derived resistivity values were $<6 \times 10^{-14}$ Ω cm for both YBCO and YBCO + 15% Ag in the current/field conditions persisting after the initial 5 min of decay. A 44–G field was observed at the center of a stack of 15 rings operating in the persistent mode. When the stack was installed on the Reliance core (see above) and a current was induced in the rings, a persistent field of >200 G, exclusive of the remnant field of the core, was sustained in a 3.7–mm gap of 24–mm diameter.

2.3.4 Detection of Structural Defects

The presence and locations of any relatively large structural defects in the products, particularly in coils, can be detected readily using the unique electrical behavior of superconductors at the onset of normal conduction. At the conclusion of a J_c test, one of the microvoltmeter contacts is lifted from the sample and attached to a probe. The sample current is then adjusted to a value about 10-20% higher than the critical current found for the sample as a whole, and the probe is used to scan the voltage gradient in the sample at 77 K. If the critical current is limited by a singular defect or zone, a major step in the gradient will be found at the limiting site. For some of the coil samples tested in this way, it was found that J_c of the whole coil was limited by defects near the ends of the coil and that the more central turns displayed a greater value.

Several such coils have been examined by microfocus X-ray technique to find the nature of the structural defects (voids, cracks, or inclusions). Typical defects are shown in Fig. 17. The alignment of cracks from turn to turn suggests that a seam in the coil-winding form may have produced the conditions for crack initiation. More generally, the results suggest that the cause of defects can be subtle. Thus, either greater care in the forming process or a formulation less susceptible to cracking is needed. This X-ray technique, as well as a direct film-contact technique, is being used to evaluate the progress of formulation and process improvements.

2.3.5 Evaluation of Magnetic Repulsion Force/Hysteresis

Certain potential applications of ceramic superconductors, e.g., in diamagnetic bearings or in the levitation of vehicles, would utilize the magnetic repulsion effect, rather than transport current properties. Quantification of the repulsion available from the ceramicproducts, particularly those in coupon form, serves the materials development effort for such applications and also provides a basis for application designs.

Results of measurements of the magnetic repulsion force of YBCO powders and block-form products at 77 K showed that the repulsion performances of the blocks could be correlated with those of the powders from which the blocks (identically pressed, sintered, and oxygen-annealed) were made. It may thus be possible to reject unsatisfactory material at the powder stage and improve manufacturing efficiency. The repulsion force of small pellets also may be tested to evaluate aspects of the processing procedures prior to the making of larger objects.

In the procedure established for Meissner-force measurements, a 5–mm thick, 12.7–mm diam, 3–kg permanent disk magnet is held parallel to the faces of the ceramic superconductor sample being tested. The opposite faces of the disk magnet form the two

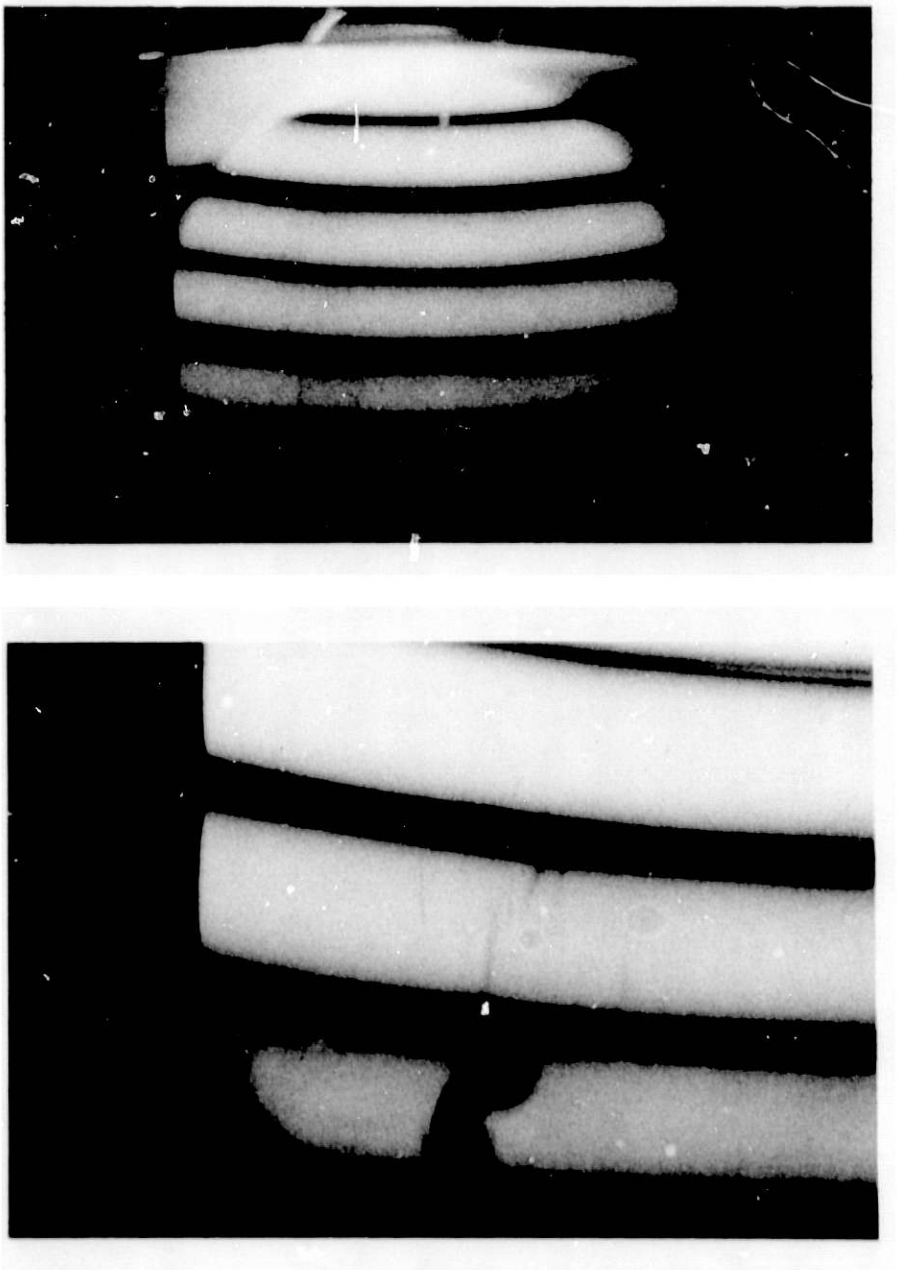

Fig. 17. Cracks and Fracture in YBCO Coil Revealed by Radiography after Firing (photos courtesy of W. Ellingson, ANL).

magnetic poles. The ceramic sample, typically much larger than the magnet, is held at 77 K and the magnet is moved toward and away from the surface. A balance is used to measure the repelling force as a function of the distance. An example of recent results from the most highly repelling YBCO disk measured to date is shown in Fig. 18. The repelling force is greater during the approach than during the retreat, an effect of induced flux retained by the sample. For some YBCO samples made by earlier techniques, the net force became slightly attractive during the retreat before going to zero at a large distance. At present the quality of samples made for repulsion applications is rated in proportion to the repelling force near contact and inversely to the amount of hysteresis.

A method of dissipating a remnant field in YBCO while maintaining the repulsion field was successfully tested. The remnant field effects were removed by the application of an AC field of somewhat greater intensity than that of the small remnant field.

In initial tests, the transport J_c values of samples did not correlate well with repulsion behavior. While their relationships to transport properties remain unclear, the repulsion measurement results seem likely to reflect bulk properties important to the transport performance.

2.3.6 T_c Test Facility

A T_c test facility has been provided to supplement the existing computerized facilities. The new probe incorporates a temperature sensor that can be installed directly on the sample, thus avoiding errors due to temperature gradients in the probe. The instrumentation can determine T_c in the range of 77-300 K and provide analog signals for recording. Adaptation to digital processing of data is planned.

2.3.7 Monitoring Viscosity Effects

Viscosity effects in the plasticized ceramic material used in the extrusion of superconductor wires and tubes are monitored during the process of mixing before extrusion. Instrumentation was constructed to monitor and record the values of the current drawn by the mixer motor as the mixture is adjusted by the addition of plasticizer and solvent or by the vacuum extraction of solvent during mixing. The monitor has been used to operationally quantify the effects in order to enable reproducibility among batches or verify that desired amounts of adjustment have been made to the highly viscous material. Plans have been made to fabricate a long capillary fitting for use with the extrusion press to allow standard measurements of the viscosity of the material being extruded.

2.3.8 Mechanical Properties

2.3.8.1 Ag additions

For most practical applications of high-T_c superconductors, both good superconducting properties (T_c, H_{c2}, and J_c) and mechanical properties (strength and fracture toughness) are desirable. It has been observed that YBCO is generally very brittle with unacceptably low strength (Crabtree et al.,1987; Cook et al., 1987). This problem is compounded by generally limited J_c values for these materials (Ekin, 1987). In view of

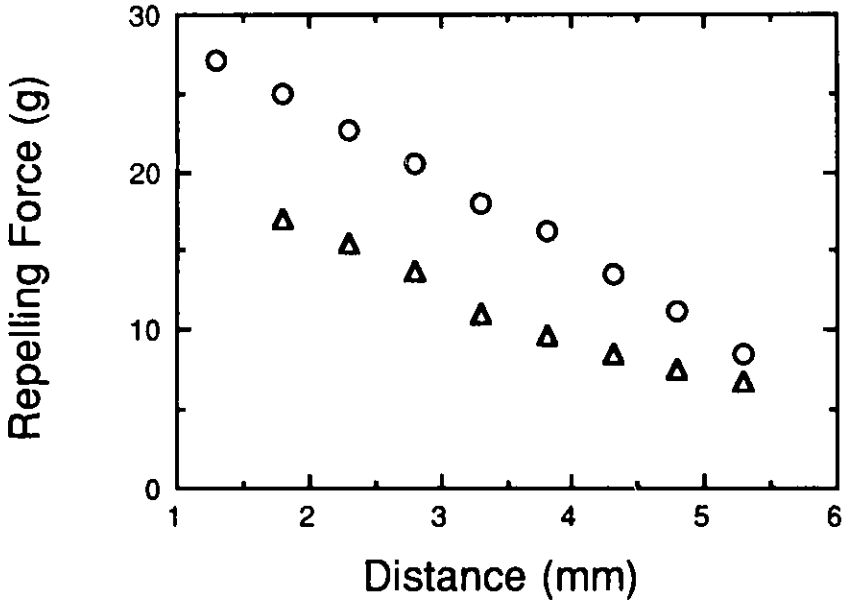

Fig. 18. Force versus Distance for YBCO Disk and Rare-earth Magnet.

these problems, effort has been directed toward improving the microstructure of YBCO to obtain both high J_c and improved mechanical properties. In a recent paper (Singh et al., 1989), it was reported that the addition of Ag powder to YBCO has greatly improved the flexibility of YBCO tapes without adversely affecting their superconducting properties. The effort at ANL has been directed toward improving both the mechanical properties and the critical current density of YBCO by understanding and optimizing the microstructure through process control. Specifically, a study was initiated in 1988 to develop and optimize composite microstructures of YBCO with Ag or Ag_2O additions, in order to obtain improved properties. Some of the results obtained in this study were included in the 1988 annual report (Poeppel, 1989). In the present report, measurements of the mechanical and superconducting properties of rectangular bars, thin tapes, and wires of YBCO and its composites with Ag or Ag_2O are presented. The correlations of these properties with microstructure will be discussed.

The YBCO powder was made by solid-state reaction of the constituent oxides Y_2O_3, CuO, and BaO, as described previously (Poeppel, 1989). The Ag and Ag_2O powder had a particle size (as indicated by the supplier) in the range of 2 to 3.5 μm. The YBCO powder and the composites with Ag or Ag_2O powder were used to make rectangular bars and thin tapes. The bars (5.1 x 0.6 x 0.3 cm) were uniaxially pressed in a steel die at 150 MPa. Tape specimens were prepared by the doctor blade technique, which is fully described elsewhere (Poeppel, 1989). Small disks (2.54-cm dia.) were punched out from the tapes for mechanical tests.

Rectangular bars and small disks of thin tapes were sintered in flowing oxygen in the temperature range of 920-980°C, followed by a predetermined annealing treatment. The strength of the sintered bar was measured in a four-point bending mode, with a support span of 0.49 cm, a loading span of 0.95 cm, and a crosshead speed of 0.127 cm/min. The fracture toughness (K_{IC}) was measured by a single-edge notch-beam technique (Brown, Jr.,

et al., 1966), and the elastic modulus was measured by pulse-echo technique (Krautkrämer and Krautkrämer, 1966). The strength of the thin tapes was measured in a piston-on-three-ball biaxial mode (Wachtman et al., 1972). The diameters of the support circle and loaded area were 1.27 cm and 0.16 cm, respectively.

Rectangular bar specimens of YBCO, sintered 2 h at various temperatures had a density (ρ) range of 64% (at 910°C) to 98% (at 1000°C) theoretical. The grains were of the order of 5-7 μm. For the specimens sintered at 930°C, the J_c increased with increasing density. On the other hand, for the specimens sintered at temperatures higher than 930°C, the J_c values generally did not increase with increasing density. The J_c values for specimens sintered 2 h at temperatures ≥930°C remained approximately constant at 300 A/cm^2. It is believed that, at temperatures higher than 930°C, second phases may be formed around grains and that these second phases may be detrimental to current transport, thus limiting the J_c. Flexural strength was generally observed to increase with density, as shown in Fig. 19. The strength increased from 28 MPa at ρ = 64% to 62 MPa at ρ = 92%. A slight decrease in strength at higher density (≈95%) is believed to be due to the presence of microcracks at higher density. Similar observations have been made elsewhere (Alford et al., 1988). Correspondingly, the elastic modulus of the sintered specimens increased with increasing density, and an average value of 105 GPa was observed for ≈90% dense specimens (Fig. 20).

The mechanical property data presented above clearly indicate that the strength values of the sintered YBCO specimens are unacceptably low for practical applications. Densifying YBCO specimens at higher temperatures may result in less than optimum values of J_c because of the presence of undesirable second phases. Hence, there is a need for sintering these specimens to a relatively high density at low temperature, with improved microstructure to maintain both good J_c and strength. Because the addition of Ag does not degrade the superconducting properties of YBCO compounds (Singh et al., 1988a), various amounts of Ag or Ag_2O were added to YBCO to improve its sinterability and microstructure.

Rectangular bars of YBCO/Ag and YBCO/Ag_2O composites were sintered for 4 h in flowing O_2 at 930°C followed by 8 h annealing from 435-385°C. A typical microstructure of polished surface of a sintered YBCO + 15 vol.% Ag bar specimen is shown in Fig. 21. The Ag phase is randomly distributed in discrete globules. The density of the sintered specimens was observed to increase from 85 to 95% with addition of 20 or more vol.% Ag or Ag_2O. A density of ≈95% theoretical was obtained at 30 vol.% Ag content. The increase in density is believed to be due to the Ag acting as sintering aid. The grains of a YBCO + 20 vol.% Ag specimen were typically 15 μm in size. These grains are about twice as large as those for YBCO specimens without Ag addition. This increase in grain size is believed to be caused by the presence of a liquid phase as a result of Ag addition. A similar effect of densification was also observed for Ag_2O addition.

Figure 22 shows the effect of Ag or Ag oxide addition on the flexural strength of composite YBCO bar specimens. The strength was observed to increase with increasing Ag content; a value of ≈90 MPa was obtained at 30 wt.% Ag addition. The addition of 30 vol.% Ag resulted in an increase in elastic modulus from 75 to 117 GPa and an increase in the average value of hardness from 137 to 243 kg/mm^2. Similar increases were also obtained with Ag_2O additions. The 2.2-fold increase in strength, 1.5-fold increase in elastic modulus, and 1.8-fold increase in hardness are believed to result primarily from the

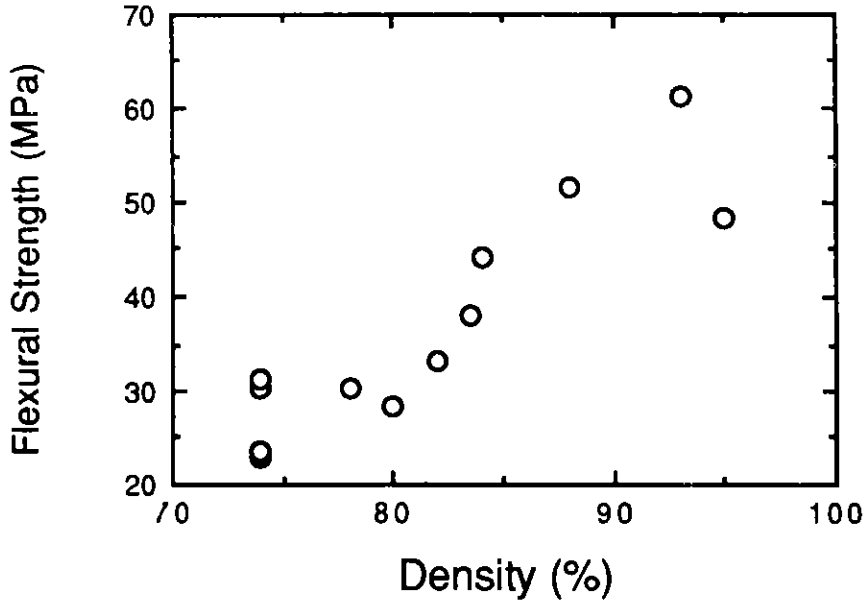

Fig. 19. Dependence of Flexural Strength on Density of Sintered Bars.

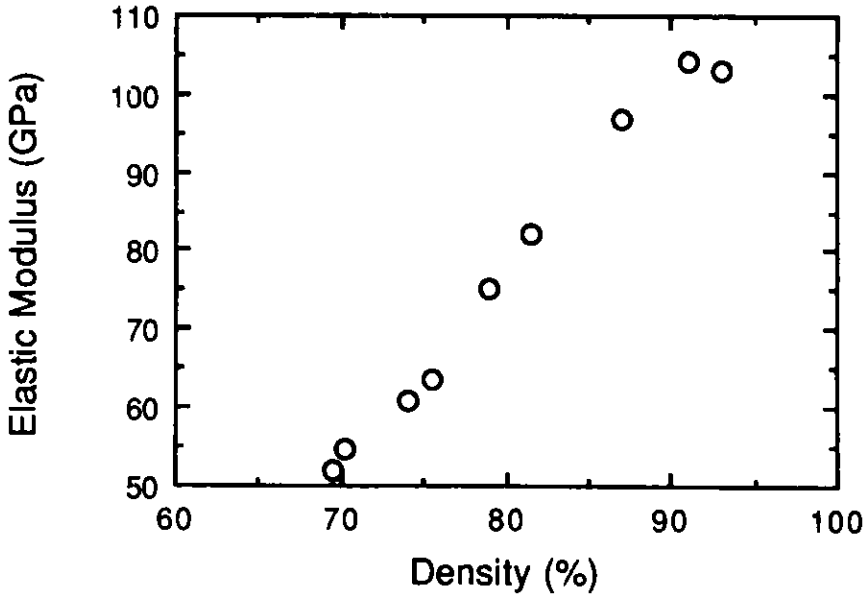

Fig. 20. Dependence of Elastic Modulus on Density of Sintered Bars.

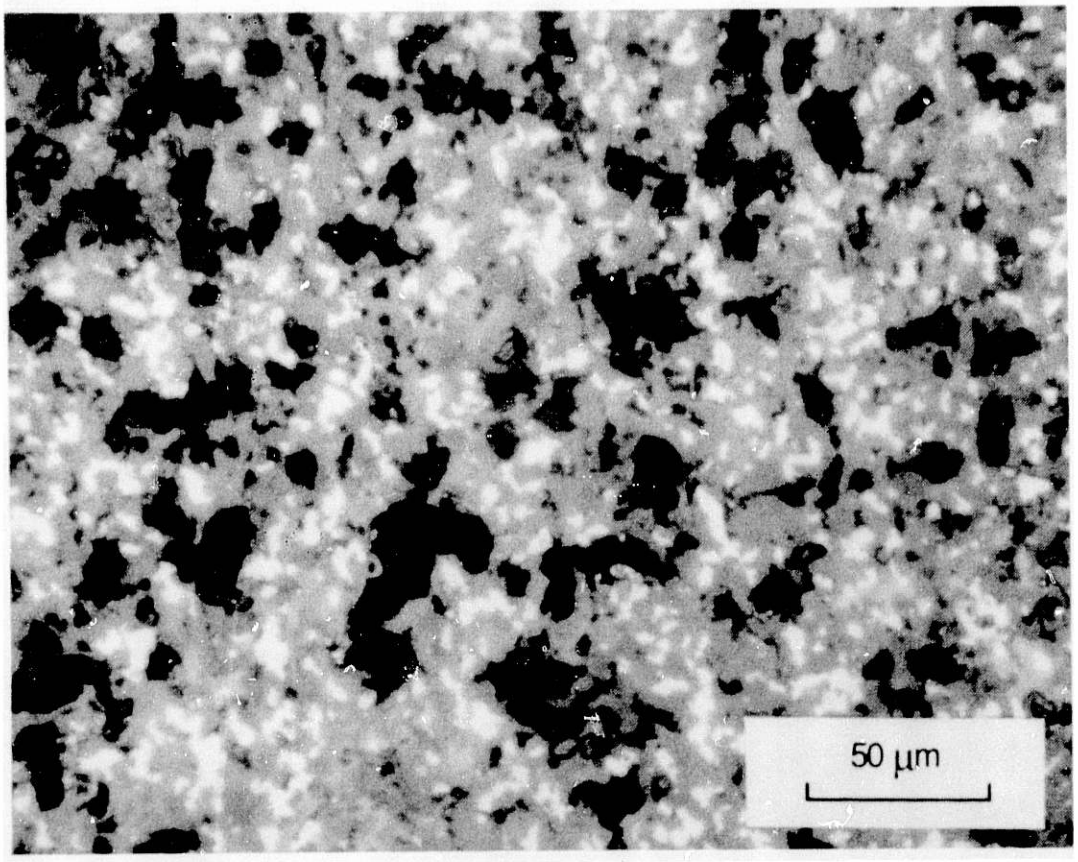

Fig. 21. Polished Surface of YBCO + 15 vol.% Ag.

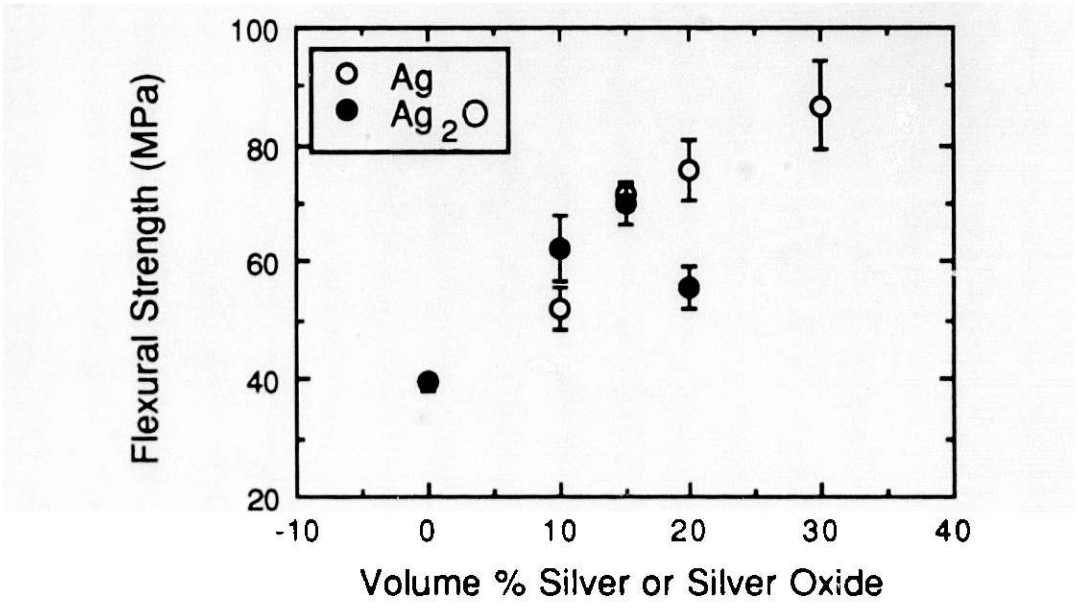

Fig. 22. Dependence of Flexural Strength of the Composite YBCO + Ag (Ag_2O) Bar Specimen on Ag (Ag_2O) Content.

increase in density of the YBCO specimen as a result of Ag or Ag_2O addition. Furthermore, these second-phase inclusions (Ag, Ag_2O) may also relax residual stresses resulting from the expansion anisotropy of grains and provide increased resistance to crack propagation by pinning the propagating crack and thus increasing the strength.

The average value of K_{IC} of the bar specimens increased from 0.95 to 1.40 MPa$\sqrt{m}$ with an addition of 15 vol.% Ag powder. The K_{IC} value for YBCO compares well with that obtained by Alford et al. (1988). It is to be noted that, although the strength and fracture toughness of YBCO specimens increase with Ag addition, the critical temperature for YBCO specimens was not adversely affected. The T_C was ≈88K for YBCO-Ag composite specimens, regardless of Ag content up to 30 vol.% tested in this study. The T_C drop encountered by Nishi et al. (1988), with 1% Ag addition in YBCO, was not observed in the present study, probably because less Ag actually entered the crystal structure of the YBCO. The excess Ag is likely to be better able to collect in single-phase regions. In addition, all T_C transitions were found to be relatively sharp. This supports past work (Chang, 1988), which hypothesized that the superconducting transition was sharpened by grain-boundary Ag improving the "weak link" between the grains. Ag doping also resulted in an order-of-magnitude decrease in room-temperature resistivity because of Ag's lower normal resistivity. Similar observations were made by Prasad et al. (1988) for a 60/40 YBCO and Ag composite. This result has important implications for applications involving conductor stability.

The J_c in zero applied field was also observed to increase with Ag addition. A 20 vol.% Ag addition resulted in a twofold increase (from 145 to 300 A/cm^2) in J_c value (Fig. 23). A similar increase in the J_c for specimen with 20% Ag_2O was also observed. In a related study, measurements made on a limited number of specimens in an applied field of up to 100 gauss indicate the J_c values of YBCO + 15% Ag composites were approximately twice the values for pure YBCO; this result suggests an additional beneficial effect of Ag additions to YBCO. It has been hypothesized that the increase in J_c value is probably caused by better contact between grains, resulting from the increase in density without forming undesirable grain-boundary phase due to a low-temperature sintering as a result of Ag addition. The present results suggest that addition of up to 20 vol.% Ag to YBCO can substantially improve its mechanical properties without degrading superconducting properties. However, for 30 vol.% Ag content, the J_c was markedly reduced, as shown in Fig. 23. The decrease in J_c value at 30 vol.% Ag content is believed to result from the presence of a continuous Ag phase, as well as the nonsuperconducting tetragonal phase at higher Ag content.

X-ray diffraction shows the presence of the tetragonal phase in YBCO with 30 vol.% Ag. The presence of the tetragonal phase was not detected by X-ray diffraction in YBCO + 20 vol.% Ag specimens. It was observed that the increase in density following Ag addition slows oxygen penetration into the sample, resulting in an oxygen-deficient structure (tetragonal) in the interior of the specimen. This hypothesis was substantiated by X-ray diffraction at various specimen depths. The specimen was ground to predetermined depths, and X-ray diffraction patterns were obtained at different depths. The X-ray patterns at different depths were used to estimate normalized lattice parameters c/a. Based on these values of c/a, the oxygen content was estimated from a lattice-parameter-vs.-oxygen-content plot constructed from the literature values (Goodenough et al., 1988; Manthiram et al., 1987). The distributions of the estimated value of oxygen content as a function of specimen depth for composites with different Ag/Ag_2O contents are shown in

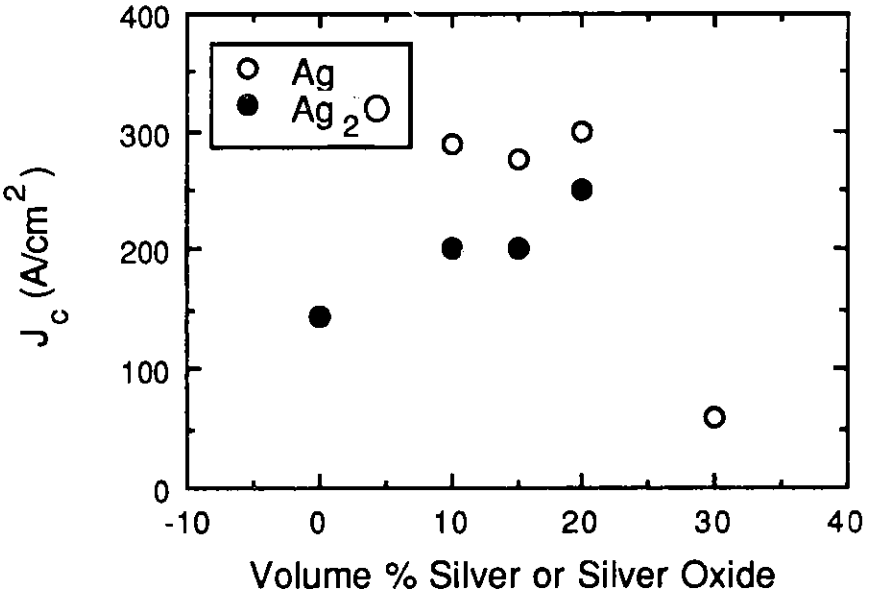

Fig. 23. J_c for YBCO + Ag (Ag_2O) Bars.

Fig. 24; oxygen content for composites with 20 vol.% of Ag or Ag_2O seems to be independent of depth. On the other hand, the oxygen content decreases rapidly with depth for the composite with 30 vol.% Ag.

These results suggest that a 30 vol.% Ag composite has an increasingly oxygen-deficient structure well below the surface, and that eventually a tetragonal phase appears. It is to be pointed out that the effects of internal microstresses were neglected in these analyses and therefore the exact values of the estimated oxygen content may change, depending on the extent of internal stresses. Although these analyses are based on simplified assumptions, the data clearly suggest a possibility of oxygen-deficient structure at greater depth in composites of YBCO with 30 vol.% Ag content, which may explain the drop in J_C for such composites.

To evaluate fabrication effects on mechanical and superconducting properties, a study was also conducted on selected composite tapes of YBCO with Ag addition. The influence of Ag on the properties of tape specimens were similar to those obtained for bar specimens. The T_C value of the YBCO tapes did not change with Ag addition and was measured to be ≈88 K. On the other hand, the J_C value increased from ≈150 A/cm^2 to ≈300 A/cm^2 with 15 vol.% Ag addition. Similar to results obtained for the bars, the biaxial strength of the thin composite tapes increased from 90 MPa to 120 MPa as a result of a 10 vol.% Ag addition. Although the variation of strength as a function of Ag content for the composite tapes is similar to that of the bar specimens, the absolute values of strength for tapes were approximate 30% higher than those for bar specimens. The relatively higher values of strength for the tape is probably due to the reduced probability of obtaining a large critical flaw in tape specimens because of their reduced volume.

It is to be noted that due to grain anisotropy, large internal stresses may result in YBCO specimens. These stresses may cause subcritical growth of inherent flaws and hence degrade the long-term strength of the components made from YBCO. Therefore, an effort

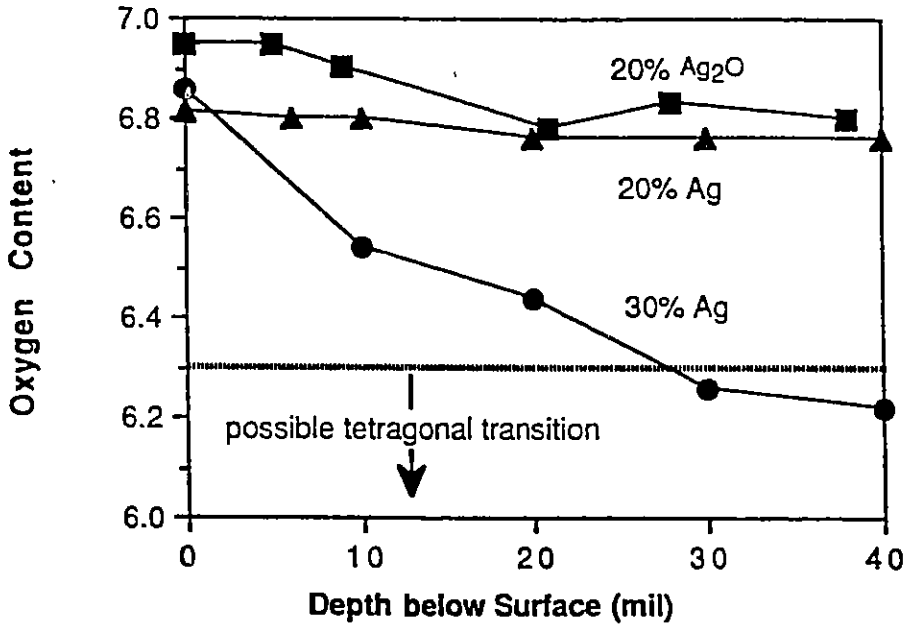

Fig. 24. Distribution of Oxygen across Cross Section of Specimen.

has been initiated to characterize the subcritical crack-growth behavior of YBCO in order to evaluate long-term mechanical behavior. Toward this end, the strength of YBCO tapes has been measured as a function of loading rate at room temperature in air. These tape specimens were sintered at 930°C for 2 h in flowing oxygen. The density of these specimens was approximately 95% theoretical. Initial results indicate that strength increases with loading rate. From a log-loading-rate/vs.-log-strength plot, a value of the subcritical crack-growth parameter, N, of ≈13 was estimated for YBCO tapes. This value of N suggests that the resistance to subcritical crack growth of these specimens is similar to that of soda-lime glasses. A limited number of tape specimens of YBCO were also made with 15 vol.% Ag addition. These tapes were sintered under identical conditions, as described earlier. For these YBCO + 15 vol.% Ag composite tapes, the value of the subcritical crack-growth parameter N as obtained from the measured dependence of strength on loading rate was calculated to be 26. The larger value of N for the composite tapes suggests an improvement in the resistance to subcritical crack growth as a result of Ag addition. A detailed evaluation of the subcritical crack-growth behavior of YBCO and its composites with Ag is currently in progress.

An evaluation of the correlations between microstructure and mechanical/superconducting properties of extruded wires with and without Ag/Ag_2O additions has been initiated in an effort to optimize processing parameters for extrusion. Initial results indicate substantial improvements in mechanical properties of extruded wires as a result of Ag addition. A flexural strength of ≈160 MPa has been obtained for 0.7-mm sintered extruded wires of YBCO with 15 vol.% Ag addition. A limited number of specimens with and without Ag additions were tested for their thermal shock resistance. The specimens were subjected to thermal shock by thermal cycling between room temperature and liquid nitrogen. Damage due to the thermal shock was estimated by measuring J_C of the specimens before and after each thermal cycle. The specimens were allowed to come to thermal equilibrium after each cycle. There was a continuous decrease

in J_c after the second cycle, and an approximate 35% drop in J_c value was observed after seven cycles for the specimens without Ag. The drop in J_{cc} is believed to be due to the formation of microcracks as a result of thermal cycling. On the other hand, no such degradation in J_c was observed for the specimens with 15 vol.% Ag. This observation suggests that Ag addition improves resistance to crack formation due to thermal shock. Although these results are preliminary, they suggest the potential for improvement in thermal shock resistance of YBCO as a result of Ag addition. Further detailed evaluation of the thermal shock resistance of YBCO and its composites with Ag is in progress.

2.3.8.2 ZrO_2 Additions

The mechanical properties of all high-temperature superconductors are poor. In particular, the fracture toughness (K_{IC} -- the ability of a material to resist fracture) is only about 1 MPa$\sqrt{m}$. Structural ceramics have values of 4 or more, and toughened ceramics can have K_{IC} values of up to 20 MPa$\sqrt{m}$. As described in the previous section, additions of particulate Ag improve K_{IC} appreciably. A second approach has recently been shown successful for improving K_{IC}. Additions of ZrO_2 toughen many ceramics (see, for example, Becher, 1986). ZrO_2 is not compatible with YBCO, however: the two compounds react to form $BaZrO_3$, and a semiconductor results (Goretta et al., 1990).

The problem of reaction between YBCO and ZrO_2 has been mitigated by additions of Y_2BaCuO_5 (211). The 211 phase is compatible with YBCO. A preliminary set of experiments have yielded the following: addition of 10 vol.% ZrO_2 improved the K_{IC} to 3 MPa$\sqrt{m}$, nearly triple the value of pure YBCO; by adding 3 vol.% 211 in addition to the ZrO_2, superconductivity is maintained (Goretta et al., 1990); T_c is reduced only 1-2 K, and systematic J_c measurements are pending.

Future work will concentrate on reducing the amount of 211 needed through use of 211 coatings on ZrO_2, on increasing K_{IC} further through optimized processing, and on determining effects of these additions on J_c.

2.3.8.3 Neutron Diffraction Studies

Since the discovery of superconducting materials with relatively high T_c values, there has been a considerable effort to understand the reason for the high T_c and to improve the mechanical properties (the latter has been a limiting factor for practical applications). The compounds have received considerable attention because of their high T_c and high upper critical magnetic field. Additions of Ag have recently been shown to improve mechanical properties (toughness and strength) of these compounds (Singh et al., 1989). Furthermore, addition of Ag can improve the conductive path between grains of superconducting YBCO and possibly help reduce the weak-link effect (Jin et al., 1989). Whereas the addition of a low-volume fraction of Ag does not adversely affect superconductivity, the introduction of transition metals to YBCO can be detrimental to superconducting properties. Also, the addition of Ag has a minimal effect on the stress-free lattice spacing. During fabrication of YBCO/Ag composites, differential thermal expansion upon cooling can lead to potentially troublesome residual stresses. Because the Ag contracts more than the YBCO, good bonding between the ceramic and silver could lead to tensile stresses in the silver and compressive stresses in the YBCO with relatively small percentages of Ag (Majumdar et al., 1988). These residual stresses could lead to premature failure of the composite, debonding of the YBCO

and Ag, and/or microcracking, all of which will affect the flow of superconducting current and the life expectancy of components made from this material. An understanding of the nature and magnitude of these stresses will help improve the design of these composites.

Neutron diffraction is a powerful method for measuring bulk residual strains, from which residual stresses can be calculated (Allen et al., 1985). Neutrons can provide a bulk measurement because they can penetrate deeper than X-rays. For the present work, the Intense Pulsed Neutron Source (IPNS) and the General Purpose Powder Diffractometer (GPPD) at ANL were used to measure the residual thermal strains in YBCO composites. The neutron diffraction measurements have been used to assess the (1) magnitude of the thermal residual tensile stresses in the Ag, (2) role of Ag in creating bulk stresses in the YBCO, (3) occurrence of yielding in the Ag, and (4) effect of variations in Ag content on the strain of the composite constituents and on the YBCO stoichiometry.

Samples to be examined were fabricated from a mixture of YBCO and Ag powders, using 0, 15, 20, and 30 vol.% Ag. The YBCO powder was made by solid-state reaction of the constituent oxides Y_2O_3, CuO, and BaO. Powders of Y_2O_3, CuO, and $BaCO_3$ were mixed in appropriate proportions and were wet-ball-milled for approximately 12 h. The dried powder was calcined at 890°C for 24 h and then crushed into fine powder; these procedures were repeated three times. After milling, the calcined powder had a measured average particle size of ≈5 μm. The phase composition of YBCO powder was confirmed by X-ray analysis. The composites of YBCO with Ag were made by mixing various amounts (10-30 vol.%) of Ag powder with YBCO powder. The Ag powder had a particle size range of 2-3.5 mm, as indicated by the supplier. Both the YBCO and composite powders were formed into rectangular bars (≈5.1 x 0.6 x 0.3 cm) by uniaxial pressing in a steel die at 150 MPa. Rectangular bars of composite YBCO/Ag were sintered in flowing O_2 at 930°C for 4 h and then annealed for 8 h from 435 to 385°C. Examination of polished surfaces of sintered YBCO/15% Ag bar specimens by SEM showed that the Ag phase was randomly distributed in discrete globules. Density of the sintered specimens was observed to increase with increasing Ag content. A density of 95% theoretical was obtained at 30 vol.% Ag content. This density increase probably occurs because the Ag acts as a sintering aid. Examination of the fracture surface of a sintered specimen of YBCO/20 vol.% Ag showed a typical grain size of 15 μm, which is about twice that of the YBCO specimens with no Ag addition. Resistivity was measured by a conventional four-probe technique, and critical current density values were determined with a criterion of 1.0 μV/cm at 77 K and zero magnetic field.

Thermal neutrons with velocities of up to 1000 m/s are of interest for neutron diffraction. At these energies, the wavelengths are on the order of the lattice spacing, and Bragg's Law of diffraction can be applied. In the experiments described here, Bragg's Law is used first to determine the lattice spacing d for a particular hkl reflection from both YBCO and Ag averaged over a volume of the strain-free powder. The stressed composite fabricated from these powders is examined next. The lattice strain associated with the hkl plane of a given phase in the composite is given by

$$\varepsilon = (d - d_0)/d_0 ,$$

where d_0 is the unstrained hkl spacing (powder) and d is the spacing for the composite.

Fast neutrons from the IPNS are moderated and produce beams at various instruments such as the GPPD, which is used for powder diffraction experiments. The GPPD is about 20 m from the target. Neutrons are detected with banks of ^{3}He proportional counters (140 total) encircling the sample chamber on a 1.5-m scattered flight path, at 20, 30, ±60, ±90, and ±148°C relative to the neutron forward direction. Lattice spacings can be measured to an accuracy of ±0.0002 Å. The main advantage of the pulsed source is that many diffraction peaks can be measured at the same time. Results reported here combine the data from the 90 and 148° detectors.

Figure 25 shows the average bulk strain at room temperature in the Ag as a function of volume percent Ag in the composite and the crystallographic direction. The Ag diffraction peaks for which data are presented are clearly isolated from the YBCO diffraction peaks. The potentially complex loads and the relatively large error in absolute measurement of strain makes it difficult to reach conclusions by comparing strains in various crystallographic directions. However, there is a trend toward decreasing Ag strain as Ag volume fraction increases (the relative error in strain between samples of varying Ag content is about half the uncertainty in the absolute values). The strain, however, is expected to be proportional to the difference between the thermal expansion coefficient of Ag and that of the composite (which increases with increasing Ag) (Selsing, 1961). The difference between the thermal expansion coefficients of Ag and YBCO is about 2 x 10^{-6}/°C. An increase in Ag content from 15 to 30 vol.% should increase the composite coefficient of expansion by about 2%. The observed decrease in strain is much larger than can be explained by the ≈2% change in thermal expansion coefficient. It is possible that the strain is relieved by creep, microcracking, or yielding of the Ag. Analysis of the diffraction peak full-width-at-half-maximum (FWHM) shows insignificant broadening, which is consistent with little or no yielding. The Ag hydrostatic stress calculated from the strain values and the Ag bulk modulus ranges from 130 ± 65 MPa for 30% Ag to 229 ± 65 MPa for 15% Ag. These relatively low values also support the conclusion that no yielding of the Ag occurs. Another possible explanation for the low strain in the 30% Ag material is that the Ag content is so large that it is not surrounded by enough YBCO to keep the Ag in tension. If this were true, the YBCO would not experience significant compressive stress, on the average.

Measuring strains in the YBCO is difficult because the stoichiometry can change with Ag content. Thus the shifts in YBCO diffraction peaks may not be solely the result of strain. Figure 26 shows the change in the diffraction pattern with Ag content for several Ag and YBCO peaks. The pattern for the 30% Ag composite is clearly different from the others and indicates a nearly tetragonal structure. Destructive analysis, combined with X-ray diffraction analysis of sections of a 30% Ag sample, shows that the stoichiometry for the 30% sample changes gradually from $\delta = 0.1$ at the outer surface (orthorhombic superconducting phase) to $\delta \approx 0.8$ near the center of the specimen (nonsuperconducting tetragonal phase). This finding is consistent with the observation that the 30% Ag sample shows a dramatic decrease in critical current density compared with samples with 0, 15, and 20% Ag content.

Because the lattice spacings for the three principal directions of YBCO are known as a function of stoichiometry, it is possible to estimate the diffraction peak shift resulting from strain (for some diffraction lines) by correcting for stoichiometry. For example, because the

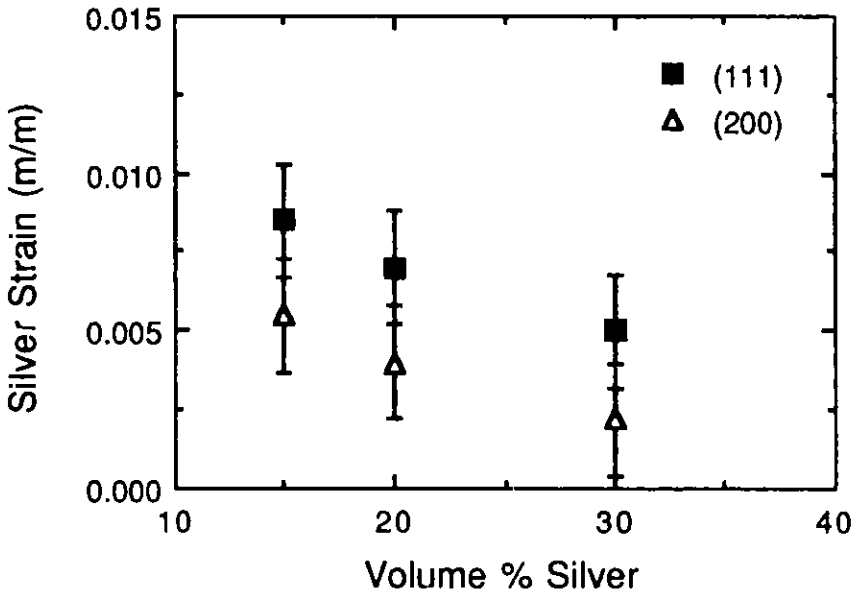

Fig. 25. Room-temperature Tensile Strain in Ag as Function of Ag Content and Crystallographic Orientation (90–148° average).

(111) diffraction peak is a single peak and the shifts are unambiguous, we can predict the change in the spacing of the (111) plane as a function of stoichiometry from the relationship

$$1/d_{111}^2 = 1/a^2 + 1/b^2 + 1/c^2,$$

where the values of a, b, and c as a function of d are determined by neutron diffraction (Jorgensen, 1989). The value of d for YBCO in the present composites was estimated by comparing relationships that are primarily due to stoichiometry rather than strain with those of materials with known δ (Fig. 27). We have assumed that the addition of 15% Ag does not significantly change the YBCO stoichiometry. The stoichiometry of the 30% Ag sample is assumed to be nearly tetragonal (bulk average), and the 20% Ag sample is assumed to be intermediate in stoichiometry between 15 and 30% Ag samples (Shaked, 1989). These assumptions are consistent with Fig. 27. The lattice parameter is predicted to increase as the stoichiometry approaches the tetragonal phase (with increasing Ag content). Experimentally, however, the spacing for the (111) planes decreases as the Ag content increases from 15% to 20%, indicating an average compressive stress in the YBCO (Fig. 28). This result is in qualitative agreement with expectations, because the Ag strain is tensile. At 30% Ag, the difference between measured and stress-free lattice spacing indicates negligible YBCO strain. This finding is consistent with the low strain measured for Ag in the YBCO/30% Ag composite and is probably a result of creep of the composite.

We have shown that neutron diffraction techniques can be applied to YBCO composites to measure residual strains in the constituent parts caused by differential thermal contraction after fabrication, as well as to determine the effect of Ag on stoichiometry (and thus on critical current density). We have observed residual tensile strains in Ag as a function of crystallographic direction; these strains range from as high as 0.085% in 15 and 20% Ag

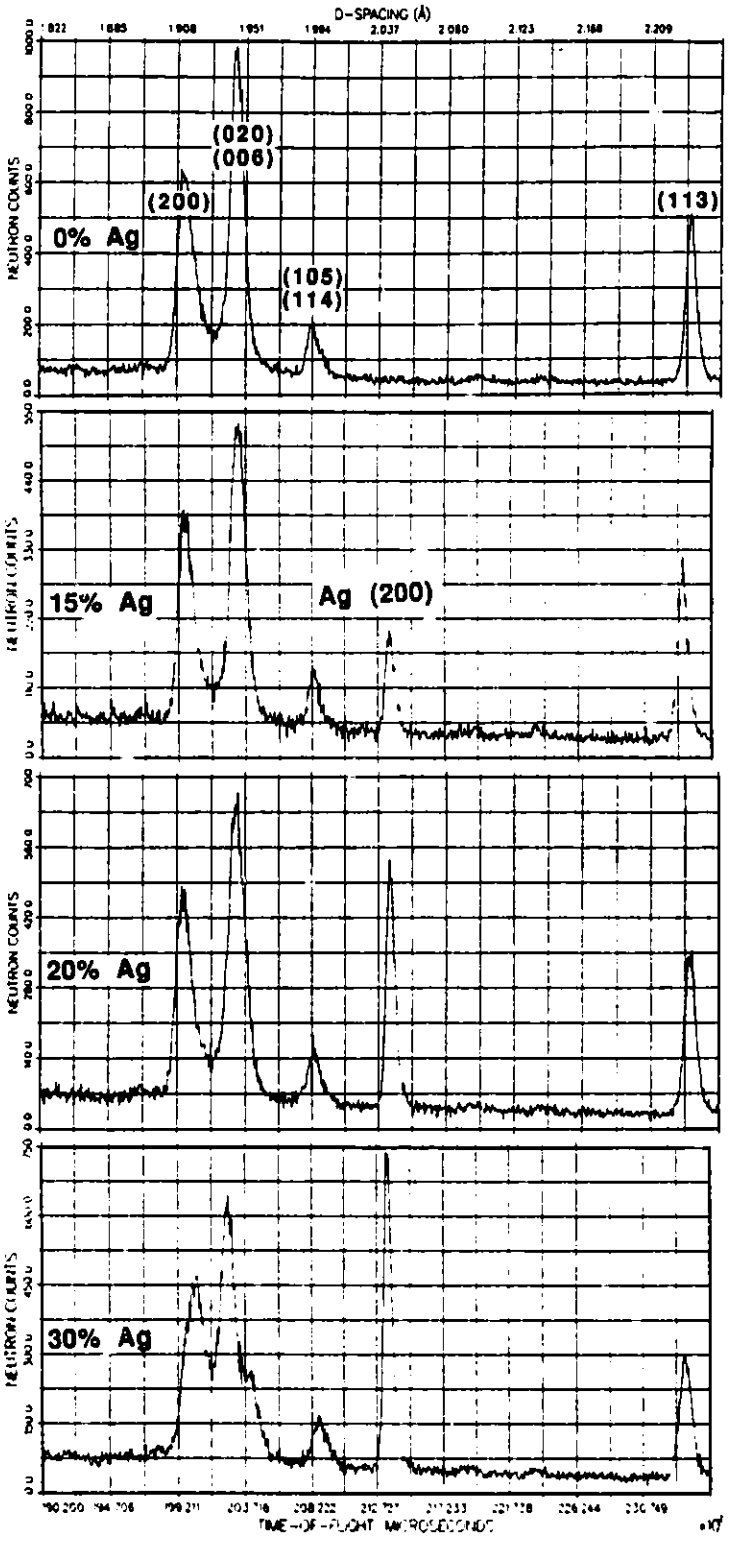

YBCO/Ag

Fig. 26. Neutron Diffraction Spectrum as Ag in YBCO Varies from 0 to 30 vol.%; the YBCO (200), (020)/(006), (105)/(114), and (113) and the Ag (200) Lines Are Shown.

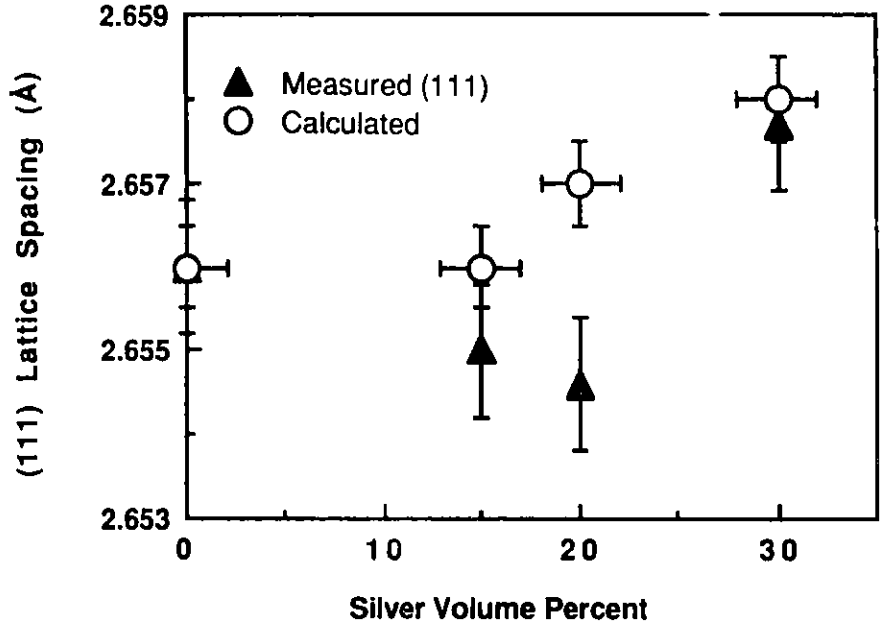

Fig. 27. Calculated and Measured Lattice Spacing for YBCO (111) Plane as Function of Stoichiometry.

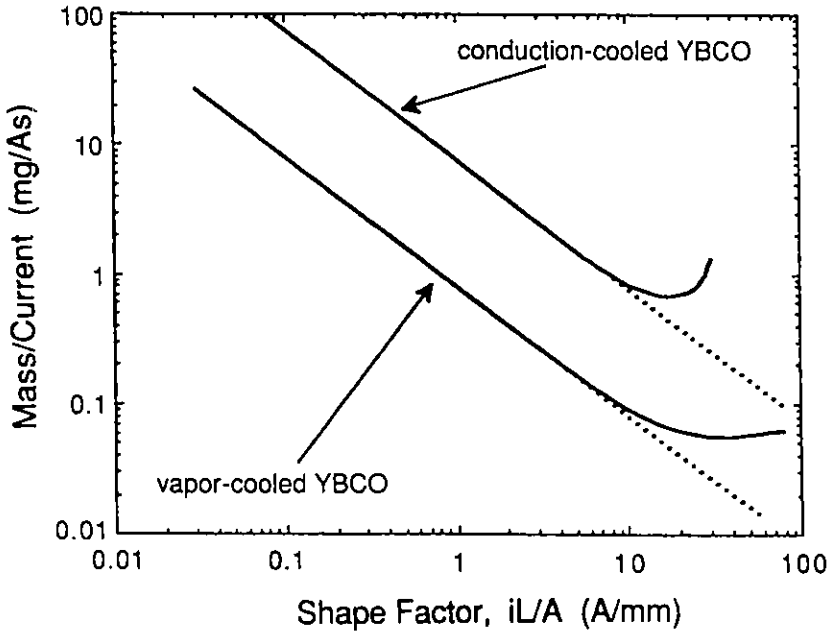

Fig. 28. Helium Flow Rate Generated by YBCO Current Lead.

samples to as low as about 0.02% in a 30% Ag sample. Compressive strains in the YBCO (111) crystallographic direction were estimated by correcting for the diffraction peak shift due to changes in stoichiometry with Ag content. The estimated compressive-strain values vary from 0.04% (15% Ag) to 0.09% (20% Ag) to 0.01% (30% Ag), with an uncertainty of about 0.03%. The decrease in strain in YBCO is consistent with the decrease in Ag strain and may be due to variation in creep properties of the composite, which are sensitive to

stoichiometry. The presence of significant average tensile strain in the Ag, particularly for 15 and 20% Ag samples, indicates good interface bonding between the YBCO and the Ag.

Strains were also measured at liquid nitrogen temperatures, and only small changes were detected. The absence of any relaxation of strain suggests that little or no cracking occurred as the temperature was lowered to the superconducting transition point.

2.3.9 Acknowledgments

The authors wish to thank J. D. Jorgensen, H. Shaked, and J. Faber, Jr., for helpful discussions, and B. Tani for X-ray diffraction data. This work has benefited from the use of the Intense Pulsed Neutron Source at Argonne National Laboratory.

References for Section 2.3

N. Alford, et al., Brit. Ceram. Proc. *40*, 149 (1988).

A. J. Allen, M. T. Hutchings, and C. G. Windsor, Advances in Physics *34*, 445 (1985).

P. F. Becher, Acta Metall. *34*, 1885 (1986).

W. F. Brown, Jr., and J. E. Srawley, American Society for Testing and Materials Special Technical Publication No. 410, 13 (ASTM, Philadelphia, PA, 1966).

Chin-An Chang, Appl. Phys. Lett. *52*, 927 (1988).

R. F. Cook, T. M. Shaw, and P. R. Duncombe, Adv. Ceram. Mater. *2*, 606 (1987).

G. W. Crabtree, et al., Adv. Ceram. Mater. *2* (3B), 444 (1987).

J. W. Ekin, Adv. Ceram. Mater. *2* (3B), 586 (1987).

J. B. Goodenough and A. Manthiram, Intern. J. of Modern Phys., *B*, *2*, 379 (1988).

K. C. Goretta, et al., J. Mater. Sci. Lett., in press, 1990.

S. Jin, et al., Appl. Phys. Lett. *52*, 2074 (1988).

J. D. Jorgensen, Argonne National Laboratory (private communication, 1989).

J. Krautkrämer and H. Krautkrämer, Ultrasonic Testing of Materials, Springer-Verlag, New York (1983).

S. Majumdar, D. Kupperman, and J. P. Singh, J. Am. Ceram. Soc. *71*, 858 (1988).

A. Manthiram, et al., J. Am. Chem. Soc., *109*, 8886 (1987).

Y. Nishi, S. Moriya, and S. Tokunaga, J. Mater. Sci. Lett. *7*, 596 (1988).

R. B. Poeppel, Practical Superconductor Development for Electrical Power Applications, Annual Report for FY 1988, Argonne National Laboratory Report ANL-88-37 (1989).

Ram Prasad, et al., Mater. Lett. *7* (1-2) 9 (1988).

J. Selsing, J. Am. Ceram. Soc. *44*, 419 (1961).

H. Shaked, Argonne National Laboratory (private communication, 1989).

J. P. Singh, et al., Mater. Lett. *7*, 72 (1988).

J. P. Singh, et al., J. Appl. Phys. *66*, 3154 (1989).

J. P. Singh, D. Shi, and D. Capone II, Appl. Phys. Lett. *53*, 237 (1988).

J. B. Wachtman, Jr., W. Capps, and J. Mandel, J. Mater. *7*, 188 (1972).

2.4 Thin Films

Practical superconductors must carry high current densities reliably. For high-T_c superconductors, thin films alone have demonstrated this potential. Developing practical superconductors with thin film coatings has been addressed extensively for the case of NbN, which also has far superior superconducting properties when made by thin-film techniques. The solutions to many of the problems have been at least partially solved, and the road to commercialization has begun in several areas. In particular, we have experience in sputter-coating fine filaments and tapes for potential use as high-current, high-field conductors. Such techniques could be extended to high-T_c superconductors after some additional thin film development, but this is complicated by the need for a high formation temperature and the consequent problems of substrate interdiffusion and loss of the highly-volatile chemical species. This program addresses high-T_c film fabrication in a single-step deposition process that eliminates the necessity of a detrimental high-temperature annealing. This task is specifically aimed at the fabrication of such films using sputtering together with in-situ analysis techniques (such as X-ray or Raman scattering) to efficiently evaluate in-situ processing (such as pulsed laser annealing). Optical in-situ techniques have been chosen because of their compatibility with all forms of vapor deposition, including chemical vapor deposition, which has the advantage of the very high throughput that is desired for large-scale practical applications. This study concentrates on the Bi- and Tl-based high-T_c because they have been shown to be compatible with a wider variety of substrates, routinely grow with the preferred c-axis orientation, and do not produce insulating phases because of small deviations from stoichiometry. Progress has been made on transverse-section transmission electron microscopy (TEM) of thin-film high-T_c superconductors. The TEM work is in collaboration with TRW, Inc., while compositional analysis and processing studies are supported by the Argonne Pilot Center. The in-situ analysis is also funded by the National Science Foundation Science and Technology Center.

2.4.1 Technical Progress

2.4.1.1 Facilities

A new chamber for laser annealing and in-situ analysis of sputtered superconducting films has been completed. The excimer laser has been installed and tested by the factory representatives and has met specifications for the pulse energy using the ArF line at 193 nm. The necessary special UV mirrors, lenses, and windows to transmit this laser output into the chamber are also in place. Films are grown in a DC magnetron sputtering system equipped with a load-lock mechanism and turbomolecular and liquid nitrogen sorption pumps. A single-source composite target of the $Bi_2Sr_2CaCu_2O_x$ (BSCCO) superconductor has been installed and a three-target source has been built. The first in-situ analysis involves reflectivity with a He-Ne laser source, but there are provisions for X-ray and Raman scattering. An X-ray source, together with detectors for in-situ X-ray fluorescence and energy-dispersive Bragg scattering, are in the testing stages prior to mounting on the sputtering chamber. We have completed construction of a precision grinding rig that is expected to increase the yield of high-quality TEM samples.

2.4.1.2 Research

To obtain a baseline of the system operation, films of the Bi-based high-T_c superconductor were made at low substrate temperature in our sputtering system and subsequently annealed at high temperature. These were superconducting, with T_c between 65 and 70 K, but were considerably improved to T_c values of up to ≈80 K by additional anneals. An extensive study of film composition by energy-dispersive X-ray (EDS) has been undertaken, since this is such a convenient, nondestructive technique. The effects of film thickness and electron energy have been investigated to overcome the substrate effects on the quantitative analysis. Unannealed films were used to avoid the complications of possible loss of highly volatile elements during annealing. The results have been checked against ICP-AES and with the use of single crystals. Several approaches appear promising. With the use of only a low voltage of 15 keV, substrate effects are eliminated for films thicker than 500 nm. Another approach uses very high energies so that the film appears thin and uniformly excited. In either case, the usual analysis must be modified. Finally, the use of a low glancing angle of electron incidence reduces the substrate effects.

The pulsed excimer laser was used to process films during growth and after growth. The optical transmission of unannealed amorphous films relative to the annealed metallic films, which are opaque, provided a means of evaluating the processing procedure and was the motivation behind the in-situ reflectivity studies. The influence of peak laser power level was studied through measurements of the temperature-dependent resistivity and by optical and SEM observations. At high power, films irradiated during growth showed a Bi loss, while similar exposures onto completed, unannealed films caused island formation. Thus the laser may be improving adhesion of the film to substrate. In addition, at low powers, films irradiated during growth showed improved uniformity (when examined by optical analysis) and less segregation (when examined by SEM analysis). However, it was difficult to maintain a uniform and precise temperature rise by the pulsed laser when starting from low temperatures. The total energy reproducibility from pulse to pulse and spatial homogeneity was inadequate. It was thus felt necessary to start from an elevated substrate temperature to reduce the effects of laser pulse imhomogeneities.

Thin films of BSCCO were sputtered onto elevated temperature substrates using the composite target. Preliminary results on the temperature-dependent resistance of films made at ≈600°C indicate evidence of superconductivity onsets as high as 110 K *without the usual high-temperature annealing step.* X-rays showed crystalline structure of the 2212 phase, i.e., $Bi_2Sr_2CaCu_2O_X$. However, EDS analysis indicates reduced Bi for films made above ≈600°C, and virtually no Bi for >650°C. With a Bi-enriched target ($Bi_2SrCaCu_{1.6}O_X$), superconducting films of $Bi_2Sr_2CaCu_2O_X$ were sputtered in a one-step, in-situ process at a substrate temperature, T_s, of only ≈650°C, compared to the usual annealing temperature of ≈865°C. It was found to be imperative to slow-cool (5°C/min) the films in oxygen (400 mtorr) to obtain good superconducting properties. The best resistive transition is shown in Fig. 1; it extrapolates to zero at 56 K. There is a narrow temperature window for formation of the 2212 phase in-situ: for T_s <630°C, films are disordered and semiconducting, while for T_s >660°C they are insulating with severe Bi deficiency. X-ray diffraction indicates broad peaks of the $Bi_2Sr_2CaCu_2O_X$ phase with a high degree of orientation of the c-axis perpendicular to the substrate.

The exact mechanism by which crystallization occurs for the low-temperature, in-situ processing is not yet known, but we may speculate that for in-situ processing the surface atoms are less constrained and thus have a smaller barrier to overcome in forming the correct crystal structure. Atoms in the low-deposition-temperature amorphous films must overcome the barrier associated with the three-dimensional lattice of interconnected bonds.

Although this represents a considerable breakthrough, SEM analysis indicates that the films are not dramatically smoother and that some segregation into nonsuperconducting grains occurred. For example, there is significant segregation into Bi- or Cu-rich regions or the Ca-poor 2201 phase of BSCCO, and CaO and CuO have been found. In order to quantify the segregation, an SEM was used to provide microscopic compositional analysis through energy–dispersive X-rays (with a resolution of ~1 μm) and electron backscatter (with a resolution of ≈0.3 μm, but sensitivity only to average atomic number). The segregation clearly becomes worse with higher substrate temperature, although the smaller grain size found at lower temperatures, relative to the SEM resolution, may hide the extent of their segregation.

A series of films deposited at 200°C and annealed from 800 to 865°C also revealed increasing segregation with annealing temperature, but below 800°C there was no segregation. It was concluded that details of the in-situ processing are responsible for both the segregation and crystallization. We speculate that the enhanced surface mobility at 600-675°C allows nonsuperconducting compounds to nucleate and grow preferentially during film growth at a lower temperature than would be required for post-annealed films. However, it is also possible that the existence of surface energies for the in-situ processing can change the relative stability of the various possible phases in this complex five-component chemical/metallurgical system.

The critical current density, J_c, is of utmost importance for superconducting applications. We are addressing issues of flux pinning in high–T_c, both from the standpoint of improving J_c and to understand the reversible (poor-pinning) behavior found in magnetization measurements in even modest magnetic fields near T_c. An important issue is the relationship of the transport J_c to that determined by magnetization, together with a suitable criterion for defining each. We are in the process of evaluating each of these points.

An unusual loss mechanism has been commonly observed in high–T_c superconductors in a magnetic field near the zero-field transition temperature. This loss manifests itself as a current-independent resistance (for sufficiently low currents) that severely broadens the transition in an uncharacteristic manner. In conventional superconductors, magnetic fields shift the resistive transitions to lower temperatures with relatively small broadening, so the shift can be regarded as a measure of the upper critical field, H_{c2}. For high–T_c superconductors in a magnetic field, there is relatively little change in temperature of the initial drop of resistance, at T_c (onset), whereas after an initial decrease, the resistance appears to be activated, i.e., it increases approximately exponentially with inverse temperature. These effects are more dramatic in BSCCO and $Tl_2Ba_2CaCu_2O_x$ (TBCCO) materials but are also found in $YBa_2Cu_3O_7$ (YBCO). Additionally, magnetization measurements in YBCO single-crystals indicate that H_{c2} is larger than that determined from any extrapolation to zero resistance or even by using the resistive midpoints.

This unusual behavior has led many to suggest the existence of thermally activated magnetic flux creep, flux line melting, or another unknown loss mechanism. We have measured resistive transitions of highly c-axis-oriented TBCCO thin films as a function of field perpendicular to the c-axis, for the current *both perpendicular and parallel to the field.* The data for these orientations are essentially the same over a span of five orders of magnitude below the normal state resistance (just above T_c). Since the Lorentz force is zero for the current parallel to the magnetic field, it cannot play a role in this loss mechanism. This new insight has important implications for understanding discrepancies between magnetic and transport measurements in high-T_c superconductors and thus seriously questions any explanation of the losses based on magnetic flux motion.

Progress has been made on transverse-section transmission electron microscopy (TEM) of thin-film high-T_c superconductors. The work is done in collaboration with TRW, Inc., and the Argonne Pilot Center for Superconductivity. During this initial period, the work has focused on learning the techniques associated with cross-section sample preparation and their application to the films of interest. This effort has met with some success, yielding an electron-transparent sample for a film of TBCCO. Preliminary examination showed that the film consists of several phases. Semiquantitative energy-dispersive spectroscopy (EDS) showed that several regions were of similar composition, near 33Tl-30Ba-9.5Ca-27.5Cu (at.%), while other regions were approximately 50Tl-50Ca (at.%) and one region was essentially pure Ba. The oxygen content could not be determined since the detector used was protected by a Be-window which absorbed oxygen X-rays. No preferred orientation was observed for any of the phases. Further analysis will be carried out to establish the identity of the phases.

Planar TEM sections of BSCCO films were prepared following standard techniques involving grinding and ion milling from the back side of the substrate. Preliminary observations of these films indicated that the 2212 phase had grown in plates parallel to the substrate with the c-axis normal to the substrate surface, but no particular orientation between adjacent plates was observed. For example, a layered structure produced by overlapping plates is often evident while lattice fringes as well as moiré fringes are also observed. The lattice fringes have a spacing of ≈25Å and correspond to the b-axis supercell, while the moiré fringes are the result of a rotation between two plates. The spacing of the moiré fringes indicates a relative rotation of ≈18° about the c-axis. Second-phase particles in the form of rods were also observed. It is not yet clear how these particles form or what their influence may be on the growth or properties of the films.

As a part of the collaboration with TRW, Inc., we sputtered and annealed films of TBCCO on $LaAlO_3$ substrates provided by TRW. They in turn made successful superconducting quantum interference devices (SQUIDs), using the ability to isolate single grain boundaries by lithography, on these large-grained TBCCO films to provide the necessary localized weak link.

2.4.2 Status

2.4.2.1 Facilities

Several changes in the sputtering system are contemplated to better access the in-situ analyses techniques, better control the substrate position during deposition, and include

three metallic sputtering targets for better control of the stoichiometry of the films. The in-situ X-ray analysis equipment will be installed on the sputtering chamber after bench testing. The energy–dispersive X-ray fluorescence (EDXRF) detector will have a diamond window, allowing access to the very–low-energy characteristic X-ray for oxygen. At the same time, the three-target source will be installed. This combination will greatly enhance our ability to evaluate one-step, low-temperature processing of films of high T_c. In addition, a source of activated or atomic oxygen will be installed on the system. The value of ex-situ TEM evaluation of our sputtered films is becoming increasingly evident. We will continue to upgrade the sample preparation facilities to ensure the rapid and reliable production of electron-thin sections.

2.4.2.2 Research

X-rays can potentially provide at least three independent in-situ analyses on growing films. EDXRF gives the chemical composition (although oxygen can only be found with some difficulty) that is independent of the structure. Energy–dispersive Bragg scattering gives structural information, and near-edge adsorption can be determined on, e.g., the copper atoms for more detailed information on its chemical valence. *By working at a glancing angle of incidence, each of these probes can be sensitive to thin surface layers (perhaps 10 nm).* It seems that an ordinary 3–kW X-ray tube will suffice for all of these. For example, the Bi concentration can be continuously monitored by EDXRF during film growth, as a function of substrate temperature, and the sputter rate of the metallic Bi target can be changed to compensate. In addition, studying the oxygen concentration can evaluate activated oxygen sources directly. Finally, energy–dispersive Bragg scattering can be used in-situ to determine whether the correct high–T_c phase is growing.

Studies of one-step in-situ processing will continue by evaluating the effect of excimer laser pulses on the minimum substrate temperature for formation of the high–T_c phase. However, because the formation of the superconducting phase in-situ has such a narrow window for the substrate temperature, it will first be necessary to implement a scheme to more adequately measure and reproduce such temperatures. A study the dynamics of the laser annealing process through the effect of pulse duration is anticipated. If it is established that UV frequencies are required for annealing, the excimer laser may be used as an amplifier, driven by a dye laser with shorter pulse length. If lower light frequencies are acceptable, the excimer laser could act as a high-power pump for a dye laser at lower frequency. The key idea is to minimize the pulse length and consequent heating of the film, and especially the film/substrate interface, to avoid interdiffusion.

Our efforts to maximize J_c have focused on learning how to minimize the large spatial inhomogeneities in the film due to recrystallization and segregation. One of the crucial ex-situ analytical tools for studying J_c will be transverse-section TEM samples and their analysis. This will allow us to see the structural, and eventually compositional, cross-sections of films and to correlate them with J_c and the growth conditions. In particular, searches will be made for impurity phases that may precipitate out as "grain-like," poorly conducting boundaries. The occurrence of segregation during in-situ processing of high–T_c films will continue to be our most important initiative. We plan to study the effects of interfacial energies between the substrate and the various film phases, including impurities. The extent to which segregation is due to incorrect overall composition or to disproportionation will be established, and methods to overcome these potential problems

will be studied. The key point here is to eliminate such inhomogeneity in order to enhance and even make a meaningful measure of J_c.

A TEM study of transverse sections of BSCCO films grown in-situ has begun, and this research, including substrate and buffer-layer effects, will be addressed. Such analysis can lead to changes in preparation conditions to avoid segregation into bad regions and thus improve superconducting properties. Similar research on superconducting NbN films has been done here in the past.

In another approach to improving J_c, the introduction of fine-scale inhomogeneities as pinning centers will also be addressed. In these experiments, the transport J_c of high-T_c films will be measured before and after neutron irradiation. Such irradiation is known to produce localized damage cascades of ≈2.5 nm, i.e., very comparable to the superconducting coherence length and thus ideal for flux pinning. This effort will be done in collaboration with TRW, which will supply high-quality YBCO films made by sputtering, and possibly with Superconducting Technologies, Inc., which would supply TBCCO films made by laser ablation deposition.

The Lorentz force independence of the resistive losses at high temperature and field is an unexpected and provocative result. Our goal here is to determine the cause of this loss so that it can be eliminated or so that its effect on applications can be evaluated. As a first step to such an understanding, studies of conventional superconductors are needed to establish whether the phenomena is restricted to high T_c. We will study NbN, NbN/AlN multilayers (which will emulate the anisotropy of high-T_c Cu-O planes quite closely), and Nb. The results will help to pin down possible explanations and suggest experiments to verify them. The importance of understanding such losses cannot be overestimated for applications of high-T_c.

The collaboration with TRW to made high-T_c SQUIDs will continue. We will prepare films of BSCCO on appropriate substrates that TRW will pattern in devices and then test. In addition, we are beginning to study the YBCO films made by TRW and used in their present attempts to make engineered weak links for used in SQUIDs.

2.5 Applications

Current leads introduce heat into cryostats by thermal conduction and, if the leads are not superconducting, by Joule heating. It is desirable to minimize this heat input to reduce the amount of cryogenic fluid boiled off in an open system or to reduce the power consumption in a cryostat cooled by a closed-cycle refrigerator. Cryostat designers have been interested in optimization of current leads for some time, and several reviews are available (e.g., Buyanov, 1985). The discovery of high-T_c superconductors that remain superconducting at temperatures above the boiling point of nitrogen offers the potential to reduce current-lead heat flow into cryostats in a number of different applications that include space missions and superconducting magnetic energy storage systems. Advantage of high-T_c superconductivity can be taken by operating the superconducting part of the lead between 77 K and 4 K.

Several researchers have recognized that high-T_c superconductors have advantages in application to cryostat current leads, but have not performed detailed analyses (Mumford

1989; Matrone et al., 1989). Analysis performed at ANL (Hull 1989a, 1989b) indicates that presently available high-T_c materials are sufficient for most current lead applications, and low-loss current leads should be one of the first applications for the high-T_c superconductors. This indication of near-term application is generating increasing interest in a number of companies and laboratories involved in the commercialization of high-T_c materials.

Bulk high-T_c superconductors have yet to exhibit high current densities in strong magnetic fields and are unlikely to replace conventional superconductors in most magnet designs until they do. However, current leads can usually be placed in low magnetic fields, low current densities can be tolerated with thick leads, and the leads are relatively short. Thus, the leads should represent a small fraction of the total system cost and could be manufactured with relatively low-cost equipment. A number of fabrication techniques have already produced meter lengths of wires with current densities of 100 to 1000 A/cm^2 in magnetic fields of 1 to 5 mT at a temperature of 77 K. The magnetic field that can be tolerated increases as temperature decreases. Joints between high-T_c superconductors and normal conductors, such as copper, can now be routinely made with a surface resistivity lower than $10^{-10}\ \Omega\ m^2$ at 77 K. Ceramic high-T_c superconductors have extremely low thermal conductivities compared to those of metallic normal conductors or to low-T_c metallic superconductors. This gives the high-T_c materials additional advantages in applications where the leads experience a relatively low-duty cycle. Therefore, high-T_c superconductors that are manufacturable with present technology appear well suited for cryogenic current leads.

In the analysis of cryostat current leads, the product of electrical resistivity, ρ, and thermal conductivity, λ, integrated over the temperature range of operation, is the figure of merit in the design of cryostat current leads, with lower $\rho\lambda$ values resulting in lower cryogen boil-off. It is of interest to compare the $\rho\lambda$ product for high-T_c materials with that for pure metals. The most studied of the high-T_c materials is YBCO, for which reported values of ρ and λ vary significantly (with most of the variation attributed to differences in sample porosity). Thermal conductivity increases approximately as T^2 from very low values at low temperature, begins to level off below 10 K, reaches a maximum of 2 to 10 W/mK in the 40 to 50 K range, and flattens out to about 2 W/mK at temperatures above the critical value. The electrical behavior of YBCO is similar to that of metals. The normal-state resistivity of YBCO increases linearly with temperature above the critical temperature from a value of about $0.5 \times 10^{-6}\ \Omega m$ for single crystals and $1.5 \times 10^{-6}\ \Omega m$ for the best bulk polycrystalline samples, although values can be up to about 10 times higher in poorer-quality bulk samples. These thermophysical data suggest that performance of high-T_c leads, even if operated totally in the normal state, should be nearly as good as that of pure metal leads.

Most of the thermal conductivity measurements reported in the literature have been made on samples that exhibit significantly poorer critical current densities and normal state resistivities than the material made at ANL, and it is uncertain whether the conclusions made from these measurements will be valid when applied to "good" materials. A better data base is required before high-T_c current leads can be properly designed. Therefore, ANL has initiated a task to obtain thermal conductivity measurements on several of its best samples. A subcontract has been issued to the Astronautics Corporation of America to measure thermal conductivity on a number of samples in zero magnetic field

and a field of 5 T. The samples include compositions of YBCO, Ag/YBCO composite, (Pb,Bi)-Sr-Ca-Cu-O, and Tl-Ba-Ca-Cu-O. Results from these measurements should be available early in FY90. In addition, several samples have been sent to Professor W. P. Kirk of the Department of Physics at Texas A&M University for thermal conductivity measurements.

The use of high-T_c superconductors for cryostat current leads has been analyzed for operation between liquid helium and liquid nitrogen temperatures in both conduction-cooled and vapor-cooled cases. Conduction-cooled cases have been solved analytically; vapor-cooled cases have been solved numerically. Results of the ANL analysis indicate possible design opportunities and problems that have not been experienced with conventional superconductors.

The helium flow rate generated by a YBCO lead per current carried is shown in Fig. 28 as a function of the shape factor (i.e., ratio of lead length times current to area), iL/A, for both the conduction-cooled and vapor-cooled leads operating between temperatures T_H = 77 K and T_C = 4.2 K. In the case of the vapor-cooled lead, we assume that heat entering the cryostat via other paths does not contribute to cooling the lead and that all heat entering the cryostat via the current lead contributes to cooling the lead. For a given value of i, the vapor-cooled configuration always produces a significantly lower helium flow and has its optimum L/A at approximately twice the value of the conduction-cooled case.

The solid curves in Fig. 28 correspond to YBCO completely in the normal state. If the lead is superconducting, the helium flow rate is given by the straight-line dashed curve for each configuration. Thus, as long as the lead remains superconducting, the helium flow rate can be made arbitrarily small by increasing L/A. If one designs the lead for optimal length for operation in the normal state, the transition to the superconducting state will reduce the helium flow to 0.58 that of the normal state in the conduction-cooled configuration, and to 0.40 that of the normal state in the vapor-cooled configuration.

For leads longer than the normal-state optimum, the helium boil-off in the superconducting state can be reduced further, but the system must be guarded against the possibility of thermal runaway. If the lead is too long, it will burn up. For lengths less than the maximum to prevent burnup, under a temperature perturbation, the lead may enter a metastable state where a large fraction of the length remains normal, and the helium boil-off remains high. This result in shown in Fig. 29.

In Fig. 29, the helium flow rate is plotted as a function of T_S, the superconducting transition temperature, T_S, for several conduction-cooled YBCO leads that are longer than the optimal length of the normal state (T_S = 0). As T_S increases, the flow rate decreases. As the lead becomes longer, the helium boil-off increases at small T_S but decreases for large T_S. For iL/A > 26.67 A/mm (i.e., a critical value about 1.53 times the optimal length), the solution splits into two separate metastable parts, with the lower curve corresponding to $dT/dx > 0$ at $x = L$, and the upper curve corresponding to $dT/dx < 0$ at $x = L$. A third solution between these two is unstable. As iL/A increases beyond the critical value, the separation between m/i for the two solutions increases, the domain of the lower solution decreases (i.e., the minimum T_S for the solution approaches T_H), the domain of the upper solution increases (i.e., the maximum T_S for the solution increases), and the domain of overlap increases. For iL/A >29.70 A/mm, the domain of the upper solution begins at T >77 K.

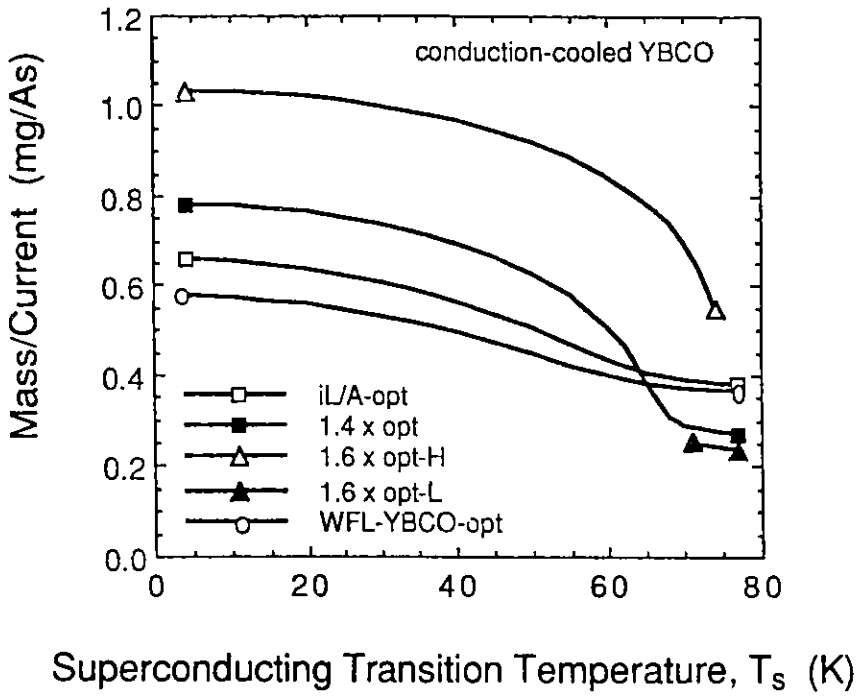

Fig. 29. Helium Flow Rate as Function of Superconducting Transition Temperature in Conduction-cooled YBCO Leads.

As an example of the potential problems associated with a design in the multiple-solution region, consider a lead whose length is longer than the critical value. Originally, it is totally superconducting and operating on the lower branch of the solution where helium boil-off is low. As a result of an external disturbance, the superconducting temperature drops below the lowest value of the lower-solution curve. Operation is then forced to transit to the higher-solution curve with the larger helium boil-off. After the external disturbance has passed, operation remains on the higher-solution branch until the current is decreased.

For current or magnetic field perturbations, the lead may enter a hybrid partially superconducting state in which the effective resistivity is about 0.1 that of the normal state. In designs for these latter cases, the helium boil-off is greatly reduced relative to that for pure metal leads.

Basic heat transfer analysis indicates that operation at presently obtainable current densities of 100 to 1000 A/cm^2 results in adequate steady-state cooling and thermal stability for most designs. This stability is obtained without the use of normal metal stabilizer.

Future work on this topic will be oriented toward design and fabrication of high-T_c current leads that will be tested with typical cryogenic apparatus. A 1-A current lead has already been sent to NASA Goddard Space Flight Center for testing in one of their cryostats. Several other laboratories (LBL and FNAL) have offered to test 500-A leads for ANL. Such leads have not yet been fabricated because of the substantial effort involved, and, in

addition, several companies have submitted proposals to the ANL Pilot Center to study current leads of approximately this current capacity.

References for Section 2.5

Y. L. L. Buyanov, Cryogenics *25*, 94 (1985).

J. R. Hull, Proc. Intersociety Energy Conversion Engineering Conf., Washington, DC, 459 (1989a).

J. R. Hull, Cryogenics (1989b, accepted for publication).

A. Matrone, G. Rosatelli, and R. Vaccarone, IEEE Trans. Magn. *25*, 1742 (1989).

F. J. Mumford, Cryogenics *29*, 206 (1989).

2.6 Interactions

2.6.1 Belden Wire and Cable Company

The purpose of this collaboration is to study the shielding effectiveness of YBCO superconductor at 77 K. Potential shielding applications include computer transmission line protection from external fields and equipment protection from large electromagnetic fields generated by magnetic resonant imaging equipment. Shielding of small magnetic fields is necessary for monitoring human brain waves (Shigematsu et al., 1989).

The exploration of AC magnetic shielding effectiveness is a unique feature of this work. Many other research groups have studied the DC magnetic shielding properties of YBCO. Electromagnetic shielding by normal conductors, such as copper, is limited by the skin effect and the conductivity of the material. High-T_c superconductors may be an alternative, and experiments have been carried out to determine the effects of frequency and magnetic field strength on shielding effectiveness.

The major contribution of ANL to this effort has been in the fabrication and characterization of YBCO specimens. Tubes of YBCO have been made by extrusion, and Belden has assisted by making a series of extrusion dies of different geometry. Three different wall thicknesses have been extruded in lengths up to 36 cm. Great care was taken in heat treating these samples, owing to a large amount of organics in the unfired state. Several factors had an influence on the final geometry, and continual interaction was maintained with Belden to design sample-size and test-fixture arrangements.

The apparatus for the near-field experiment is shown in Fig. 30. The AC current is supplied to the outer power coil by an HP 4194-A impedance-gain phase analyzer and power amplifier. The inside coil picks up the transmitted signal that passes through the high-Tc superconducting tube. The shielding effectiveness of YBCO has been found to be superior to copper or cold-rolled steel at magnetic fields below 10 G.

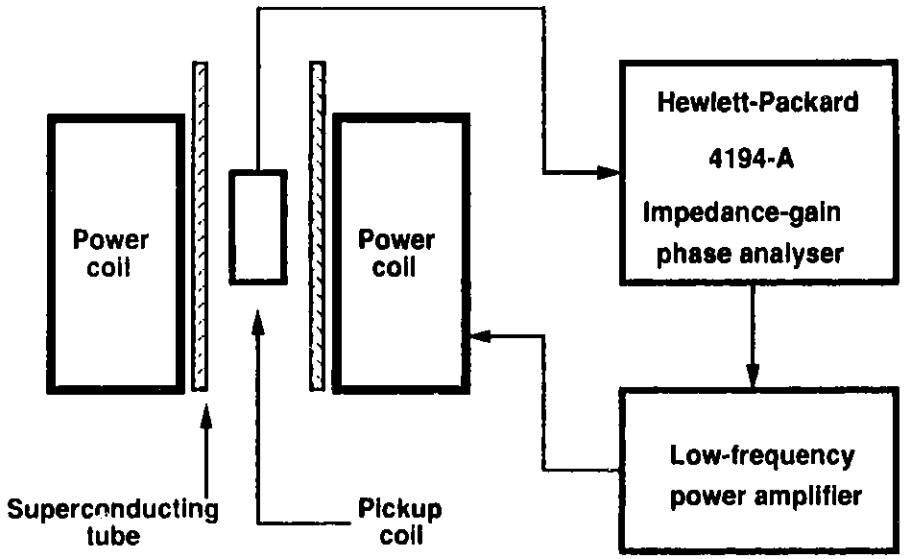

Fig. 30. Near-field Apparatus Experimental Setup.

A recent experiment has been to determine the effect of a DC magnetic field on AC shielding properties. Current leads were attached to the ends of the YBCO tube, and the intensity of the static magnetic field is proportional to the applied current. Results of the study are shown in Fig. 31. The low-frequency shielding properties degrade in the 5-A range, which corresponds to a magnetic field of 1.5 G. The mechanism for degradation in shielding effectiveness is still under consideration, but is probably due to the breakdown in superconducting current paths as magnetic field is increased. This phenomenon has also been seen in critical current density measurements.

In conclusion, this collaboration has resulted in many useful experiments and has elucidated the electromagnetic shielding properties of YBCO. Several technical papers on this work have been presented (Pienkowski et al., 1988a, 1988b, 1989).

2.6.2 Pennsylvania State University

The green phase, Y_2BaCuO_5, is chemically compatible with the superconducting YBCO compound, and has been used as an insulation layer in composite structures. We have fabricated Y_2BaCuO_5 pellets and sent the specimens to Drs. A. Bhalla and D. Moffatt for dielectric characterization. The dielectric constant and loss have been measured from 10^2 to 10^6 Hz at temperatures of -160 to 200°C. Initial data confirm the semiconducting behavior observed by DC measurements. A joint publication on the properties of Y_2BaCuO_5 was published (S. E. Dorris, et al., 1989).

2.6.3 Northeastern University

High-T_c superconductors potentially have very low surface resistance at microwave frequencies and may be useful for many applications. Large area coatings of RF cavities may be used for band pass filters in communications, particle beam accelerators, and frequency stabilization for oscillators. ANL has great expertise in the use of low-T_c superconductors in RF cavities and has extended that knowledge to the high-T_c materials.

Dr. S. Sridhar and Dr. K. Zahopoulos of Northeastern University have designed and machined a cavity to act as a filter in the 8 to 12 GHz range. The cavity was fabricated from silver, as requested by ANL. Silver has been found to be a compatible substrate for the YBCO system. ANL coated the cavity by a thick film process and carried out the heat treatment. Preliminary results are encouraging, with the Q of the cavity increasing by a factor of 5 as the cavity was cooled below the superconducting transition temperature.

2.6.4 General Dynamics Corporation

General Dynamics (GD) has extensive experience in the fabrication and characterization of large niobium-titanium magnets and is interested in studying YBCO coils. GD has the capability of measuring both DC and AC electronic properties of coils. Specimens were made at ANL, and the critical current densities were measured prior to shipping to GD. The first critical current density measured by GD was within 5% of that measured at ANL, and it was found that certain portions of the coil quenched before other sections. AC measurements carried out at 50 Hz indicate that losses for YBCO at 77 K are about five times larger than losses in the state-of-the art NbTi materials at 4.2 K. Work will continue to achieve better electrical properties in high-T_c coils.

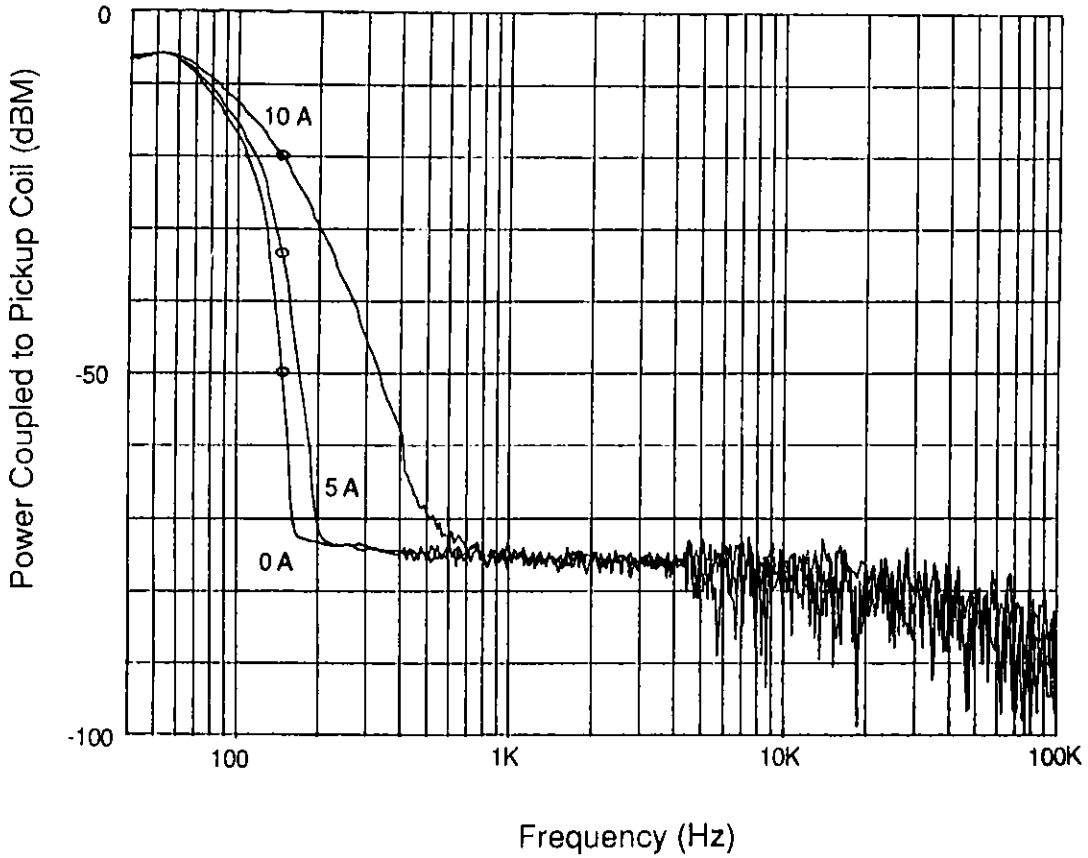

Fig. 31. Near-field Magnetic Shielding of YBCO as a Function of DC Current (Power level is 0 dBm).

2.6.5 ATEK Metals Center, Inc.

We have been interacting with Atek Metals Center Inc., of Cincinnati in the area of high-pressure, hot extrusion of ceramic superconductors. The hot extrusion work was done by ATEK using powders provided by ANL. The powder compacts are encapsulated in a metal can and then extruded. The YBCO powder was synthesized by the conventional calcination technique. The conclusions of the experiments are:

- Plastic deformation of 123 was achieved by coextrusion in metal cans between 650 and 850°C and pressures between 408 and 1360 MPa, respectively.

- Conditions were identified that allow the YBCO to be hot-extruded by streamlined flow in a metal can from a pellet to an integral rod without apparent fracture.

- Densities approaching the theoretical maximum can be produced by compacting pressures of 1360 MPa at temperatures as low as 450°C.

- A combination of high-quality starting material and optimal extrusion holds promise for producing solid orthorhombic oxide rods.

2.6.6 United Technologies Research Center

As part of the Pilot Center Program between ANL and the United Technologies Research Center (UTRC), ANL is processing Bi-based ceramic superconductor blocks. UTRC is interested in the development of superconducting magnetic bearings using high-T_c materials. We have shipped large sintered blocks and calcined powders of Pb/BSCCO to UTRC. Magnetometry measurements were done on the sintered samples at UTRC. The plots showed a single diamagnetic transition in both field-cooled and zero-field-cooled data, with an onset of 110 K. Force versus field measurements are being done at this time.

2.6.7 Naval Surface Warfare Center

This collaboration is focused on microscopic distribution of silver in YBCO powders. Silver is added in the form of silver nitrate using a melt process. The YBCO powders are synthesized at ANL by a vacuum calcination technique. Pellets made from the powder containing 15 wt.% Ag and sintered at 885°C in 1% oxygen exhibited a critical current density (J_c) of ≈200 A/cm^2 at 77 K.

2.6.8 NASA-Marshall Space Flight Center

This collaborative work involves the use of a magnetic decoration technique to study where on the sample surface the flux pinning occurs, i.e., in the grains or at the grain boundaries. Also, tests will be done to characterize the superconductors using magnetic "attractive" levitation. Our role is to prepare superconducting 123 and YBCO /Ag samples of appropriate dimensions.

2.6.9 CPS Superconductor Corporation

We evaluated YBCO powders received from CPS. This powder was phase-pure by X-ray diffraction and could be readily sintered to very high density (~96% of theoretical value). The J_c of the pellets sintered at various temperatures is ≈100 A/cm^2.

2.6.10 Oregon Graduate Center

Professor N. G. Eror is collaborating with ANL in characterizing the YBCO powders using a sensitive X-ray diffractometer. Two joint publications have resulted.

2.6.11 Northwestern University

We are collaborating with Professors T.O. Mason and D. L. Johnson in studying solid-state reaction kinetics and effects of sinter forging on ceramic superconductors. The following resulted from this collaboration:

"Impedance Spectra During Solid State Powder Reactions of Oxide Superconductors," submitted to the Journal of the American Ceramic Society in August 1989.

Four abstracts were submitted to the Fall Meeting of the Materials Research Society, Boston, Nov. 27-Dec. 2, 1989:

- "Processing and Fabrication of $YBa_2Cu_4O_8$ and $YBa_2Cu_4O_8/YBa_2Cu_3O_x$ Composites."

- "Microstructure and Superconductivity in $YBa_2Cu_{3+x}O_y$."

- "The Effects of the Solution Structure on the Microstructure and Properties of Sinter-forged Sol-gel-derived Superconductors."

- "High-T_c Oxide Solid State Reaction Kinetics via Complex Impedance Spectroscopy."

2.6.12 University of Notre Dame

Collaborative work between Professor Paul McGinn of the University of Notre Dame and ANL is underway in the area of melt-texturing of ceramic superconductors; J_c is enhanced by melt-texturing. McGinn has zone-melted YBCO wire samples that were extruded and sintered at ANL. The binder burnout and sintering has been carried out by ANL. The zone-melted samples are characterized at ANL. The J_c versus field measured in a small piece of zone-melted sample is shown in Fig. 32. As seen from this figure, a J_c of at least 500 A/cm^2 at an external applied field of 5000 G is observed in this sample. The grains are more than 1 mm long and ≈300 μm wide. Zone melted samples are porous and contain many cracks. Zone-melting parameters are now being optimized to eliminate the cracks and improve the density. Magnetic susceptibility measurements showed a sharp transition at 90 K. The magnetization curve at 77 K showed a very large hysteresis, and the magnetization appears to be greater than that for a single crystal.

2.6.13 DuPont

Funding is now in place for a collaborative effort between ANL and DuPont on the design and fabrication of a solenoid to be made from the YBCO superconductor. Such a solenoid has potential as a low-voltage actuator, for example in mining equipment, where safety concerns limit the electrical power used. The envisioned solenoid would be approximately 3 in. long, 1.5 in. O.D., and 5/16 in. I.D. It would consist of approximately 2500 turns carrying a current of 0.15 A and would have a working field of ≈200 oersted. Fabrication of this solenoid should be feasible without dramatic increases in the critical current density of YBCO, since the solenoid would be operated at low current. The superconducting solenoid thus has potential as a practical application of the high-T_c superconductor in the near term.

The first step was to determine the best YBCO powder available for fabrication of the solenoid. Toward this goal, YBCO powder provided by DuPont was characterized in terms of powder characteristics and superconducting properties of fired samples. Particle size analysis with the Microtrac analyzer showed that the DuPont YBCO powder was significantly coarser than our solid-state-derived YBCO powders, with a mean particle size of ≈15 μm and no particles smaller than ≈5 μm. Examination of the powder with SEM supported this approximate particle size and showed that the large particles are agglomerates. Slips of this powder became much more viscous upon milling, indicating that the agglomerates are fairly soft and can be fairly readily broken down. X-ray analysis of the powder showed the presence of very minor amounts of $BaCuO_2$ and/or Ba_2CuO_3.

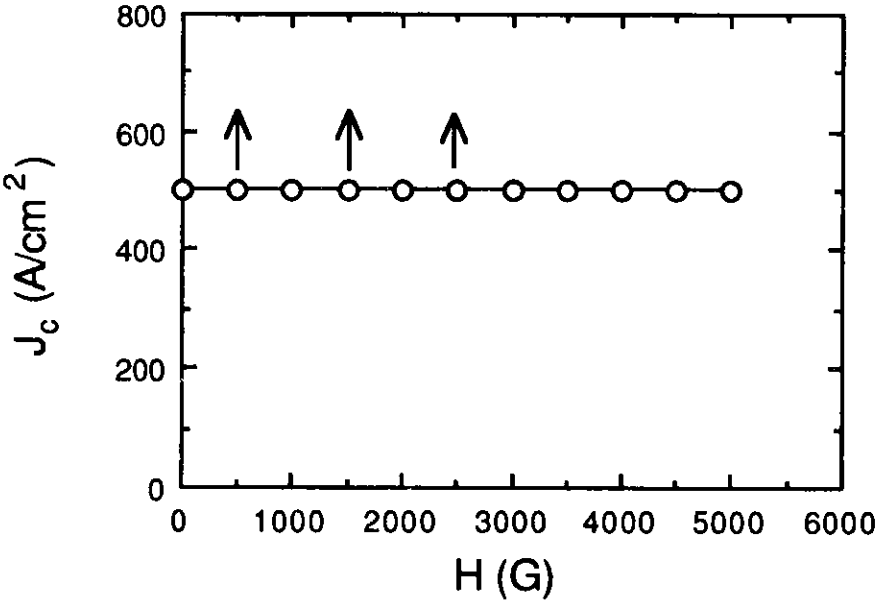

Fig. 32. Lower Limit of J_c of Melt-textured YBCO versus Applied Field.

Tapes were cast from the DuPont powder, and wires and coils were extruded. The samples were fired, and their critical current densities (J_C) were measured. Fired coils have been given to Dennis Kountz at DuPont, so that they can also characterize the superconducting properties. On the average, J_C was about twice as large for coils made from ANL-produced powder, based on measurements made at ANL. For this reason, fabrication of coils at ANL will be done with ANL-produced powder.

A meeting between ANL and DuPont representatives was held at the DuPont Experimental Station in late June 1989. It was decided at that meeting that future efforts should focus on the extrusion of multilayer coils. As mentioned earlier, this will require that the extruded wire be coated with an insulating layer. The 211 material is being used as the insulating material, and two methods for applying 211 are currently being explored: dip-coating of the wire is being investigated at ANL, and plans are being made to explore coextrusion at DuPont, either by DuPont personnel or by an ANL representative through a personnel exchange. The next meeting between ANL and DuPont representatives is tentatively scheduled for late September 1989, at which time it is hoped that a multilayer coil will have been produced.

2.6.14 Interactions with Industry on Thin Films

Our program with TRW, Inc., of Redondo Beach, CA, involves collaborative research on TEM analysis of transverse sections of high-T_c thin films and the fabrication of thin-film SQUIDs. In addition, we will study the effects of neutron irradiation on J_c. This "work-for-others" contract has matching funds provided by the Argonne Pilot Center for Superconductivity.

Collaborations with Superconducting Technologies, Inc., Santa Barbara, CA, have begun with ANL coating that firm's substrates with unannealed TBCCO to allow the company to

check its annealing process against that of ANL. In addition, we plan to neutron-irradiate the company's laser-ablation-deposited TBCCO films to evaluate J_c increases due to artificial pinning centers.

Preliminary discussions about possible collaborative efforts on high-T_c films have begun with the Microelectronics and Computer Technology Corporation of Austin, TX. An ANL staff member has visited their research laboratory and continued the discussion about possible collaborative ventures.

An interaction with the Solar Energy Research Institute of Golden, CO, has been maintained, and A. J. Nelson has made preliminary measurements of the Auger and electron energy loss signals at 100 K and 300 K, which have an interesting temperature dependence. We have sent a new TBCCO film with higher T_c to allow measurements below T_c in a new variable-temperature stage to help determine the significance of these measurements to the electronic states in high-T_c superconductors.

We have begun informal discussions with David Ginley of Sandia National Laboratory about collaborative research, including our TEM studies. It would be of interest to examine Sandia's films by TEM and also to trade unannealed films of the Tl-based high-T_c superconductors for annealing to establish whether the unoriented films found only by Sandia are due to the annealing procedures or the synthesis technique. The latter is more likely, since Sandia uses a multilayer approach whereas ANL sputters all elements simultaneously, and the annealing procedures are not very different.

2.6.15 Interactions with Universities on Thin Films

We have established closer ties with the University of Illinois at Urbana-Champaign, Northwestern University, and the University of Chicago as a result the NSF-funded Science and Technology Center for Superconductivity. A program is being developed to establish standards for compositional analysis of thin films using EDS, including round-robin testing. A similar program is being considered to establish universal criterion for J_c measurements, including the problems of contacts. In addition, a graduate student from Northwestern joined ANL in June 1989 and began studies of in-situ analysis of growing films using X-ray fluorescence and Bragg scattering. An additional post-doctoral appointee, funded by this center, will join the thin film group with his primary research focus on in-situ high-T_c film fabrication, as well as on a new initiative using the scanning tunneling microscope for evaluating the structural and electronic properties of such films.

Within the context of the Science and Technology Center, Kenneth Gray of ANL talked with representatives of three companies, each of which is interested in thin film research. They include Dr. Bill Mitchell, 3M Company, Minneapolis, MN; Dr. James Bray, General Electric, Schenectady, NY; and Dr. David Taschler, Air Products, Allentown, PA. Collaborations with 3M may include evaluation of their ion-beam sputtering technique and exchange of films for analysis. Air Products has indicated a desire to support thin film research in the S&T center with real money.

A collaboration with A. M. Goldman of the University of Minnesota has begun with studies of the penetration depth and the fluctuation conductivity in our Tl-based high-T_c

films. Results for the latter show strictly two-dimensional behavior in agreement with the highly 2–D character of H_{c2} we had already reported.

K. C. Woo, University of Illinois at Chicago, is conducting studies of the high-field properties of our films, including measurements at the National Magnet Laboratory (FBNML). Hall-effect measurements, for identifying the carrier concentration and sign, have been partially completed. Further studies have included the measurement of the new loss mechanism found in high–T_c superconductors at high temperatures and even modest magnetic fields, as well as the comparison of J_c from transport and magnetization measurements.

D. E. Farrell of Case Western University has made torque measurements on our TBCCO films and confirms the giant anisotropy of >70 measured by us resistively. Further investigations into fluctuations and losses are in progress.

References for Section 2.6

U. Balachandran, et al., in Ceramic Superconductors II, ed. M. F. Yan (Am. Ceram. Soc., Westerville, OH, 1988), p. 198.

U. Balachandran, et al., Mater. Lett. *8*, 454 (1989).

S. E. Dorris, et al., Jpn. J. Appl. Phys. *28*, L1415 (1989).

T. Pienkowski, et al., presented at IEEE 1989 National Symp. on Electromagnetic Compatibility, Denver (May 23-25, 1989).

T. Pienkowski, et al., Superconductivity, '88 Oct 19, 1988, Boston (1988a).

T. Pienkowski, et al., Proc. Wire and Cable Symp., 24-28, Nov. 15-17, 1988, Reno, NV (1988b).

K. Shigematsu, et al., Jpn. J. Appl. Phys. *28*, L813 (1989).

2.7 Selected Publications on High-Temperature Superconductors

Mechanical and Superconducting Properties of Sintered Composite $YBa_2Cu_3O_{7-\partial}$ Tape on Silver Substrate

J. P. Singh, D. Shi and D. W. Capone II

Appl. Phys. Lett. **53**, 237-239 (1988)

Electrical Conductivity and Chemical Diffusion in Sintered $YBa_2Cu_3O_y$

J.-H. Park, Peter Kostic and J. P. Singh

Mater. Lett. **6**, 393-397 (1988)

120 K Superconductivity in the (Bi,Pb)-Sr-Ca-Cu-O System

U. Balachandran, D. Shi, D. I. Dos Santos, S. W. Graham, M. A. Patel, B. Tani, K. Vandervoort, H. Claus and R. B. Poeppel

Physica C **156**, 649-651 (1988)

RF Measurements on High-T_c Superconductors at Argonne National Laboratory

J. R. Delayen, K. W. Shepard, K. C. Goretta and R. B. Poeppel

Proc. 3rd Workshop on *RF Superconductivity* ed. K. W. Shepard (Argonne National Laboratory, Argonne, IL, September 14-18, 1987, ANL-PHY-88-1, January 1988), pp. 229-232

A Time-Temperature-Transformation Curve for the Orthorhombic to Tetragonal Phase Transition in $YBa_2Cu_3O_{7-x}$

D. Shi, D. W. Capone II, K. C. Goretta, G. T. Goudey and K. Zhang

J. Appl. Phys. **63**, 5411-5414 (1988)

Ceramic Processing of High-T_c Superconductors

R. B. Poeppel, J. P. Singh, M. T. Lanagan, K. C. Goretta, J. T. Dusek and D. W. Capone II

In Sensing, Discrimination, and Signal Processing and Superconducting Materials and Instrumentation, SPIE Proc. Vol. 879, 1988, pp. 170-173; invited paper

Fabrication of Bulk Superconducting Ceramics

K. C. Goretta, J. T. Dusek, J. P. Singh, M. T. Lanagan, U. Balachandran, S. E. Dorris and R. B. Poeppel

In World Congress on Superconductivity, ed. C. G. Burnham and R. D. Kane (World Scientific, Singapore, 1988), pp. 311-320; invited paper

Cu Adatom Interactions with Single- and Polycrystalline $Bi_2Ca_{1+x}Sr_{2-x}Cu_2O_{8+y}$ and $YBa_2Cu_3O_{7-x}$

D. M. Hill, H. M. Meyer III, J. H. Weaver, C. F. Gallo and K. C. Goretta

Phys. Rev. B **38**, 11,331-11,336 (1988)

Sintering of $YBa_2Cu_3O_{7-x}$ Compacts

D. Shi, D. W. Capone II, G. T. Goudey, J. P. Singh, N. J. Zaluzec and K. C. Goretta

Mater. Lett. **6**, 217-221 (1988)

Electronic Structures of the $YBa_2Cu_3O_{7-x}$ Surface and Its Modification by Sputtering and Adatoms of Ti and Cu

H. M. Meyer III, D. M. Hill, T. J. Wagener, Y. Gao, J. H. Weaver, D. W. Capone II and K. C. Goretta

Phys. Rev. B **38**, 6500-6512 (1988)

Calcination of $YBa_2Cu_3O_{7-x}$ Powder

K. C. Goretta, I. Bloom, N. Chen, G. T. Goudey, M. C. Hash, G. Klassen, M. T. Lanagan, R. B. Poeppel, J. P. Singh, D. Shi, U. Balachandran, J. T. Dusek and D. W. Capone II

Mater. Lett. **7**, 161-164 (1988)

Shielding Effectiveness of Superconductive Particles in Plastics

T. Pienkowski, J. Kincaid, M. T. Lanagan, R. B. Poeppel, U. Balachandran and K. C. Goretta

37th International Wire and Cable Symp. Proc. (U.S. Army Communications -- Electronics Command, Fort Monmouth, NJ, 1987), pp. 24-28

RF Properties of an Oxide-Superconductor Half-Wave Resonant Line

J. R. Delayen, K. C. Goretta, R. B. Poeppel and K. W. Shepard

Appl. Phys. Lett. **52**, 930-932 (1988)

Oxygen Diffusion in $YBa_2Cu_3O_{7-\delta}$

J. L. Routbort, S. J. Rothman, L. J. Nowicki and K. C. Goretta

Mater. Sci. Forum **34-36**, 315-321 (1988); invited paper

Texturing of $RBa_2Cu_3O_{7-x}$ Superconductors

K. C. Goretta, D. W. Capone II, T. L. Tolt, R. B. Poeppel, J. P. Singh, A. J. Schultz, D. Shi, J. T. Dusek, D. S. Applegate and J. S. Kallend

In Ceramic Superconductors II, ed. M. F. Yan (Am. Ceram. Soc., Westerville, OH, 1988), pp. 323-331

Superconducting Properties of $LaBa_2Cu_3O_{7-x}$ and $YBa_2Cu_3O_{7-x}$

U. Balachandran, K. C. Goretta, D. Shi, R. B. Poeppel and N. G. Eror

In Ceramic Superconductors II, ed. M. F. Yan (Am. Ceram. Soc., Westerville, OH, 1988), pp. 198-203

Reactivity and Passivation for Bi Adatoms on $YBa_2Cu_3O_{6.9}$ and $Bi_2Ca_{1+x}Sr_{2-x}Cu_2O_{8+y}$

H. M. Meyer III, D. M. Hill, J. H. Weaver, D. L. Nelson and K. C. Goretta

Appl. Phys. Lett. **53**, 1004-1006 (1988)

Ceramic Fabrication Technology for High-T_c Materials

M. T. Lanagan, R. B. Poeppel, K. C. Goretta, J. P. Singh, J. T. Dusek, G. T. Goudey and D. I. Dos Santos

In Superconductivity and Its Applications, ed. H. S. Kwok and D. T. Shaw (Elsevier, New York, 1988), pp. 118-123

Observations of Preferred Orientation in High-T_c Oxide Superconductor Tapes
J. P. Singh, U. Balachandran, D. Shi, J. K. Degener and R. B. Poeppel
Mater. Lett. **7**, 72-74 (1988)

Effect of Heating Rate on Properties of $YBa_2Cu_3O_{7-x}$
N. Chen, K. C. Goretta, M. T. Lanagan, D. Shi, M. A. Patel, I. Bloom, M. C. Hash, B. S. Tani and D. W. Capone II
Super. Sci. & Tech. **1**, 177-179 (1988)

Processing and Electrical Properties of High-T_c Superconductors
R. B. Poeppel, M. T. Lanangan, J. P. Singh, K. C. Goretta, J. T. Dusek, S. E. Dorris, U. Balachandran, C. L. Bonn and J. R. Delayen
In Thirteenth International Conference on Infrared and Millimeter Waves, SPIE Proc., Vol. 1039, 1988, pp. 197-198

Ceramic Fabrication Processes for High-T_c Superconductors
R. B. Poeppel, K. C. Goretta, M. T. Lanagan, J. T. Dusek and J. K. Degener
Proceedings of American Power Conference, Volume 50, ed. P. Dawkins, 1988, pp. 450 - 453; invited paper

Reports on International SC Global '89 Conference
U. Balachandran
Cold Facts **5**, 6 (1989)

Fabrication of High-T_c Superconductors
K. C. Goretta, M. T. Lanagan, J. P. Singh, J. T. Dusek, U. Balachandran, S. E. Dorris and R. B. Poeppel
Mater. & Manufact. Proc. **4**, 163-175 (1989); invited paper

Superconducting Wires
M. T. Lanagan, R. B. Poeppel, J. P. Singh, D. I. Dos Santos, J. K. Degener, J. T. Dusek and K. C. Goretta
J. Less-Common Met. **149**, 305-312 (1989); invited paper

Shape Forming of High-T_c Superconductors
R. B. Poeppel, S. E. Dorris, A. J. Youngdahl, J. P. Singh, M. T. Lanagan, U. Balachandran, J. T. Dusek and K. C. Goretta
J. Met. **41**[1] 11-13 (1989); Invited Paper

Swaged Superconductor Wires
D. Shi and K. C. Goretta
Mater. Lett. **7**, 428-432 (1989)

Resonant Inverse Photoemission of $Bi_2Ca_{1+x}Sr_{2-x}Cu_2O_{8+y}$ and $YBa_2Cu_3O_{7-x}$, Unoccupied Oxygen States, and Plasmons
T. J. Wagener, Y. Hu, Y. Gao, M. B. Jost, J. H. Weaver, N. D. Spencer and K. C. Goretta
Phys. Rev. B **39**, 2928-2931 (1989)

RF Surface Resistance of Large-area Bi-Sr-Ca-Cu-O Thick Films on Ag Plates
C. L. Bohn, J. R. Delayen, U. Balachandran and M. T. Lanagan
Appl. Phys. Lett. **55**, 304-306 (1989)

Slip Casting of High-T_c Superconductors
D. E. Bloomberg, D. S. Applegate, T. L. Tolt, M. T. Lanagan, J. T. Dusek, R. B. Poeppel and K. C. Goretta
J. Mater. Sci. Lett. **8**, 759-761 (1989)

Single Crystal $YBa_2Cu_3O_{7-x}$ and $Bi_2Ca_{1+x}Sr_{2-x}Cu_2O_{8+y}$ Surfaces and Ag Adatom-induced Modification
H. M. Meyer III, D. M. Hill, T. J. Wagener, J. H. Weaver, C. F. Gallo and K. C. Goretta
J. Appl. Phys. **65**, 3130-3135 (1989)

High-temperature Deformation of $YBa_2Cu_3O_{7-d}$
A. W. von Stumberg, N. Chen, K. C. Goretta and J. L. Routbort
J. Appl. Phys. **66**, 2079-2082 (1989)

Influence of Oxygen Concentration on Processing $YBa_2Cu_3O_x$
N. Chen, D. Shi and K. C. Goretta
J. Appl. Phys. **66**, 2485-2488 (1989)

Effect of Heat Treatment Time and Temperature on the Properties of $YBa_2Cu_3O_{7-x}$
I. Bloom, B. S. Tani, M. C. Hash, D. Shi, M. A. Patel, K. C. Goretta, N. Chen and D. W. Capone II
J. Mater. Res. **4**, 1093-1098 (1989)

Recent Improvements in Bulk Properties of Ceramic Superconductors
R. B. Poeppel, U. Balachandran, I. Bloom, S. E. Dorris, J. T. Dusek, K. C. Goretta, M. T. Lanagan, V. A. Maroni, J. J. Picciolo, D. Shi, J. P. Singh and C. A. Youngdahl
In High Temperature Superconducting Compounds: Processing & Related Properties, ed. S. H. Whang and A. DasGupta (Minerals, Metals and Materials Society, Warrendale, PA, 1989), pp. 59-71; invited paper

SIMS Measurement of Oxygen Tracer Diffusion in $YBa_2Cu_3O_{7-d}$
S. J. Rothman, J. L. Routbort, J. E. Baker, L. J. Nowicki, K. C. Goretta, L. J. Thompson and J. N. Mundy
In Diffusion Analysis & Applications, ed. A. D. Romig, Jr. and M. A. Dayananda (Minerals, Metals and Materials Society, Warrendale, PA, 1989), pp. 289-305; invited paper

Impedance Spectra During Solid State Powder Reactions of Oxide Superconductors
E. A. Cooper, T. O. Mason, M. E. Biznek and U. Balachandran
J. Am. Ceram. Soc., submitted

Properties of Sputtered Superconducting Films of $Bi_2Sr_2CaCu_2O_x$ Made by Low-temperature, In-situ Growth

R. T. Kampwirth, P. H. Anderson, D. B. McDonald, D. J. Miller, K. E. Gray, Z. F. Sungaik, U. Balachandran and A. Wagner

Appl. Phys. Lett., submitted

Processing of Y- and Bi-Based Superconductors

U. Balachandran, D. I. Dos Santos, A. W. von Stumberg, S. W. Graham, J. P. Singh, C. A. Youngdahl, K. C. Goretta, D. Shi and R. B. Poeppel

Xth Winter Meeting on Low Temperature Physics, Cocoyoc, Morelos, Mexico, January 1989, in press; invited paper

Y_2BaCuO_5 as a Substrate for $YBa_2Cu_3O_x$

S. E. Dorris, M. T. Lanagan, D. M. Moffat, H. J. Leu, C. A. Youngdahl, U. Balachandran, A. Cazzato, D. E. Bloomberg and K. C. Goretta

Jpn. J. Appl. Phys., in press

Application of Neutron Diffraction NDE to High-Temperature Superconducting Composites

D. S. Kupperman, J. P. Singh, S. Majumdar, A. C. Raptis and R. L. Hitterman

Proc. of 16th Annual Review of Progress in Quantitative NDE, Brunswick, ME, July 23-28, 1989, in press

Production of Wires and Coils from High-temperature Superconducting Materials

M. T. Lanagan, U. Balachandran, S. E. Dorris, J. T. Dusek, K. C. Goretta, R. B. Poeppel, J. P. Singh and C. A. Youngdahl

Proc. of Workshop on High-T_c Superconductivity, Huntsville, AL, May 1989, in press

Application of Neutron Diffraction to Characterization of Residual Thermal Strains in $YBa_2Cu_3O_{7-\delta}/Ag$

D. S. Kupperman, J. P. Singh, J. Faber, Jr. and R. L. Hitterman

Appl. Phys. Lett., in press

The Effect of Composition and Processing on High T_c Superconductors Containing Bismuth

A. S. Nash, K. C. Goretta and R. B. Poeppel

Advances in Powder Metallurgy - 1989, in press

Oxygen Diffusion in High-T_c Superconductors

S. J. Rothman, J. L. Routbort, L. J. Nowicki, K. C. Goretta, L. J. Thompson and J. N. Mundy

DIMETA-88, International Conference on Diffusion in Metals and Alloys, Balatonfüred, Hungary, September 1988, in press; invited paper

Synthesis and Sintering of $Tl_2Ca_2Ba_2Cu_2O_x$

K. C. Goretta, D. Shi, B. Malecki, M. C. Hash and I. Bloom

Super. Sci. & Tech., in press

Synthesis of Phase-Pure Orthorhombic $YBa_2Cu_3O_x$ Under Low Oxygen Pressure
U. Balachandran, R. B. Poeppel, J. E. Emerson, S. A. Johnson, M. T. Lanagan, C. A. Youngdahl, D. Shi, K. C. Goretta and N. G. Eror
Mater. Lett., in press

Effect of Silver and Silver Oxide Additions on Mechanical and Superconducting Properties of $YBa_2Cu_3O_{7-\delta}$ Superconductors
J. P. Singh, H. J. Leu, E. Van Voorhees, G. T. Goudey, K. Winsley and D. Shi
J. Appl. Phys., in press

$YBa_2Cu_3O_x$ Toughened by ZrO_2 Additions
K. C. Goretta, O. D. Lacy, U. Balachandran, Donglu Shi and J. L. Routbort
J. Mater. Sci. Lett., in press

Mechanical Properties of CuO
J. K. Lumpp, Nan Chen, K. C. Goretta and H. M. Herro
High Temp. Mater. Proc., in press

Lorentz-Force Independence of Resistance Tails for High-Temperature Superconductors in Magnetic Fields near T_c
K. C. Woo, K. E. Gray, R. T. Kampwirth, J. H. Kang, S. J. Stein, R. East and D. M. McKay
Phys. Rev. Lett., submitted

Transport Critical Current Behavior and Grain Boundary Microstructure in $YBa_2Cu_3O_x$
D. Shi, J. G. Chen, M. Xu, A. L. Cornelius, U. Balachandran and K. C. Goretta
J. Appl. Phys., in press

Fabrication of a Superconducting Coil for Solenoid Applications
H. J. Leu, J. P. Singh, S. E. Dorris and R. B. Poeppel
Supercond. Sci. Tech., in press

Microstructure and Electrical Properties of Bulk High-Tc Superconductors
U. Balachandran, M. J. McGuire, K. C. Goretta, C. A. Youngdahl, D. Shi, R. B. Poeppel and S. Danyluk
Proc. of 3rd Annual Conf. on Superconductivity and Applications, Buffalo, NY, September 1989, in press

O 2p Holes: Temperature Effects and Surface Characteristics of Cuprate Superconductors
T. J. Wagener, H. M. Meyer III, Y. Hu, M. B. Jost, J. H. Weaver and K. C. Goretta
Phys. Rev. B, in press

Surface Reactivity and Interface Morphology for Ti Growth on $YBa_2Cu_3O_{7-x}$, Y_2BaCuO_5 and CuO
H. M. Meyer III, J. H. Weaver and K. C. Goretta
J. Appl. Phys., in press

Lorentz-Force Independence of Resistance Tails for High-Temperature Superconductors in Magnetic Fields near T_c

K. C. Woo, K. E. Gray, R. T. Kampwirth, J. H. Kang, S. J. Stein, R. East and D. M. McKay
Physica C, in press

A Superconducting Coil Made of Filamentary Composites

D. Shi, M. Xu, J. G. Chen, S. G. Lanan, D. Miller and K. C. Goretta
Mater. Lett., in press

TECHNOLOGY TRANSFER INFORMATION (STEPS Laboratories)

2. Patents Arising from OESD–funded Research

Number of Invention Disclosures 18 : Patent Applications 5

Summary of Patent Information

File Date	Title	Inventors	DOE Case No.	Serial Number
9/28/87	Preferential Orientation of Metal Oxide Superconducting Materials	*D. W. Capone R. B. Poeppel	S–101,821	
9/28/87	Metal Oxide Superconducting Powder Comprised of Flake–Like Single Crystal Particles	*D. W. Capone J. T. Dusek	S–101,771	
9/28/87	Preferential Orientation of Metal Oxide Superconducting Materials by Mechanical Means	*D. W. Capone R. B. Poeppel	S–101,818	
9/28/87	Acoustic Plane Wave Preferential Orientation of Metal Oxide Superconducting Materials	*D. W. Capone R. B. Poeppel T. L. Tolt	S–101,819	
9/28/87	Magnetic Preferential Orientation of Metal Oxide Superconducting Materials	*D. W. Capone R. B. Poeppel J. T. Dusek T. L. Tolt *B. D. Dunlap *B. Veal	S–66,537	S–101,820
	Processing Method for Superconducting Metal Oxides	I. D. Bloom B. K. Flandermeyer R. B. Poeppel	S–66,566	

Summary of Patent Information (Contd.)

File Date	Title	Inventors	DOE Case No.	Serial Number
	Composite of Superconducting Metal Oxide with Silver Particles Between Superconducting Grains Sintered on Silver Substrate	J. P. Singh *D. Shi *D. W. Capone J. T. Dusek	S-67,757	
	Monolithic Superconducting Coil with Integral Stabilizer and Insulation	R. B. Poeppel J. P. Singh *K. C. Goretta *D. W. Capone *D. Shi	S-67,768	
	Meissner Motor	R. B. Poeppel D. S. Giroux D. S. Kupperman R. L. McDaniel		
	Synthesis of Bi-Sr-Ca-Cu Oxide Superconductor by Solution Technique	D. I. dos Santos U. Balachandran		
	Improved Current Density in Bi-Sr-Ca-Ci-O Systems	U. Balachandran		
	Extrusion Process for Metal Oxide Superconducting Wire	J. T. Dusek		
	Calcination and Solid-State Reaction of Ceramic-Forming Components to Provide Single-Phase Ceramic Product having Fine Particle Size	U. Balachandran R. B. Poeppel J. E. Emerson		
	High-Temperature Superconducting Leads for Cryogenic Apparatus	J. R. Hull		

Summary of Patent Information (Contd.)

File Date	Title	Inventors	DOE Case No.	Serial Number
	Cryogenic Liquid Depth Sensor	M. T. Lanagan		
	Electrostatic Separation of Metallic Ceramics from Nonmetallic Ceramics	**K. C. Goretta J. T. Dusek		
	Superconducting $YBa_2Cu_3O_x/ZrO_2$ Composites	K. C. Goretta		
	Improved Substrate for $YBa_2Cu_3O_x$ Superconductor	S. E. Dorris **K. C. Goretta		
	Low Pass Filter with a High-T_c Superconducting Shield	+M. T. Lanagan ++T. Pienkowski		
	Method of Degaussing Ceramic Superconductors	C. A. Youngdahl		

*Work supported by Basic Energy Sciences–Division of Materials Sciences.

**Primarily funded by Basic Energy Sciences–Division of Materials Sciences.

+Partial support through the ANL Pilot Center for Superconductivity.

++Cooper Industries – Belden Wire and Cable Company.